Development of Cell Lysis Techniques in Lab on a chip

by

Mehdi Shahini

A thesis

presented to the University of Waterloo

in fulfillment of the

thesis requirement for the degree of

Doctor of Philosophy

in

Systems Design Engineering

Waterloo, Ontario, Canada, 2013

AUTHOR'S DECLARATION

I hereby declare that I am the sole author of this thesis. This is a true copy of the thesis, including any required final revisions, as accepted by my examiners.

I understand that my thesis may be made electronically available to the public.

Abstract

The recent breakthroughs in genomics and molecular diagnostics will not be reflected in health-care systems unless the biogenetic or other nucleic acid-based tests are transferred from the laboratory to clinical market. Developments in microfabrication techniques brought lab-on-a-chip (LOC) into being the best candidate for conducting sample preparation for such clinical devices, or point-of-care testing set-ups. Sample preparation procedure consists of several stages including cell transportation, separation, cell lysis and nucleic acid purification and detection. LOC, as a subset of Microelectromechanical systems (MEMS), refers to a tiny, compact, portable, automated and easy-to-use microchip capable of performing the sample-preparation stages together. Complexity in micro-fabrications and inconsistency of the stages oppose integration of them into one chip.

Among the variety of mechanisms utilized in LOC for cell lysis, electrical methods have the highest potential to be integrated with other microchip-based mechanisms. There are, however, major limitations in electrical cell lysis methods: the difficulty and high-cost fabrication of microfluidic chips and the high voltage requirements for cell lysis. Addressing these limitations, the focus of this thesis is on realization of cell lysis microchips suitable for LOC applications.

We have developed a new methodology of fabricating microfluidic chips with electrical functionality. Traditional lithography of microchannel with electrode, needed for making electro-microfluidic chips, is considerably complicated. We have combined several easy-to-implement techniques to realize electro-microchannel with laser-ablated polyimide. The current techniques for etching polyimide are by excimer lasers in bulky set-ups and with involvement of toxic gas. We present a method of ablating microfluidic channels in polyimide using a 30W CO_2 laser. Although this technique has poorer resolution, this approach is more cost effective, safer and easier to handle. We have verified the performance of the fabricated electro-microfluidic chips on electroporation of mammalian cells.

Electrical cell lysis mechanisms need an operational voltage that is relatively high compared to other cell manipulation techniques, especially for lysing bacteria. Microelectro-devices have dealt with this limitation mostly by reducing the inter-distance of electrodes. The technique has been realized in tiny flow-through microchips with built-in electrodes in a distance of a few micrometers which is in the scale of cell size. In addition to the low throughput of such devices, high probability of blocking cells in such tiny channels is a serious challenge. We have developed a cell lysis device featured with aligned carbon nanotube (CNT) to reduce the high voltage requirement and to improve the throughput. The vertically aligned CNT on an electrode inside a MEMS device provides highly strengthened electric field near the tip. The concept of strengthened electric field by means of CNT has been applied in field electron emission but not in cell lysis. The results show that the incorporation of CNT in lysing bacteria reduces the required operational voltage and improves throughput. This achievement is a significant progress toward integration of cell lysis in a low-voltage, high-throughput LOC.

We further developed the proposed fabrication methodology of micro-electro-fluidic chips, described earlier, to perform electroporation of single mammalian cell. We have advanced the method of embedding CNT in microchannel so that on-chip fluorescent microscopy is also feasible. The results verify the enhancement of electroporation by incorporating CNT into electrical cell lysis. In addition, a novel methodology of making CNT-embedded microfluidic devices has been presented. The embedding methodology is an opening toward fabrication of a CNT-featured LOC for other applications.

Acknowledgements

I hereby acknowledge all the efforts have been taken in order to educate me during my life. The efforts are contributed by my parents, family members, my teachers from elementary schools to graduate universities, and many others whose relation with me had impact on my thoughts and understandings of life. This PhD work would have never been accomplished without the kind support from my supervisor, committee members, lab-mates, office-mates, family members and many of friends.

First and foremost, I express my deep sense of appreciation to my supervisor, Prof. John Yeow, for all of his technical supports and kind supervision. In addition to the technical/scientific leanings I acquired from him, I have gained a variety of problem-solving tactics that can be applied in other aspects of my life.

I would like to sincerely thank members of the committee in my comprehensive examination and PhD defense; Professor Maud Gorbet, Professor Abdel-rahman Eihab and Professor Michael Tam for their valuable hints and suggestions. I should also thank Professor Nasser Mohieddin Abukhdeir and Professor Sushanta Mitra from University of Alberta for accepting to be my examiners in my thesis defense, and for their precious suggestions and comments for the revision of my thesis.

I should thank Prof. Pu Chen and his nice grad students for helping me in the biological part of my research and for providing me with mammalian cells; many thanks to Ms. Ran Pan, Ms. Baoling Chen (Sophie) and Dr. Mousa Jafari. In addition, a thank you to Professor Perry Chou for his permission to access their lab for culturing bacteria.

My lab-mates are my best friends who have had remarkable impact on my research. My deepest thanks go to Manu Pallapa, Morteza Ahmadi, Zhenhao Li, Shruti Nambiar and all other labmates for their kind supports and for making Micro/Nano Device lab such a friendly environment.

I owe my thanks to the co-op and internship students who worked for my projects. Their contribution to my research is appreciable. Good luck Kevin Joseph, Frans van Wijngaarden and Josh Reid! I wish all of you the best.

Moving to a large room-as my new office- opened up a great opportunity for meeting new students who soon became my close friends. At the times the research did not proceed well, these office friends have been the best people to sit with, have tea, relax, discuss and receive their positive encouragement along with some valuable comments from diverse points of view. Many thanks to Mahyar Vajedi, Reza Razavian, Maryyeh Chehresaz, Amir Taghavipour, Mehdi Jalalmaab and all other UW friends for making my PhD life more enjoyable.

I express my deepest appreciation sense to my families, my parents, my wife, Fatemeh, my sisters, Malihe and Motahareh and my brother, Mohsen. I am still learning from you how to make fun out of problems!

Dedication

To my parents

Table of Contents

List of Figures

List of Tables

List of Acronyms

Acronyms	Description
cDNA	complementary DNA
CHO	Chinese Hamster Ovary
CNT	Carbon Nanotube
DNA	Deoxyribonucleic acid
dsDNA	double-stranded DNA
FEP	Fluorinated Ethylene Propylene
ITO	Indium Tin Oxide
LOC	Lab on a chip
LB	Lysogeny Broth
MEMS	Microelectromechanical System
mRNA	Messenger RNA
MWNT	Multi-walled Carbon Nanotube
PCR	polymerase chain reaction
PDMS	Polydimethylsiloxane
PMMA	Poly (methyl methacrylate)
PZT	Piezoelectric transducer
SWNT	Single-walled Carbon Nanotube

Chapter 1

Introduction

1.1 Overview

Researches in the field of molecular biology and genetics have increased dramatically in recent decade. Much of the efforts in those areas are dedicated to developing efficient ways of preparing biological samples for a particular analysis. In general, sample preparation consists of transportation, separation, cell lysis, purification and detection processes employed for targeted sample analysis.

Cell lysis is one of the initial steps of sample preparation procedure. Cell lysis refers to the process through which cell membrane is disrupted and the intracellular components including DNA, RNA, proteins and organelles are released.

Prior to performing cell lysis, sample cells must undergo different treatments to be prepared for lysis in a desired location. When cell lysis procedure is complete, the released components will be directed to the next stages where the specific components of interest will be detected among and separated from other useless debris. Depending on the sensitivity of the detection system, some lysis products may need to be amplified prior to detection. In conventional methods, each step needs its separate device which is usually bulky and its operation is usually labor-intensive. Consequently, the whole process is accomplished only in specific equipped laboratories with trained technicians and through time-consuming processes.

Development of Microelectromechanical Systems (MEMS) has opened a new window to sample analysis experiments where those bulky laboratory instruments can be scaled down and integrated into one chip. This subset of MEMS, which is referred to as lab-on-a-chip (LOC) technology, makes it possible to compact point-of-care testing in a portable and automatic device. Such portable,

compact, automated biosample analysis devices are, in fact, miniaturized clinical laboratories that have enormous advantages over traditional methods including:

- Potential to integrate different functional devices into one chip;
- Reduction in required samples as well as reagents/waste;
- Faster processing time since several processes can be run at the same time;
- Automation and portability;
- Capability of microfluidic cell manipulation process;
- Possibility of analyzing a single cell.

The feasibility of sample preparation procedures in LOC is a challenge toward developments in on-chip molecular diagnostics. As an example, centrifugation is repeatedly used in biological treatments but it is not normally amenable to LOC. Therefore, the traditional approaches have to be replaced by new techniques whose establishment leads the development.

The main goal of the sample preparation project in our group in Micro/nano Devices Lab at University of Waterloo is to develop LOC systems capable of performing cell treatments required for preparing molecular components. The research project is split into sub-projects including particle/cell movement/separation, cell lysis, Polymerase Chain Reaction (PCR) and integration of these processes into one chip. The focus of this thesis is on developments of LOC devices particularly for cell lysis. Cell lysis, in our scheme, is the mechanism to lyse the cells that are hypothetically separated from debris. The products of cell lysis are the intercellular components for subsequent processes, such as PCR. We have considered the fact that the developing cell lysis devices intend to be integrated with other on-chip functions as straightforwardly as possible. In addition, novelty, simplicity and affordability of the proposed fabrication methodologies are taken into our considerations.

1.2 Research objectives and outline of the thesis

The goal of this research is to develop electrical cell lysis devices suited for LOC technology. Two overall objectives of the thesis are as follow:

i) Developing a fast and straightforward fabrication methodology for making electro-microdevices for cell lysis.

ii) Overcoming the high voltage requirements as the main barrier toward integration of electrical cell lysis with other on-chip systems, by incorporating carbon nanotube into electrical cell lysis.

The thesis content is outlined as follows:

Chapter 1 introduces cell lysis through the MEMS point of view.

Chapter 2 covers a comprehensive review over the wide range of cell lysis methods classified into four groups: mechanical, physical, chemical, electrical as well as combined methods. The review explains common advantages and disadvantages of each group. Treatments prior and after cell lysis as well as various cutting edge techniques employed in "single cell lysis" are also reviewed. The chapter envisions the future direction of on-chip cell lysis developments.

Chapter 3 presents a novel methodology for fabricating electrical microfluidic chips for single cell electroporation. We introduce a new methodology of fabricating microchannel with electrical functionalities achieved through fast and cheap processes. The performance of the chips has been tested on electroporation of single mammalian cells.

Chapter 4 reports on the effects of carbon nanotube on electrical lysis of bacteria. Voltage reduction and throughput enhancement are presented as the main benefits of incorporating CNT into electrical cell lysis.

Chapter 5 presents application of CNT in single cell electroporation. A new fabrication methodology for making CNT-embedded microchannel is introduced and the enhancement of mammalian cell electroporation by the use of CNT is explored.

Chapter 6 concludes the results of the research and summarizes the presented contributions. Directions for future works are presented in this chapter.

Chapter 2

Literature Review

2.1 Introduction

MEMS-based sample preparation techniques for molecular diagnostic have been reviewed widely [1–5]. A comprehensive review on recent achievements in lab-on-a-chip (LOC) technology under the wide title of micro total analysis systems is also available in literature [6].

We narrow the focus of this chapter to concentrate on only those techniques which specifically involve cell lysis. MEMS contributions to cell lysis methods are our interest in this chapter. We classify cell lysis methods into physical, mechanical, chemical, electrical methods as well as any combination of these methods. Traditional techniques of cell lysis associated with each class are first introduced along with their limitations and drawbacks. Then the techniques that are appropriate to on-chip integration are discussed in details and advantages and disadvantages of each classification are evaluated individually and in comparison with the other classes. A brief introduction of single-cell lysis and nucleic acid purification techniques are presented. Finally, future direction of this field of research is discussed.

2.2 Cell lysis techniques

Cell lysis involves mechanisms in which the cell membrane is broken apart and intracellular components are released into surrounding medium. The intracellular components such as DNA, RNA and proteins are the main products of cell lysis.

2.2.1 Pre-lysis sample treatment

Depending on the sample complexity and the lysate of interest, some treatments need to be accomplished prior to cell lysis. Pre-lysis treatments are required to isolate the target cells out of the complex matrix and remove those particles that interfere with the cell lysis or downstream processes. The treatments consist of several processes such as sample filtration, centrifugation, pre-concentration, dilution, target enrichment, etc. that are yet mostly performed off-chip due to their incompatibility with analytical instruments [7]. Raw samples such as whole blood are usually complex and separation of target cells out of them on chip is challenging. Conventional sample separation techniques cannot be readily scaled down to microchip devices due to the extent of hands-on tasks that they demand. For example, there has not yet been devised a chip to mimic the functionality of centrifugation, a method widely used for cell separation. However, some novel on-chip mechanisms for pre-lysis treatment have been developed.

Microfabricated filters are presented for on-chip sample filtration [8]. The micropillar gaps inside the flow-through system restrict cell movement, separating and trapping the cells based on their size. Dielectrophoresis (DEP) has been widely employed for cell separation based on the physical principle that dielectric particles experience force while exposed to a non-uniform electric field [9–12]. Dielectric particles can also be manipulated with optical tweezers instrument while focused laser beam provides with either attractive or repulsive force exerted to dielectric particles [13]. Sample derivatization refers to the chemical transformation in cells prior to analysis that make them detectable or suitable for analysis system. It is mostly achieved with fluorescent labels that tag to the cells and make them colored compounds and suitable for optical detection. Depending on the sensitivity of the detector used in the system, sometimes sample pre-concentration is required prior to detection step in order to

increase the number of sample molecules to be more detectable. A review of on-chip sample treatments prior to cell lysis has been presented by Lichtenberg et al. [14].

Upon separation of target cells through sample pre-lysis treatments, a variety of methods can be used to break apart the membrane of cells. In terms of the principles employed for cell disruption, the methods developed for cell lysis are classified in four groups: mechanical, physical, chemical and electrical. It should be noted that no well-defined boundaries can be considered between the above-mentioned groups. In many approaches, a combination of two or more methods is used. In what follows, we describe each of these methods and discuss their characteristics.

2.2.2 Mechanical methods

Mechanical method refers to cell disruption technique which is based on exerting shear stress or pressure difference across the membrane. The force is exerted on the cell as a consequence of physical contact between the cells and agitating agents such as beads.

Conventional methods- There is a wide range of mechanisms in macro scale to apply shear stress or mechanical force on cell membrane. Mechanical cell lysis has been traditionally carried out by high pressure homogenizer [15,16] or high speed bead mills [17,18].

The high pressure homogenizer consists of a high-pressure pump and a lysis chamber. The cell suspension with quantities as large as 500 ml up to even 5 liters is forced to pass through a channel at a relatively low speed but high pressure. The stream then passes through a tiny gap whose size is adjustable by a discharge valve. Thorough this gap, the pressure drops suddenly and the speed increases in return. The homogenized suspension of lysed cells is collected in the lysis chamber afterwards. Although the sudden pressure drop across the discharge valve is reported to be the main

factor of disrupting cells by high pressure homogenizer, the multiplicity of forces including shear, cavitation and impingement is involved in such conventional mechanical cell lysis [19,20].

Bead mills systems consist of a double walled grinding chamber and a rotating shaft located centrally inside the chamber. Some grinding elements are patterned on the outer side of the shaft making a helical array. The cell suspension mixed with tiny beads is loaded into the chamber. The high speed rotation of the shaft exerts shear force between liquid layers and causes collisions between cells and agitating beads. The shear forces and agitation lead to mechanical cell lysis.

On-chip methods- Depending on the mechanism by which the shear forces are produced, mechanical cell lysis can or cannot be implemented on chip. For example, techniques such as milling [21], inevitably need moving parts that are challenging to be miniaturized. Nevertheless, microfluidic chambers that function based on mechanical cell lysis have been made. An example is cell lysis via spherical beads in a microfluidic chamber in a compact disk (CD) [22]. In this pure mechanical cell lysis method, an annular microfluidic channel was patterned on a Polydimethylsiloxane (PDMS) sheet using standard soft lithography techniques. The sheet was sandwiched between two polycarbonate disks building the CD. This is illustrated in Figure 2-1a. The beads are uniformly coated on the outer wall of the chamber. While the CD is spinning, the cells are lysed due to collision and impulse between cells and beads. The large cells such as mammalian cells (about 10 µm in diameter), small sample cells such as bacterial cells and hard-to-lyse cells such as yeast cells have been successfully lysed by the device. However, the large set-up requirement to provide rotational power to the CD (Figure 2-1b) is not suitable for LOC systems that are desired to be compact and portable.

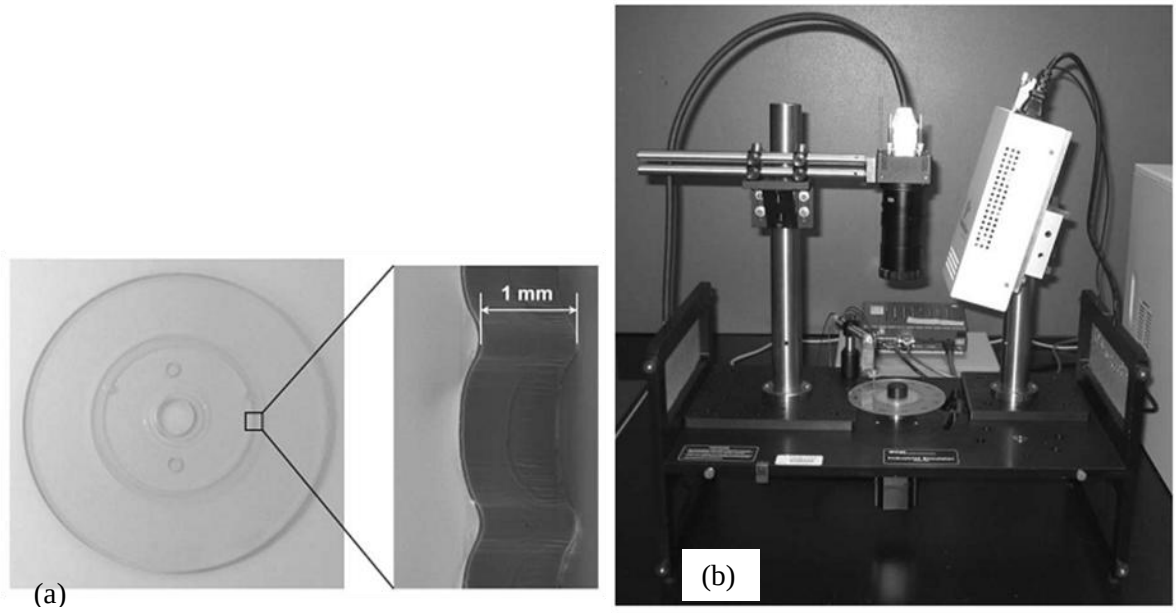

Figure 2-1 a) Mechanical cell lysis device through microfluidic channel designed in a CD. The CD spins forward and backward alternatively and the aqueous medium containing sample cells and glass beads were injected into the lysis chamber meanwhile the CD is at rest. The beads are uniformly coated on the outer wall of the chamber. The inner wall is designed wavy to get cells to stay longer there, interacting with bead particles more efficiently. b) Set-up for mechanical cell lysis via CD [22]

To avoid moving part supplies, mechanical methods in LOC are commonly limited to those integratable onto nano-sharp elements or microfluidic gaps through which sample cells are forced to pass by pump. As an example, Carlo et al. [23] efficiently lysed HL-60 and red blood cells through a microfluidic channel with nano-scale knives. The lysing gate of the device is schematically shown in Figure 2-2a-b. Figure 2-2c illustrates sharp nano-knives that have been patterned on the lysing surfaces. These nano-knives enhance cell lysis by exerting shear stress on passing cells.

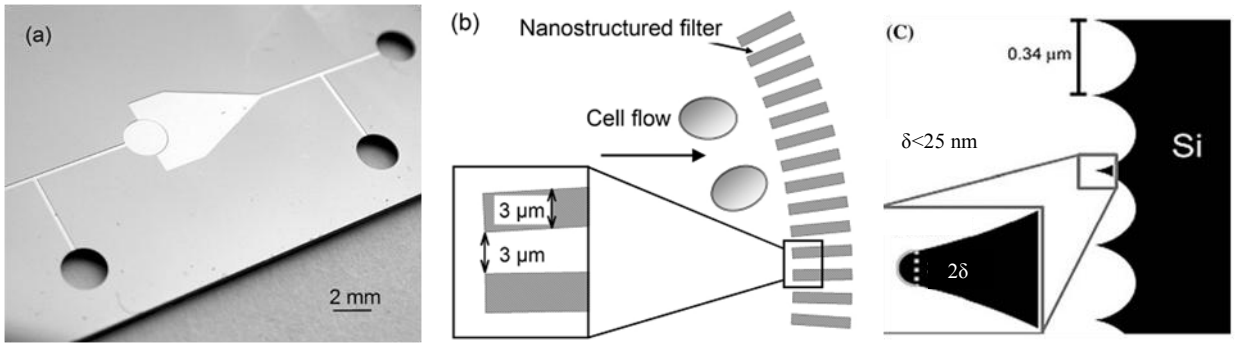

Figure 2-2- a) Mechanical cell lysis device. Cells are forced by syringe pump to pass through tiny gaps b) Dimensions of the semicircular microfilter used for mechanical cell lysis. Lysing gate surfaces fabricated by modified deep reaction etching method are vertically in 3µm distance and the gap is 3 mm in width c) Nano-knives patterned on the lysing surfaces [23]

Unlike chemical methods which are presented in section 2.2.4, usually no enzyme or chemicals are added in mechanical methods. Consequently, the mechanical methods do not chemically affect downstream processes. However, since the whole cells are broken in mechanical methods, it disfavors detection of targets including DNA or RNA which are suspended in a complex pool of debris. To achieve a high throughput cell lysis, cells are usually passed through several gaps. This requirement leads to increase in size of equipment which opposes the scope of LOC technology. For systems with flow-through gaps, adequate flow rates as well as very small channel structures are required to exert high enough shear stress on the membranes. So, with such scaled-down channels, clogging is a serious problem which necessitates considerable caution.

2.2.3 Physical Methods

Physical cell lysis methods refer to the techniques that influence physical properties of cells.

2.2.3.1 Thermal Lysis:

Thermal lysis methods make use of temperature effects on stability of cell membrane or thermostability, i.e. high temperature or cyclic heating is utilized [24].

Conventional methods- Thermal cell lysis has been traditionally achieved by immersing the sample tubes into boiling water or incubator for 10 to 30 minutes [25]. The typical temperature used for cell lysis in this technique is 50-100 °C. The period of temperature time should be carefully controlled so that only the membrane of cells is lysed and the nucleic acids remain intact. Thermal lysis techniques are naturally simple and cost-effective. However, this method is not reliable for extraction of intracellular proteins since proteins cannot stand high temperatures and they might be denatured before cell membrane is disrupted. Therefore, thermal lysis is limited to the applications whose products can safely stand such temperatures.

Boiling lysis is very common in releasing plasmid DNA from bacteria. The conventional protocol of boiling lysis which is used to provide bacterial plasmids is presented by Holmes et al. [26]. In this technique, bacteria were boiled for less than one minute after some agents were added to them. These agents were responsible for weakening bacterial cell wall prior to boiling process, facilitating the process of cell disruption at a lower temperature. The protocol has been modified several times to improve cell lysis efficiency and the yield of plasmid DNA [27–30]. The protocols require centrifugation process for debris removal after cell lysis. This requirement imposes a barrier on integration of the process into miniaturized on-chip devices.

Thermal cell lysis is commonly used in polymerase chain reaction (PCR) process through which the copies of released DNA strands are amplified after cell lysis. This is usually performed by cyclic heating and cooling processes. In PCR machines, the thermal protocol of lysis is programmed prior to PCR protocol. Belgrader et al. [31] used Advanced Nucleic Acid Analyzer (ANAA) to lyse the cells prior to PCR process. Using ANAA, they preheated sample cells at 96 °C for 15 minutes at real-time PCR. PCR-based thermal cell lysis is also realized in miniaturized devices as follows.

On-chip methods- In on-chip integration of cell lysis with PCR, the microfluidic chip is entirely put into cyclic heater [32]. The cell lysis heating time is added to the basic protocol of PCR in order to release DNA. The products is collected by a sieving medium and electrophoretically separated in terms of their size. One of the other successful integration of cell lysis and PCR is the fully integrated microchip developed by Liu et al. [33]. As illustrated in Figure 2-3, the LOC device consists of mixers, valves, pumps, channels, chambers, heaters, and sensors that are all integrated in one microchip. The target cells are pre-concentrated in the PCR chamber. The cells are thermally lysed prior to PCR cyclic heating through which the DNA sequences are amplified. Heat treatment here has been achieved by a resistive heating element attached to the PCR chamber. Piezoelectric transducer (PZT) has been used to mix the liquid solutions through the cavitation microstreaming phenomenon [34].

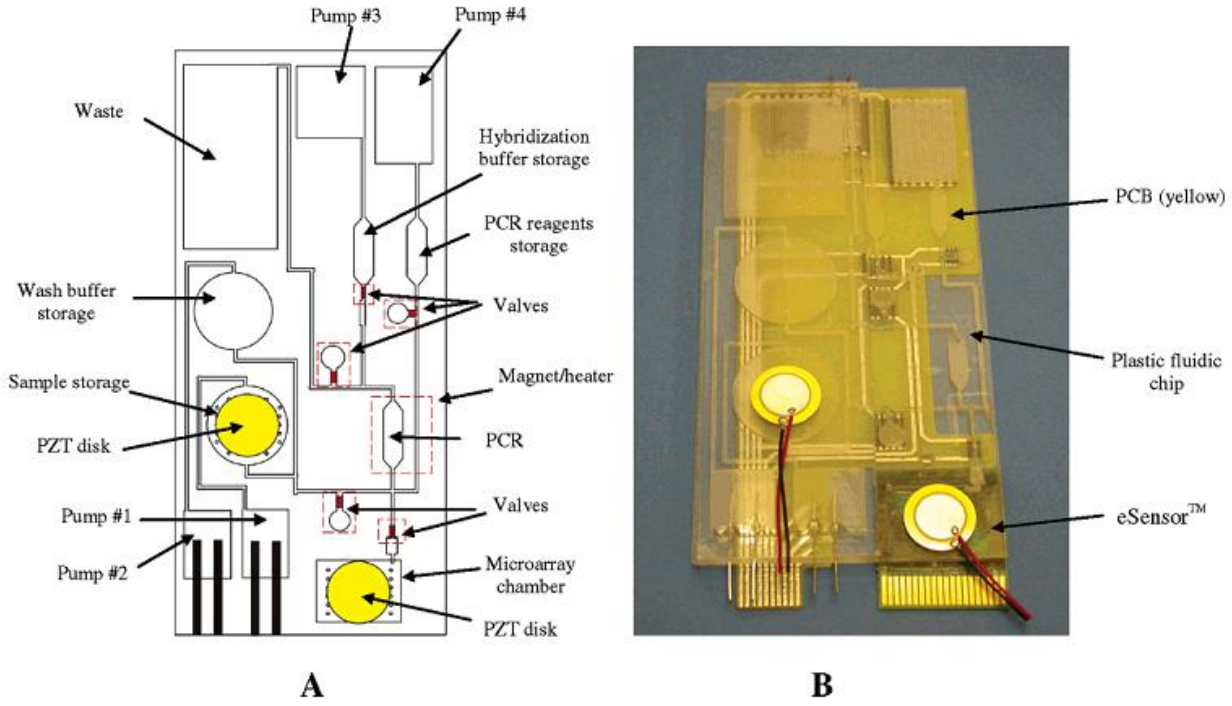

Figure 2-3 On-chip sample preparation device integrated cell lysis with PCR. A) Schematic view of microfluidic biochip consisting of mixers, valves, pumps, channels, chambers, heaters, and DNA microarray sensors. B) A snapshot of the biochip device [33].

2.2.3.2 Osmotic Lysis

Osmotic Lysis (Cytolysis and Plasmolysis) is categorized under physical method. In this technique, the osmotic pressure exerted on the membrane is imbalanced by sudden change in concentration of the surrounding medium. For cytolysis or plasmolysis, the target cell is enclosed by hypotonic or hypertonic medium, respectively. In cytolysis, excess water diffuses through membrane causing increase in osmotic pressure and, consequently, increase in volume of cell. If the membrane cannot

stand the exceeded capacity, it is disintegrated. In contrary, for plasmolysis, the osmotic pressure is decreased when cell loses too much water.

Conventional methods- Osmotic lysis has been traditionally performed by introducing some membrane pore formers such as staphylococcal α-toxin and cytolytic T-cell perforin to cell medium [35]. This method works based on the fact that cytolytic perforin, the pore-forming protein of cytotoxic T cell (CTL), creates nano-scale channels across the membrane [36].

On-chip methods- Literature contains some instances of fabricated cell lysis chips that operate using osmotic method. Commonly, those chips employ osmotic principles in conjunction with other methods.

Augmentation of osmotic lysis, as a physical method, along with mechanical lysis has been reported [37]. In this approach, the cells are principally lysed by shear stress when passing through tiny gaps. Additionally, hypotonic medium surrounding the cell facilitates the lysis by causing the cells to swell, resulting in higher shear stress through the passage.

Feril et al. [38], too, have taken advantage of cell enlargement in hypotonic medium. They have integrated this idea into an ultrasound-based cell lysis. This combination has two advantages: first, the swollen cells are bigger targets to be struck by ultrasound waves. Second, the tension between components of the membrane of the low-density, high-volume cell is dramatically higher, making the cells more susceptible to ultrasonic damage.

Prinz et al. [39] have applied osmotic lysis to lyse bacterial cells in a microchannel. The principle of the phenomenon is illustrated in Figure 2-4. The cells are directed to the T-junction lysis zone where the introduction of deionized water to the pre-weakened E. coli cells makes the cells to absorb water, swell and rupture. The weakening pretreatment is done by breaking down the peptidoglycan layer

between the inner and the outer membranes of the bacteria that otherwise would resist against the osmotic shock.

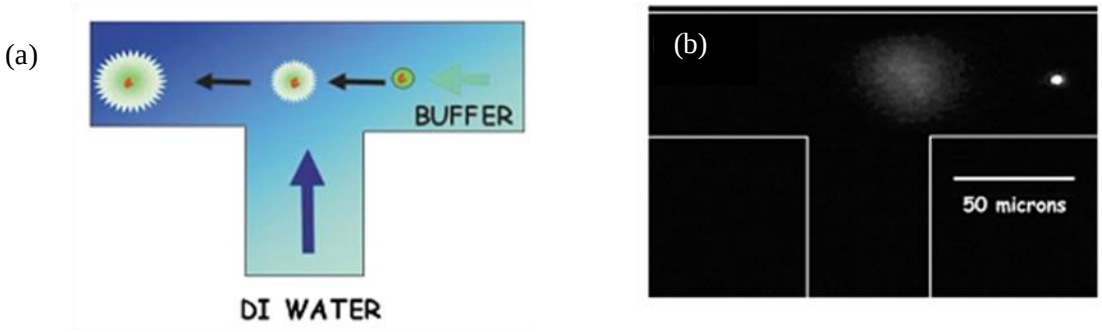

Figure 2-4 a) Illustration of an osmotic lysis microchannel, b) Images of E. coli cells while passing the lysis T-junction lysis zone [39].

2.2.3.3 Ultrasonic cell lysis

Ultrasonic cell lysis, which can also be considered as a thermal method, utilizes ultrasound waves or sonication as the source of required energy. In this method, sample cells enclosed by liquid medium are exposed to high-intensity focused energy of ultrasound. The effects of ultrasound waves on viability of living organisms have been examined extensively for many years [40,41], however the underlying principle of the reaction is not still fully understood. What plays the main role in cell disruption seems to be the generation of microbubbles which are powered by concentrated pulsed ultrasonic waves. The rapid compression and expansion of the microbubbles exerts such great shockwave on the membrane that breaks membrane integrity.

Conventional methods-In traditional ultrasound lysis system, the ultrasound power is provided by a resonant probe which is immersed into suspension of sample cells. The suspension is kept at a cylindrical vessel which is in turn placed in a mixture of ice and water to cool down the suspension during the process. Acoustic power applied to the medium will results in growth and collapse of micro bubbles during the rarefaction phase of the sound waves causing subsequent pressure on cells that leads to cell rupture [42].

Cells are required to be located as an optimum distance from the probe in order to be lysed. This criterion adds a restriction to the volume of the suspension containing sample cells in conventional ultrasonic method due to the difficulty in transferring sufficient power to bulky volume of cells. This restriction does not apply to ultrasonic cell lysis in microfluidic chip.

On-chip methods- Ultrasonic utilization has been broadly implemented into microfluidic cell lysis chips [43–46]. In these applications, the sonication is produced either by an external transducer or by a built-in piezoelectric film. In both methods, the acoustic energy must be highly concentrated in a small zone [47,48]. The external transducer delivers sonic pressure waves to the flexible surface of the flow-through channel, causing creation of micro-bubbles that leads to cell lysis. Piezoelectric transducers made of zinc oxide are deposited on the floor of microchannel. The transducers are driven by a sinusoidal source in the frequency as high as the resonance of the transducers so that the acoustic power exerting to the cell medium is amplified. Consequently, cavitation along with heat generation inside the microchannel leads to cell lysis [47].

The fabrication process for the built-in piezoelectric-based lysis is more complex than using external transducers. Through external sonicators, however, the horn tip of transducer has to be in physical contact with lysis chamber wall in order to induce pressure waves. The complete transmission of energy through interface between transducer probe and liquid medium is a challenge in this approach.

The outstanding feature of ultrasonic lysis is the capability of concentrating a high density of energy into a small lysis chamber inside the microchannel. Commercial transducers, as depicted in Figure 2-5, can be employed out of the device to focus ultrasonic irradiation into a very small scale of the lysis area [48].

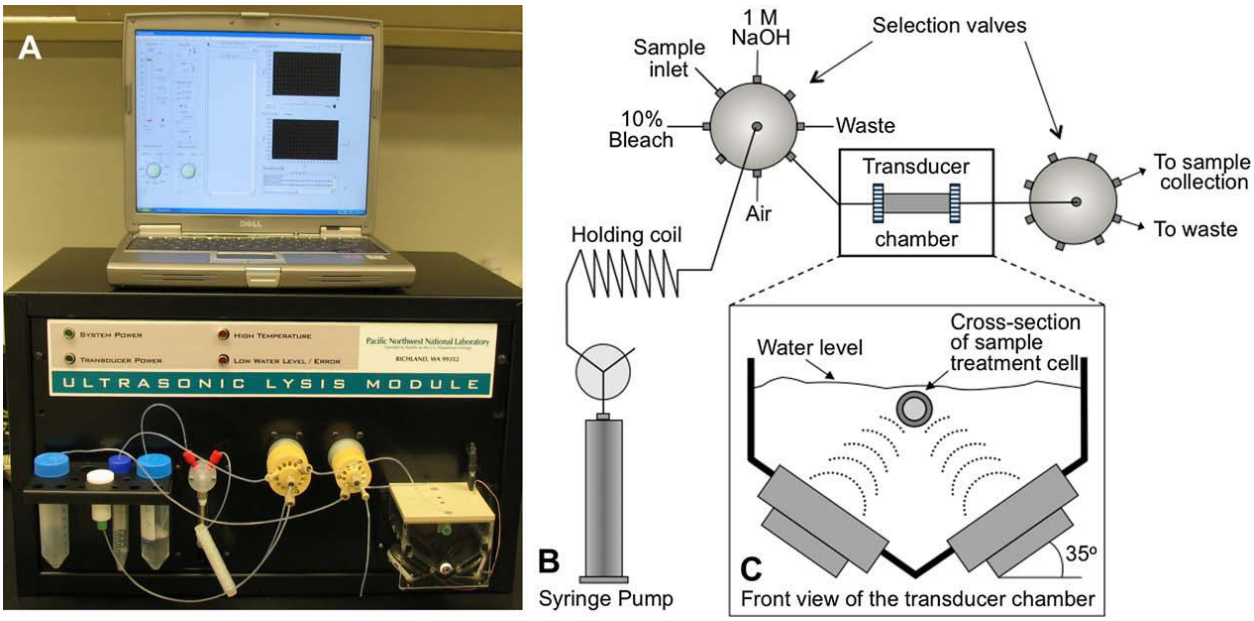

Figure 2-5a) Control system for automated cell lysis device b) schematic view of the flow-through ultrasonic lysing device c) orientation of transducers employed for ultrasonic lysis. A flow rate of 1µl/s is acquired by a syringe pump and the sample cells and other chemicals are added through selection valves. The flow-through tube is faced in parallel to two commercial transducers that exert the power of 10 W/cm2 to the tube at the frequency of 1.4 MHz [48].

The high temperature gradient in sonication systems should be taken into caution. However, the high temperature is not an issue for entire device since high energy concentration is localized only in a small region of lysis. This is favorable for the devices with some temperature-sensitive parts that

cannot endure high temperature of thermal lysis. Ultrasonic cell lysis can be implemented in such devices as an alternative for thermal lysis. Unlike chemical methods which are discussed in the following section, continuous cell lysis without a need to add any chemical can be achieved by ultrasonic cell lysis, leaving the suspension clean from any disturbing substances. Thanks to the high intensity of energy delivered to cell memberane, ultrasound methods are the best candidate for lysing hard-to-lyse sample cells such as eukaryotic cells and bacterial spores [47].

Each of the above-mentioned physical techniques suffers from some drawbacks when used alone. Therefore it is desirable to use each in conjunction with the other methods in one chip. As an example of combination of physical and mechanical methods, Khanna et al. [49] have assisted ultrasonic cell lysis by incorporating Nanocrystalline Diamond (NCD) micro spikes. As depicted in Figure 2-6a, the bottom floor of the microfluidic chamber is covered by sharp NCD micro spikes. Cell lysis of an equal number of murine melanoma cells has been repeated in three sets of experiment. Figure 2-6b compares efficiency of the cell lysis in three methods: i) control unit (only micro spike), ii) plain unit (only ultrasound) and enhanced unit (both ultrasound and micro spike). This figure clearly indicates that the combination of the two techniques has significantly increased cell lysis rate.

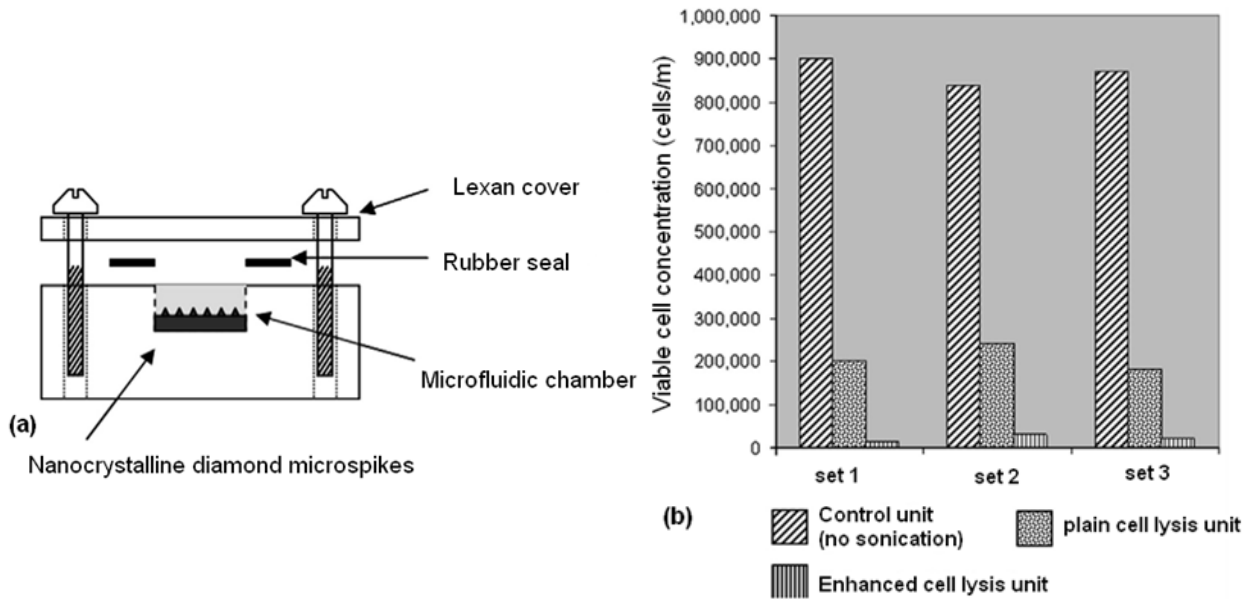

Figure 2-6- a) ultrasound-assisted cell lysis by nanocrystalline diamond microspikes b) Concentration of viable cells for different sets of experiment [49]

2.2.4 Chemical Methods

In chemical methods, membranes of cells are disintegrated by adding proper reagents to samples. The added reagents dissolve the membrane or increase permeability of the cell wall. Enzymatic lysis [50] can be considered as a chemical method where some enzymes are responsible to digest the wall of the target cells. Another sample of chemical method is viral lysis where specific viruses or bacteria are introduced to cells and they take on the task of disrupting cell membranes.

Conventional methods- Acid and alkali lysis have been traditionally employed to disrupt cells. In acid hydrolysis, concentrated acids such as HCL or H_2SO_4 at temperatures of 55 to100°C are

responsible to either rupture cells or extract intracellular components within 6-12 hours [51]. As an example, treatment with NaOH results in hydrolysis and solubilization of cell envelope, that in turn weakens or disrupts cell walls [52]. Sodium dodecyl sulfate (SDS), tweens, and triton X-100 have been traditionally employed for cell lysis [52]. These detergents disturb interaction of lipid and proteins of the cell membrane resulting in solubilization of the membrane components.

On-chip methods-Microfluidic channel networks can be employed to introduce lysing detergent to target cells. In this approach, sample cells and lysing chemicals are directed separately to the lysis chamber through Y-shaped or H-shaped or from different microchannels by electrophoresis or syringe pump. They then blend inside the lysis chamber where the membrane of cells is disrupted and intercellular components are released. A variety of lytic chemicals is often used for this purpose such as toluene, ether, phenylethyl alcohol, DMSO, benzene, methanol, and chloroform [2]. Sodium dodecyl sulfate (SDS) [53] and Triton X-100 [54] are also utilized for chemical cell lysis.

Carlo et al. [55] have reported a system which is able to release both DNA and protein by using hydroxide ion as a lysing reagent. As illustrated in Figure 2-7a-b, a filter unit lysis is sandwiched between two palladium electrodes placed with 600μm separation distance. The applied electric field of 43V/cm is strong enough to hydrolyse water, producing OH^- at the cathode and H^+ at the anode due to the following reactions:

$$in\ cathode: 4H_2O + 4e^- \leftrightarrow 4OH^- + 2H_2$$

$$in\ anode: 2H_2O \leftrightarrow 4H^+ + 4e^- + O_2$$

As depicted in Figure 2-7a-b, sample cells introduced into the lysis unit from the bottom are lysed due to the reaction illustrated in Figure 2-7c. The membrane phospholipids are cleaved and lysophospholipids are created. The cell is finally disrupted due to change in permeability of its membrane. The role of hydroxide ions in cell lysis enhancement is so significant that the cells are lysed even in regions with no electric field.

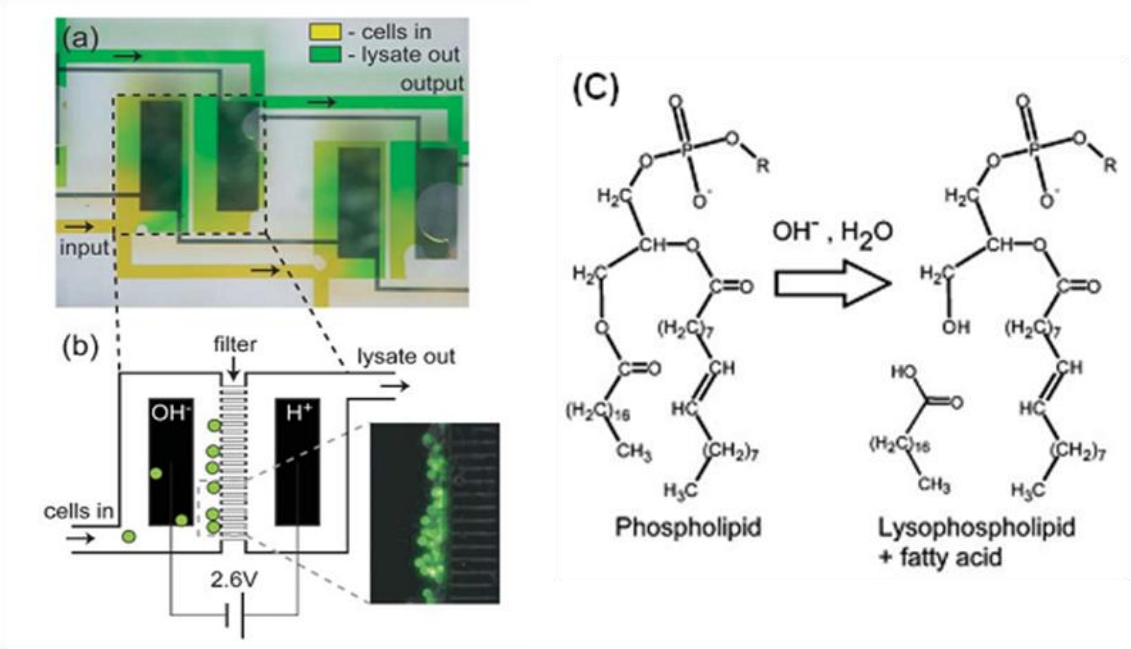

Figure 2-7- a) A view of two lysing chambers of hydroxide cell lysis device b) Schematic view of a lysing chamber c) Cleaving of membrane phospholipids by reaction with hydroxide [55]

Separation and detection of lysis products among cell suspension mixed with lysing chemical is a major challenge in chemical lysis methods. Fractionation can be employed for separation of mixing molecules based on their size. Schilling et al. developed an on-chip chemical cell lysis system integrated with fractionation process of released intracellular proteins [56]. The microfluidic channel

network, schematically displayed in Figure 2-8, was to introduce lytic agent to cell suspension separately through left and right side of the lysis chamber. Since molecules are large, they do not diffuse into the lytic agent stream and remain on the left side. The lytic agent, however, diffuses rapidly into the cell suspension and lyses the cells. Then the extracted intracellular components that have a smaller size would be able to diffuse freely to the right half side. At the end of the lysis chamber, the large molecules along with cell fragments flow out of the lysis channel. The targeted components that reach the detection chamber are introduced to detection molecule, such as a fluorogenic substrate. Bacterial cells are lysed by the device and an intracellular enzyme is detected and quantified through fluorescent enzyme assay [56].

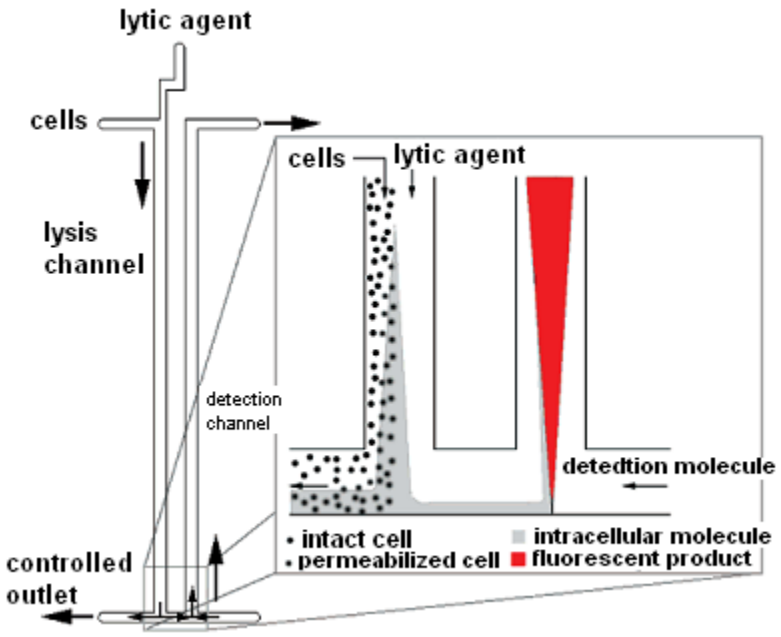

Figure 2-8 Schematic view of the chemical cell lysis microfluidic device [56]

The big drawback of enzymatic and chemical methods is the complexity of removal of the detergents, enzymes or reagents which will otherwise interfere with the following processes. Although chemical lysis techniques are usually suffering from long-time processing, especially by non-ionic detergents, they are still widely used. Thus, the purification and gene amplification steps in chemical methods are generally far more complex than other methods. The inherently slow chemical procedure becomes even slower with the fore-mentioned additional considerations for purification requirements. To diminish this disadvantage, usually a combination of different methods is more favorable. Examples of this combined method will be presented later.

2.2.5 Electrical Methods

In electrical cell lysis method, sample cells are exposed to an external electric field. Since electrical techniques create nano-sized pores across the membrane that makes membrane permeable to the outside medium, electrical cell lysis is also called *Electroporation* or *electropermeabilization*. Although electroporation has been investigated for a long time [57], the underlying physics of the electroporation process is not still well understood. One hypothesis is that cell lysis occurs due to potential difference across the membrane that causes the build-up of ions across the membrane. If this potential difference which is called transmembrane potential increases, the ions squeeze the membrane and reduce its thickness. If the applied electric field is strong enough, nano-pores create paths between the external-internal cell medium [57].

Electroporation process can be either reversible or irreversible. Reversible electroporation is used when permeability of the membrane is increased but the membrane lipids return back to their natural state once the electric field is removed. Irreversible electroporation is achieved when the applied

electric field is so strong that the induced transmembrane potential surpasses a threshold value. Then the imbalanced osmotic pressure makes the membrane lose its integrity.

Conventional methods- Electrical cell lysis has been traditionally achieved by applying an operational pulse voltage as high as 2000 V on E. coli cells. The cells are stored in cuvettes that are exposed to the electric field exerted through stainless steel [58]. The main barrier to using electrical techniques is the high voltage requirements for cell lysis that limits the incorporation of electrical systems onto LOC technology.

On-chip methods- Several solutions have been reported to reduce the required voltage in order to make the electroporation feasible on LOC devices. One idea is to create a local high voltage by narrowing the small gate through which the cells are to be lysed. Cells in the technique proposed by Lee et al. [59] pass through a narrow orifice whose width and length is 20 times shorter than the micro channel, as shown in Figure 2-9. With a 50 V DC as the operational voltage, the electric field at the orifice part will reach the strength as high as 1.2 KV/Cm. This electric field condition is enough to disrupt cells with 100% lysis rate.

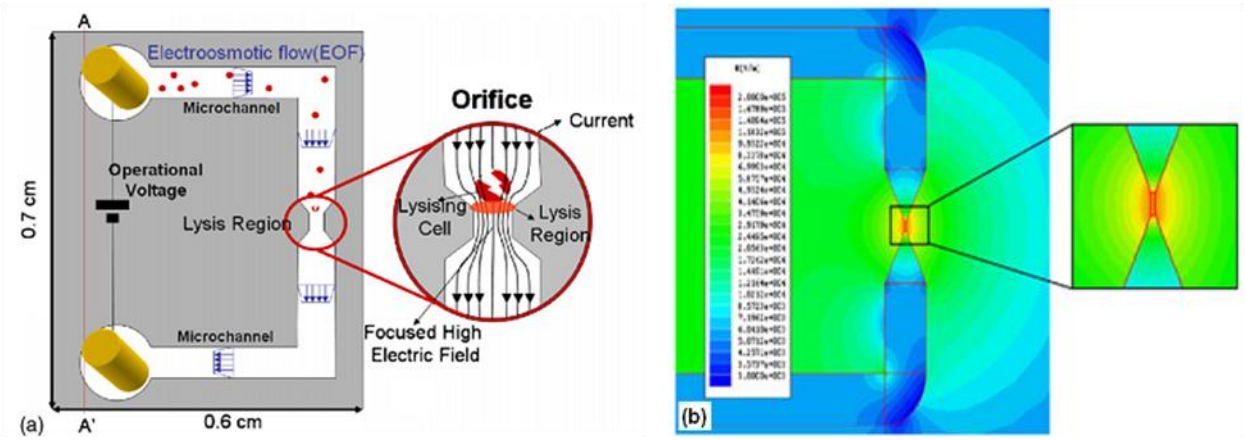

Figure 2-9 a) Schematic of microfluidic channel with lysing orifice b) Simulation of the strength of the applied electric field [59]

Figure 2-10 is an illustration of the device created by Lu et al. [60] to lyse human carcinoma cells. The saw-tooth electrodes apply non-uniform electric field in the microfluidic channel while the strongest field is at the tip of electrodes. It is found that cell lysis can be achieved with operational voltage of less than 10 V when the tip-to-tip distance is 30 μm.

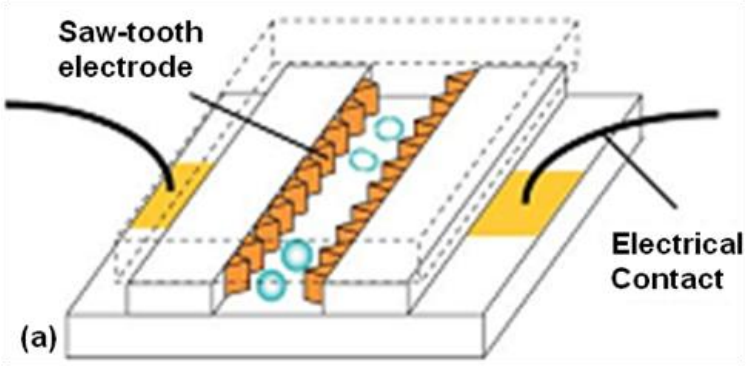

Figure 2-10- Electrical cell lysis device with Saw-tooth electrodes [60]

The high electric field required for lysis of smaller cells can also be achieved in these electrical schemes. But, it imposes shortening the inter-distance of electrodes which is not favorable in microchannels. In addition to the costly fabrications, such flow-through channels are likely to be blocked at their tiny gaps.

A successful 3-dimensional structure for electrically lysing virus has been developed by Park et al. [61]. The apparatus captures vaccinia virus particles via positive dielectrophoresis (pDEP) and then lyses them. Pairs of three-dimensional probes are patterned on silicon on insulator wafer in tiny inter-distances of 100 nm to 1.5 μm. As shown in Figure 2-11, the cells are attracted by DEP toward the probe gap where the high electric field of 10^7 V/m is applied through the same probes.

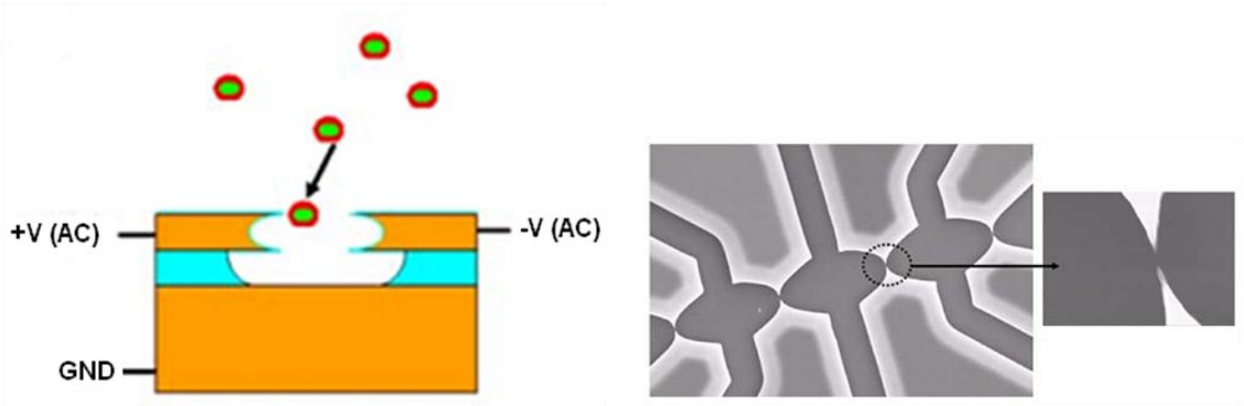

(a) (b)

Figure 2-11 a) schematic front view of the cell capture by pDEP: virus particles are attached to the probe array and electrically lysed b) Top-view SEM image showing the gap between electrodes: the tiny gap between electrodes (100 nm – 1.5 μm) provides very strong electric field (about 10^7 V/m) [61]

2.3 Single Cell Lysis

When a bulky group of cells are examined, the information obtained is usually averaged over a large number of individual cells. Since it has been understood that identical cells are quite likely to be diverse in their chemical composition and their activity characteristics, bulky-cell analysis systems are not able to see such cellular heterogeneities like variability of gene expressions levels and individual cell responses to an external particular stimulus [62,63]. Thus the single-cell analysis techniques have been increasingly taken into interests within the past few years [64]. Categorized in five classes of optical, acoustic, mechanical, electrical and chemical groups, single-cell lysis techniques have been more profoundly reviewed recently [65]. In what follows, a few examples of the works toward single-cell lysis that are implemented on LOC technology are summarized to outline the cutting edge techniques employed for single-cell lysis.

Since microfluidics has the capability of cell manipulation, automation and integration with other functional processes in a very small scale of the sample volume, microfluidics is a first-rate platform into which single-cell analysis processes can be implemented [66–70].

Chemical method is the most popular approach employed for single-cell lysis. It has been accomplished by introducing target cells to lytic agent through Y-shaped microfluidic channel [71] or by suspending the cell-containing medium that is as little as few nano-liters into lysis buffer [72]. As an example of chemical cell lysis achievement toward the analysis of single-cell manipulation, Marcus et al. [69] have developed a single-cell mRNA isolation device platformed on a microfluidic scheme to analyze gene expression in individual cells. The system has integrated cell capture, cell lysis, mRNA purification, and complementary DNA (cDNA) synthesis and purification into one microfluidic device. Using micromechanical valves, the single cells are isolated and then chemically lysed with

lysis buffer. cDNA is synthesized from the subpicogram messenger RNA (mRNA) templates extracted from single cells.

Pulsed laser beam-induced techniques are amenable to single-cell lysis schemes. The cells suspended in a droplet are entrapped inside a microfluidic chamber where the optical transparency of the chamber lets the laser pulse localize precisely onto the area of lysis. Single-cell analysis has been carried out on the target cell that is selectively encapsulated in a pico-liter aqueous droplet and being lysed using frequency-tripled Nd-YAG pulsed lasers (355 nM) with about 5-ns pulse duration [73]. It is challenging to accurately locate the individual cells at the center of the laser beam. And, the cell adhesion to channel may defect the efficiency of the system. However laser-beam induced techniques need no chemical addition and lysing process is relatively fast. Mechanical single-cell lysis is achieved by nano-structured barbs patterned into a microfluidic channel with pressure driven cell flow [23]. The size of the thorough-pass channel has to be in scale of the cell size. It causes structural complexity and increases the cost. Such a-few-micron scale schemes are more amenable to large cells rather than bacterial cells. Sonication by itself does not seem to be suitable for single-cell lysing due to the lysis time requirement that is reported to be longer than 50s for one human natural killer cell [74]. However, ultra-sonication in incorporation with the chemical detergent-based lysis has led to reduce the lysis time to 3s [75]. In contrary, electrical cell lysis method has been employed for rapid single-cell lysis, namely less than 33ms for complete lysis of a mammalian cell by applying a 1 ms pulse length [76]; but it still suffers from relatively high voltage requirement, that is to say 40V for 20-μm inter-electrode distance. The adhesion of cells and lysate to the electrodes is more challenging for single-cell cell lysis systems than the population-cell lysis systems. The coating of some known polymers such as PDMS on the channel walls usually eases the problem. An electrical fast high throughput single-cell lysis has been achieved on microfluidic platform where the cell adsorption has been reduced by adsorbing a polymer surfactant to the channels coated with PDMS [77].

2.4 Nucleic Acid Purification

After cell is lysed, the lysis products need to be collected and separated. Nucleic acid purification is performed to isolate the nucleic acid lysis product out of the debris. Phenol-chloroform extraction is the conventional method through which DNA-containing sample is precipitated with an alcohol such as phenol–chloroform solution, followed by ultra-centrifugation [78]. Since DNA is not soluble in the alcohol, the pellet of DNA is left upon centrifugation. For RNA extraction, guanidinium thiocyanate is added to an acidic solution which is containing sodium acetate, phenol and chloroform. Guanidinium thiocyanate denatures DNA and proteins and separates rRNA from ribosomes. RNA can be separated from DNA and proteins, based on phase separation technique. After centrifugation, all of the RNA is present in the aqueous phase of the acidic solution and DNA and proteins stay either in the inter-phase or in the lower organic phase [79].

Centrifugation requirement is not amenable to microchip technology so that the above-mentioned conventional techniques cannot be integrated on-chip. The developments on on-chip separation techniques have been reviewed recently [80]. Here the platforms of on-chip nucleic acid purification approaches are presented.

Silica-based solid-phase extraction is the primary technique for DNA purification implemented in LOC technology. It is based on the affinity of DNA adsorption to silica-based surfaces in the presence of a chaotropic salt. Chaotropic salt denatures cellular proteins but not DNA or RNA. The high concentration of the salt facilitates binding of the nucleic acids to the silica-based surfaces, while the other components in the lysis debris freely pass the surface. The adsorbed DNA can be washed away by an alcohol out of the device. This technique can be implemented into microfluidic channels with high surface area in contact with sample-containing solution. Oxidized silica-based channels fabricated through deep reactive ion etching [81] and silica pillars that are deeply etched in silicon [82] can

provide the high surface-area-to-volume features for DNA binding. Based on the same concept, silica beads and silica resins have also been employed for purification of DNA [83] and RNA [84]. The purification of nucleic acids implemented into LOC technology has been discussed in more detail in [85].

2.5 Envision the Future Direction of Cell Lysis in LOC

The ultimate target of LOC technology, and the main trend, is to develop a stand-alone system which encapsulates all sample preparation procedures, including cell lysis, together in one single hand-held, easy-to-use device. This of course would be a very attractive tool for biological laboratories in the way it saves them space, cost, and time. The path to reach this destination passes through the intermediate station where the LOC may not necessarily include the entire needed sample preparation, but rather, they have successfully realized the integration of two or more of those procedures in one chip. If these intermediate-level LOC are compatible with one another in such a way that the outcome product of one fits well as an input of the other, they may as well serve as the completed final-destination LOC. These techniques are widely presented under the title of micro total analysis systems (μTAS) or LOC [86,87]. To give a general overview of the lysis techniques which have been successfully integrated into μTAS, a few examples are presented here.

Hong et al. [88] have integrated cell lysis with purification of nucleic acids from small number of bacterial and mammalian cells through a microfluidic device featured by mechanical micro-valves. Integration of single-cell capture and chemical cell lysis has been studied by Irimia et al. [89], using a picoliter-scale chamber featured by four thermopneumatic actuators. Lee et al. [90] have developed an automate bio-analysis system in which cell lysis, sample transportation, sample/reagent mixing and DNA amplification are performed in a microchip. As shown in Figure 2-12, a PDMS-based

microfluidic channel is constructed on a glass substrate. The cells are thermally lysed through microheaters deposited on the glass substrate. Then they are electro-osmotically transported to the mixture reservoir where required PCR reagents are mixed to the sample cells. The released DNAs are amplified in the micro PCR chamber.

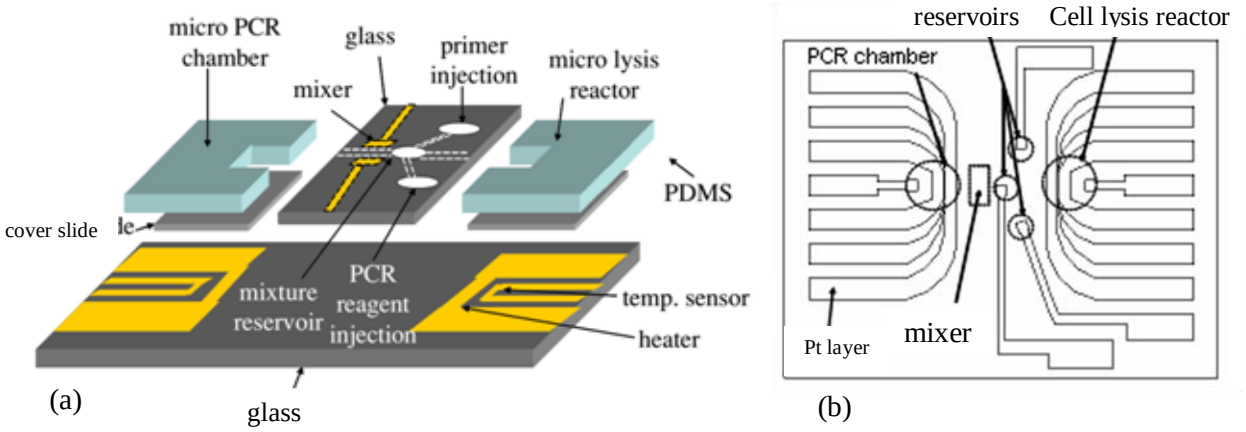

Figure 2-12 a) Schematic view of the integrated cell lysis with several sample analysis functions into one chip b) Top view of the bottom glass substrate [90]

Another trend is to increase the efficiency of cell lysis in order to release targeted intracellular components with high yield. This is particularly important when the samples are not abundant.

Most of the systems introduced are capable of lysing only specific kind of cells with limited range of properties such as size, shape, etc. Also, sometimes some pretreatments have to be done on samples prior to cell lysis. For instance, the above-mentioned systems [88–90] call for cell culturing to be performed off-chip in order to prepare sample cells for the devices. The cell culturing protocol proceeds with centrifugation for cell washing and for cell diluting/concentrating. These are necessary pre-treatments that have to be accomplished before the chip functions because each chip is designed

for specific cell types suspended in a specific buffer with a specific range of cell concentration. If a miniaturized cell lysis chip is so developed that has the flexibility in lysing different kinds of cells without pretreatment, they will highly promote research on bio-sample analysis.

2.6 Conclusions

In this chapter, different techniques for cell lysis that are used in LOC technology were presented. The methods were classified as mechanical, physical, chemical and electrical. It was demonstrated that a wide range of principles can implement cell lysis. Advantages and drawbacks of each group were discussed from the point of view of integratability onto LOC technology. The trends of future development of the technology were described.

Thermal lysis is a simple and cost effective physical method. It is not yet reliable for extraction of protein. This method is conveniently integratable with PCR. Osmotic lysis is usually combined with other methods to enhance cell lysis efficiency. Ultrasonic lysis methods are capable of lysing hard-to-lyse cells without adding any chemicals.

The problem of most mechanical techniques is the challenge to scale them down to fit LOC technology. The most common method in this category for cell lysis is applying shear stress via microfluidic channels.

Chemical methods are normally suffering from the necessity of post cell-lysis purification and detergent removal processes. The detergent removal is necessary to keep the downstream stages intact against harmful chemicals. Despite this, they can be used in combination with other techniques to ease the disruption process of cell membranes.

In electrical cell lysis, sample cells are exposed to a high voltage electric field where the ions inside cell exert a force on membrane until disrupted. The big limitation for electroporation is the high

voltage requirements. Some approaches are presented in literature to minimize this problem, namely by decreasing the distance between electrodes.

Table 2-1 summarizes the cell lysis methods that are categorized based on the principle involved. The list of advantages and disadvantages in the table are collected from the broad range of developed systems that are discussed in this chapter. It should be noted that there is not a boundary defined between each classes and different categories of the methods are found in literature.

Table 2-1 Summary of cell lysis methods implemented in LOC

Cell Lysis Method		Advantages	Disadvantages
Mechanical		No chemical necessarily added	With moving elements: challenging to be miniaturized With tiny flow-through gaps: clogging probability
Physical	Thermal	No chemical necessarily added Amenable to miniaturization	Not reliable for extraction of protein
	Osmotic	Effective in combination with other methods	A change in cell medium concentration required Pretreatments required to weaken cells prior to osmotic lysis
	Ultrasonic	Capable of lysing hard-to-lyse cells Applicable in single cell lysis	Heat generation High gradient of temperature Transmission of Energy to cell medium
Chemical		Available variety of lytic chemicals No external power required	Complexity due to removal of added chemical Slow processing
Electrical		No chemical necessarily added Highly amenable to miniaturization	Complicated fabrication of electro-microfluidic devices High voltage requirements

Since each class of the methods has its own drawback, combination of methods has attracted interests. One mechanism is to produce microchannel walls with a sharp micro textures. Combined chemical

methods can be used to imbalance osmotic pressure of cells in order to weaken their enduring strength prior to cell lysis process.

Microfluidics is the first-rate platform on which single-cell lysis techniques have been integrated. Laser beam lysis techniques have been widely employed for single-cell lysis due to its capability of concentrating energy to a very small area of interest.

It is envisaged that the integration of cell lysis with other sample preparation procedure in single LOC is going to be the main trend of the researches in this area in the following years.

As mentions in Table 2-1, the complicated fabrication of micro-electrical devices and relatively high voltage requirements are the main barriers toward development of electrical cell lysis systems. We have addressed these two limitations by developing novel systems for cell lysis that are presented in the following chapters.

The three projects that will be introduced in the following chapters are the achievements toward development of cell lysis devices suitable for LOC. The main focus of the project presented in chapter 3 is to devise a fabrication methodology for making electrical cell lysis devices through a fast and cheap procedure. Performance-enhancing of cell lysis by applying CNT in electrical cell lysis is the main achievement of the project presented in chapter 4. In the project described in Chapter 5, the fabrication of CNT-featured cell lysis device is advanced and the application of CNT in single cell electroporation is also developed.

Chapter 3

Fabrication of Electro-microfluidic Channel for Single Cell Electroporation

The content of this chapter has been published in Biomedical Microdevice, DOI 10.1007/s10544-013-9761-0

3.1 Introduction

The point of this chapter is to demonstrate the use of a quick and cheap fabrication method to realize a laser-ablated microfluidic channel for single cell electroporation. Traditional lithography of microchannel with electrode in MEMS applications has always been complicated. Most microfluidic devices are created as low-cost disposables, in order to minimize the risk of sample contamination and increase their practicality in developing countries. For this application, polymers are very well suited, being cheap, easy to work with and available with a wide range of specifications [91]. Popular polymers for microfluidic applications are Poly (methyl methacrylate) (PMMA) [92], Polydimethylsiloxane (PDMS) [93] and SU-8 photoresist [94]. Polyimide is also often used for microfluidics [95], offering excellent properties specifically for biological applications, such as good thermal stability, low uptake of water and good biocompatibility [96]. There are also no known solvents for polyimide [91], giving it an excellent chemical stability. Its low absorption of small molecules is especially advantageous when compared to the other popular polymer PDMS, which does suffer from such problems [97].

Fabrication methods used to create the microfluidic channels are mostly derived from the semiconductor industry, and include photolithography [98], etching [99] and laser ablation [100]. Laser

ablation is most often performed using excimer laser systems [101], operated at wavelengths from 193 nm to 355 nm. This technique provides good results and excellent controllability, allowing easy creation of new patterns for prototyping.

Often, electrodes are incorporated with microfluidic channels, allowing functions such as cell electroporation [102], electrochemical detection [103], the manipulation of the liquid [104] or simply as pads and wires for connecting the chip to external equipment.

Electroporation techniques require creation of electrodes in the microfluidic chip. Creation of such electrodes can be done in multiple ways; for example, by depositing thin (typically 50-250 nm) metal layers on the polymer in vacuum. However, since polymers have much greater thermal expansion coefficients, the temperature during deposition must be kept near room temperature to prevent cracking in the metal electrode layers. Another disadvantage is that lift-off lithography must be used to achieve features less than 10 μm in size, and most polymers are chemically incompatible with the photoresist and developer used in such steps. If a thick-film method is used, no vacuum is required. In such a method, a paste of metallic particles is smeared on a mask placed over the sample. The mask is then removed, and the residue left to dry. This typically yields electrode thicknesses of tens of micrometers, and worse resolution than the thin-film depositing method [91]. In contrast, glass slides coated with Indium Tin Oxide (ITO) can be easily used. If chip-wide electrodes are all that is required, no extra steps at all are required. If more intricate electrode patterns are required, lithography can be easily done on the chips, without suffering from the thermal expansion mismatch when depositing on polymers. Previously, transparent ITO substrates have been used in microfluidic applications [92,105], but never in combination with laser-ablated polyimide.

The laser ablation fabrication technique is well suited for fabricating microfluidic channels in polyimide. It is fast, detailed, controllable and very flexible. However, most laser systems used are excimer lasers, which are bulky and require sophisticated systems for handling the toxic gas used. In

this chapter, we present a method of ablating microfluidic channels in polyimide using a 30W CO_2 laser with a wavelength λ=10.6 μm. Although lacking the resolution of excimer lasers, this system is low-cost, safe and easy to handle. Laser ablation using excimer lasers of polymers is a complicated process of both photothermal and photochemical breakup of the polymer chains[106]. In contrast, the infrared wavelength of a CO_2 laser means that it always ablates the material photothermally. Although CO_2 laser ablation of polymers has been done before [107], it has not been done on polyimide. Bonding of polyimide can be performed in multiple ways, with lamination by far the most used method. When creating a polyimide-polyimide bond in this way, polyamic acid can be used as a solvent to enact diffusion of the polymer chains, yielding a very strong bond [95]. This method has the disadvantage that it results in shrinkage of the polyimide, reducing the control over the feature size. On the other hand, using polyimide with a Fluorinated Ethylene Propylene (FEP) coating (such as DuPont's Kapton™ Type FN), no additional solvents are needed, and bonding can be done by simple thermal lamination techniques.

In this work, we combine many of the easiest techniques to create a low-cost, quick and versatile method for prototyping microfluidic chips. Use of transparent ITO coated substrates will allow easy electrode creation, while retaining the ability to quickly image the channel performance using optical microscopy techniques. The use of a CO_2 laser will give great flexibility in channel design, without the difficulties normally associated with handling an excimer laser.

In the present methodology, the microchannel pattern is cut out of polyimide, bonded to two ITO-coated substrates using Teflon as an adhesion layer. ITO as a conductive material enables electric field in the channel and its optical transparency allows microscopy techniques to be utilized in characterizing the behavior of the microfluidic chip. The performance of the chip was tested on irreversible single-cell scale electroporation which requires relatively high voltages. Chinese Hamster Ovary (CHO) cells, as mammalian cells, were passed through the microchannel to experience electric

field. Cells were loaded with a fluorogenic dye, Calcein AM, and the electroporation of each was individually recorded in real-time via fluorescent microscopy. The results show promising performance of the electric microchannel in electroporation. By customizing of ITO electrodes and the design of microchannel pattern, utilization and integration of the proposed electrical microchannel in variety of other MEMS-based devices are achievable.

This method has a low start-up cost, but the cost per unit does not decrease appreciably for larger volumes. Therefore, our method will be most useful for rapid prototyping and characterization of microfluidic chips, rather than bulk-volume fabrication.

3.2 Fabrication of electro-microfluidic channel

Our microfluidic channels are made by using a 10.6 μm CO_2 laser engraving system (Universal Laser Systems, VLS2.30) to cut the channels completely through polyimide (DuPont Kapton FN 200FN919), thus yielding channels of the same height as the thickness of the polyimide layer.

Our tests on cutting 50-μm thick polyimide showed that engraving at 1% of the maximum power (30 mW) and 1% of the maximum speed (0.25 mm/s), and making 3 passes over the same pattern yields the best results. At this speed, hardly any material is ejected from the channel, but rather is left behind as residue of broken monomers. This residue is easily removed after machining using ethanol as a cleaning agent. Engraving at higher power and/or speed caused an excess of heat buildup in the sample, resulting in thermal buckling and loss of positional control of the laser spot on the polyimide. Using the same laser, access holes to the microfluidic channels are drilled in the backside of the ITO-coated slides (Sigma Aldrich, 30-60 Ω/sq, Cat. No. 703184). The experimentally optimized settings for laser cutting/engraving of all components used for the microchannel are listed in Table 3-1. PMMA cutting and engraving were performed to provide the customized chip holders.

Table 3-1 Laser settings used for different components of microchip

Material	Thickness (mm)	Power	Speed (mm/s)	Iterations
Kapton Polyimide	0.05	30 mW	0.25	3
ITO-coated microscope slide	1.1	1.5 W	0.5	10 times from each side
PMMA cutting	4.5	24 W	2.5	1
PMMA engraving	1.1	1.5 W	2.5	5

The polyimide used (Kapton FN) is pre-coated on both sides with Teflon FEP fluoropolymer as adhesive layers. This FEP coating can be bonded to ITO glass by heating it to 280˚C under pressure of a small vise, and letting it gradually cool. Samples of laser-cut polyimide before and after bonding are seen in Figure 3-1. A sample line scan by a Dektac surface profilometer made perpendicular to the channel is illustrated in Figure 3-1c. The roughness at the edges is diminished after bonding to ITO-coated cover slips. ITO-coated cover slips (SPI supplies, 30-60 Ω/sq, Cat. No. 06467-AB) was used in this sample. It should be noted that the ITO-coated cover slip, as thin as 130-170 µm, provides capability of imaging in higher magnifications where the microscope's objective lens has to be in such tiny distance to the specimen in the channel. Since CHO cells are big enough to be visible in lower magnifications, the chips used in our experiments are all made with ITO-coated glass slides.

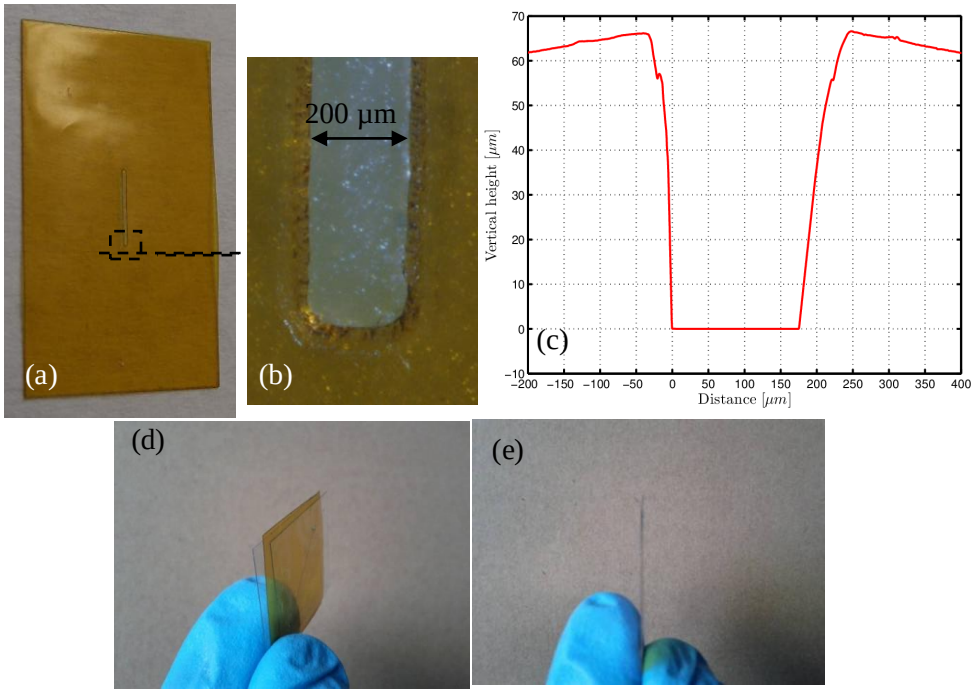

Figure 3-1 Samples of laser-ablated poyimide, a) post-cutting but pre-bonding, b) under 11.25x magnification, c) line scan made by a Dektac surface profilometer made perpendicular to the channel, d) polyimide samples after bonding to ITO-coated cover slips, e) front view of the bonded polyimide

The chip that is presented in this chapter contains simple straight channels that are 3 mm in length. The width is 200 µm. The Kapton is cut to size using the laser cutter, and the channel is cut within it. The ITO-coated slides, having a sheet resistance of 30-60 Ω/sq, are also laser-drilled. All components are then cleaned using an ultrasonic cleaner (FisherScientific, FS30D), and are rinsed thoroughly by hand using ethanol. The whole stack is bonded in a vacuum oven, and syringe tips are attached and glued in place over the access holes in the bottom ITO-coated slide. For gluing, epoxy glue thickened

with fumed silica is used. Normal epoxy glue was found to be not viscous enough, and was likely to flow into the microfluidic channels, thereby blocking them. During experiments, tubes will be attached to the syringe tips. The whole chip is then placed on a PMMA support structure, allowing top-down observation by fluorescence microscope while leaving room for the tubes to be guided away to syringes and waste disposal vials. A snapshot of the chip is depicted in Figure 3-2.

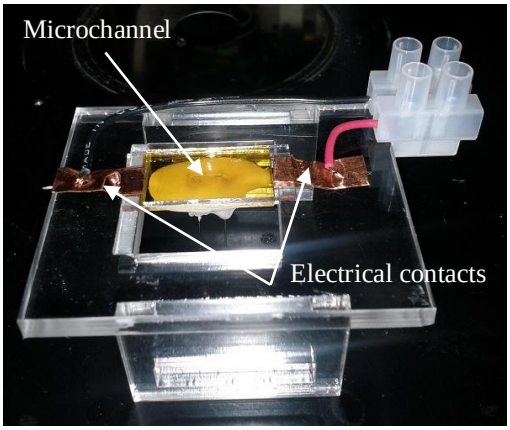

Figure 3-2 snapshot of the fabricated electro-microfluidic chip for mammalian cell electroporation

3.3 Cell Preparation and Fluorescent Microscopy

Chinese Hamster Ovary cell line CHO-K1 (ATCC, Cat. No. CCL-61) was used as a sample for mammalian cells. The frozen cells thawed in growth medium, containing F-12 Kaighns (Fisher Scientific, Cat. No. SH3052601) supplemented by 10% Fetal Bovine Serum (Fisher Scientific, Cat. No. SH3039602) and 1% Penicillin / Streptomycin (Bio Basic Canada, BS732). The cells were transferred to a cell culture flask and incubated at 37 °C, 5% CO_2. Every two days, cells were sub-

cultured as follows: the cell medium was aspirated from the cell culture flask and then, cells were washed by PBS. One milliliter of Trypsin 0.25% (Fisher Scientific, Cat. No. SH3004202) was then added to the medium in order to detach cells. After five minutes incubation in room temperature, 7 ml of cell medium was added to the trypsin to deactivate it. Cells were transferred into a centrifuge tube and centrifuged at 300 g for 1 minute. The supernatant was discarded and electroporation buffer (10 mM phosphate buffer and 250 mM sucrose, pH 7.4) containing 0.05% Calcein dye was added.

The cells were loaded with Calcein AM dye during 30 minutes incubation at 37 ºC.

Calcein AM is membrane permeant; in live cells, intracellular esterases remove the acetomethoxy group so that the non-fluorescent Calcein AM gets trapped inside and gives strong green-fluorescence. The resulting fluorescent Calcein is highly charged and therefore cannot be excised from the cytoplasm once it has infiltrated the cell unless non-selective pores are introduced. The high sensitivity of Calcein AM fluorescence makes it useful in detecting the diffusion of dye out of the cell once the cell is electro-permeated. Here, the leakage of the dye through permeabilized cell membranes has been used as an indication of cell electroporation [108].

3.4 Cell Electroporation

To show the useful and correct operation of our microfluidic chip, electroporation experiments have been done. In electrical lysis of the cells, a voltage is applied across the cell suspension. The resulting electrical field causes a voltage drop across the membrane (transmembrane potential), which introduces pores. If the transmembrane potential is large enough, and is maintained long enough, these pores can permanently disrupt the cell membrane thereby lysing the cell. The voltage applied to the chip (operational voltage) must be high enough to induce the required transmembrane potential. Electroporation depends on the strength of electric field as well as the duration of time the field is

applied. Since the threshold operational voltage is dependent on the system characteristics, the consequent external field (E_{ext}) applied to the cell-containing medium is more common in reports. The threshold values for electroporation of CHO cells have been studied by Valic et al. [109]. They have reported the threshold strength of electric field within the range of 200-250 V/cm with pulses of milliseconds in duration. Electroporation can happen within 30 ms, if suitably high voltages and channel designs are used [110]. Tweaking the pulse characteristics of a pulsed electrical field can also improve efficiency [111]. The difference between reversibly electroporating a cell and lysing a cell is mostly a matter of field strength and exposure time, both of which can easily be controlled.

3.5 Cell Electroporation Experiments

Cell electroporation was performed as one example of the applications of the proposed polyimide-made electro-microfluidic channel. Direct imaging of lysis was used as a method to determine whether the microfluidic chip was capable of electroporating cells.

The prepared cells were loaded with Calcein-AM dye and imaged using fluorescent imaging. Calcein-AM is a non-fluorescent cell-permeable compound that hydrolyses to the fluorescent anion Calcein inside the cells. Before switching on the electrical field, the cells were very visible green dots. This allowed for following the cells in real-time during lysis. Cells were pumped to the chip through silicone tubing (VWR, Cat. No. CA62999-850). The pump turned off and cells became stationary before operational voltage was applied. A data acquisition system (DAQ) was used to supply operational pulse voltage and also to measure the passing current. Images were taken by a CCD camera (CoolSNAP, Turbo 1394 Series EZ) on a fluorescent microscope (Nikon Eclipse E600FN). Schematic view of the set-up of experiment is shown in Figure 3-3.

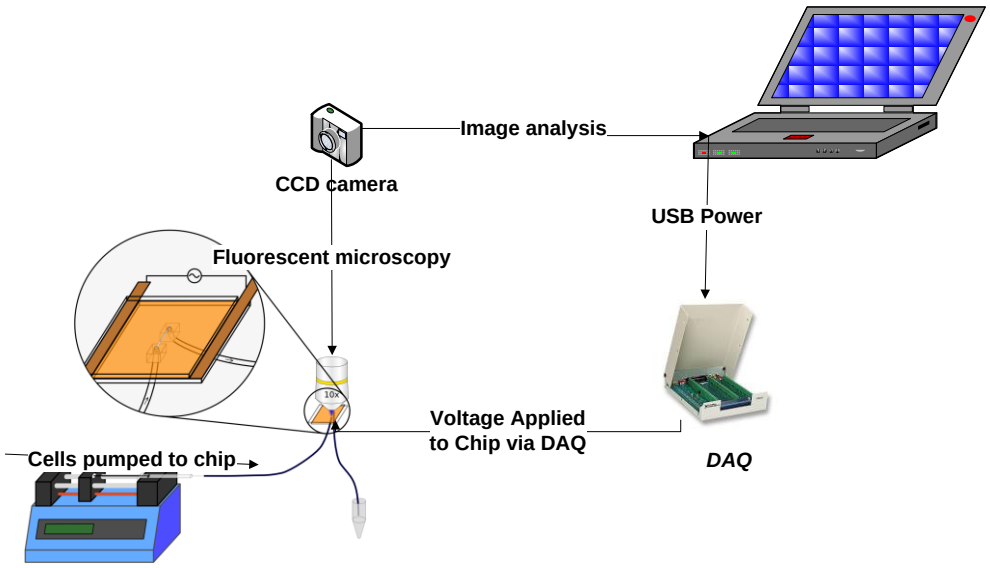

Figure 3-3 Schematic overview of the experimental setup

3.6 Results

Cell electroporation experiments were conducted as explained in previous section. When a cell was electroporated, the fluorescent dye inside the cell would flow out through the ruptured membrane, and the brightness of the cell would reduce strongly. Electroporation is thus determined by watching the intensity of the fluorescent cell over time, and correlating this with the time the electrical field is switched on. The images were taken by the CCD camera at frame rate of 2 Hz with exposure time of 30 ms.

The Calcein AM dye did show deterioration when under prolonged excitation lighting, based on polarization quenching theory[112]. This is illustrated in Figure 3-4, but this process has a time scale of about 140 seconds. It is determined by fitting the normalized measured intensity graph with:

$$I=I_0 \exp(-t/\tau) + I_{base} \qquad (3.1)$$

where I_0 (= 0.4876) is the starting intensity, I_{base} (= 0.465) is the background intensity and τ (= 141.5 s) is the decay time constant. This deterioration is thus not significant when determining cell lysis through imaging, since that process takes place over a timescale of 10-20 seconds.

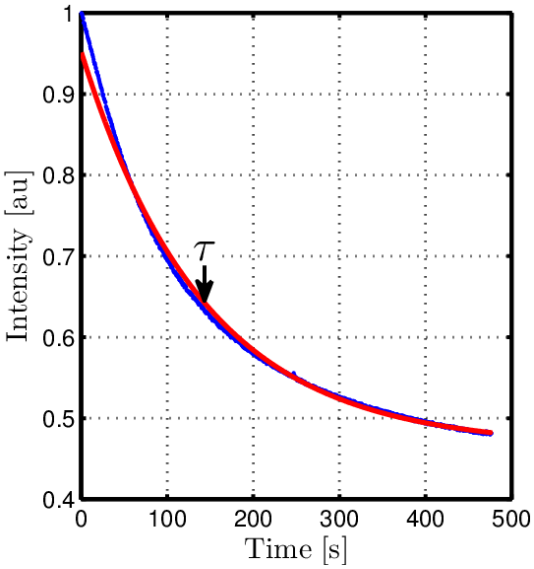

Figure 3-4 Fluorescence decay of CHO cells loaded with Calcein-AM (blue) and the fitting exponential graph (red).

Figure 3-5a) shows images of four cells staying in a microchannel under microscope light when the voltage of V=0 V (no electric field) is applied to the chip. The walls of the channel are depicted by the straight lines in the pictures. Figure 3-5b) shows images of four cells in the channel being electroporated within 20 seconds while the operational voltage of V=5 V was applied to the chip at

the time of t=5 s. The drop in color intensity of Calcein-AM loaded cells indicates electroporation for all the four target cells.

The intensity of the cell spots in Figure 3-5b is quantified by a MATLAB program and the results are shown in Figure 3-5c. The intensity of all pixels in a square zone of $20 \times 20\ \mu m^2$, surrounding each cell, is summed up and the total value is illustrated vs. time. The natural decay is also shown in the graph. The intensity of the brightest cell is normalized to start at 1, and the intensities of the other cells are normalized relative to the brightest cell using the ratio of maximum pixel values within the measured area. Even though the total intensities of the target cells are not equal at the time electric field is applied, the identical drops seen for the all cells indicate electroporation occurs within the first five seconds. It means the electric field in the channel is strong enough to electroporate cells with 100% rate. The variation of the graph is not considerable after the time of t=10 s. To confirm that 100% electroporation occurs at this voltage, more experiments have been performed at the same condition and the intensity variations of more cells are shown in Figure 3-5d. The black dot line indicates the time electric field turned on.

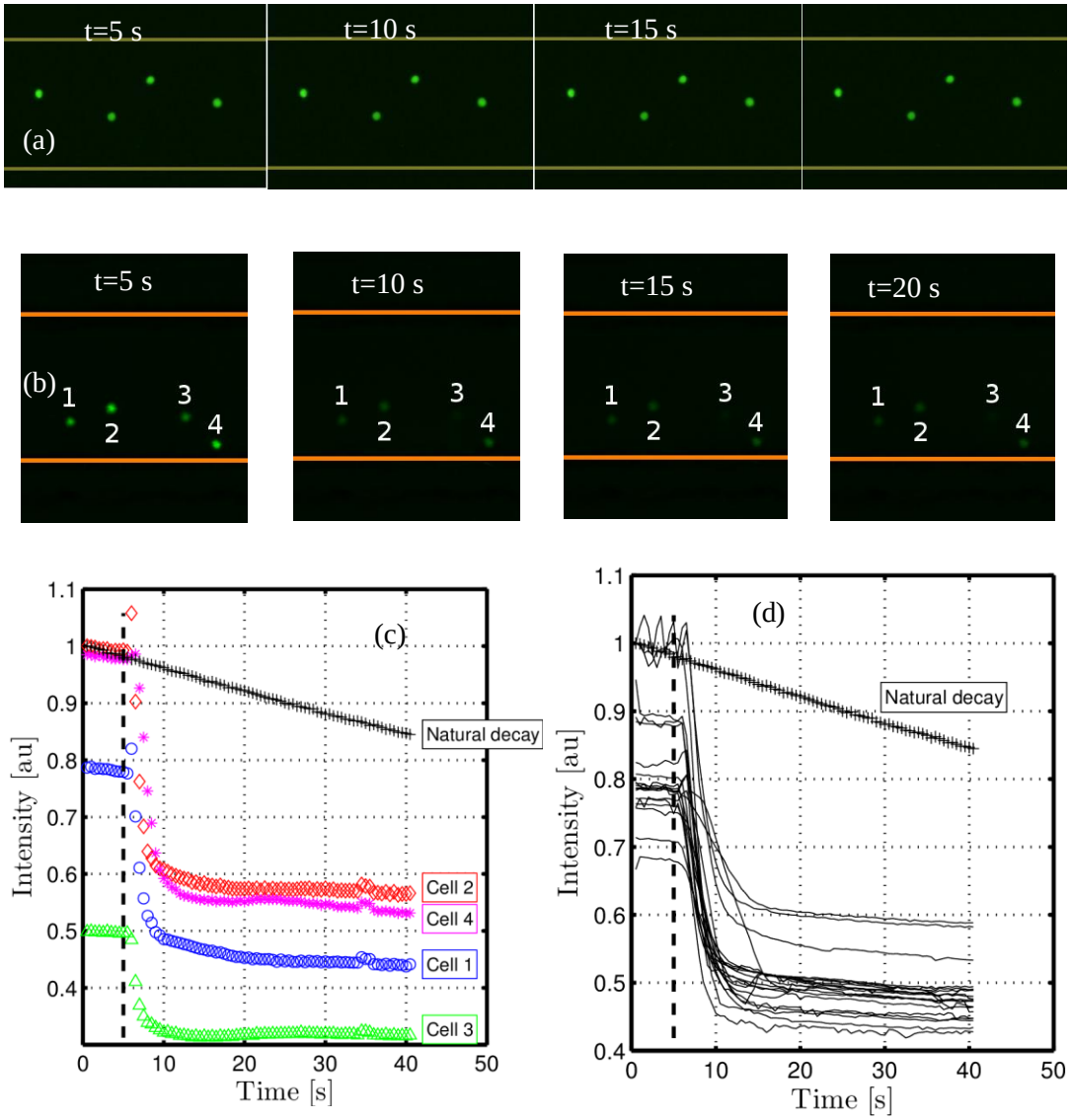

Figure 3-5 Images of four cells loaded with Calcein AM dye, a) not exposed to electric field (V=0 V), b) exposed to electric field at t=5 s and operational voltage of V=5 V, c) total intensity of the square zones surrounding the four cells labeled in (b), d) more cells experienced the same field as b (V=5 V)

The experiment was repeated with operational voltage of V=3 V. New chips were used to avoid contamination left from the previous experiments. The results for some target cells are illustrated in Figure 3-6. As seen in the graph, nine cells out of thirteen are fully electroporated. An increase in the total intensity of the electroporated cell is visible right after electric field is turned on. It should be due to the abrupt expansion of the cell size while being electroporated. [110,113,114]

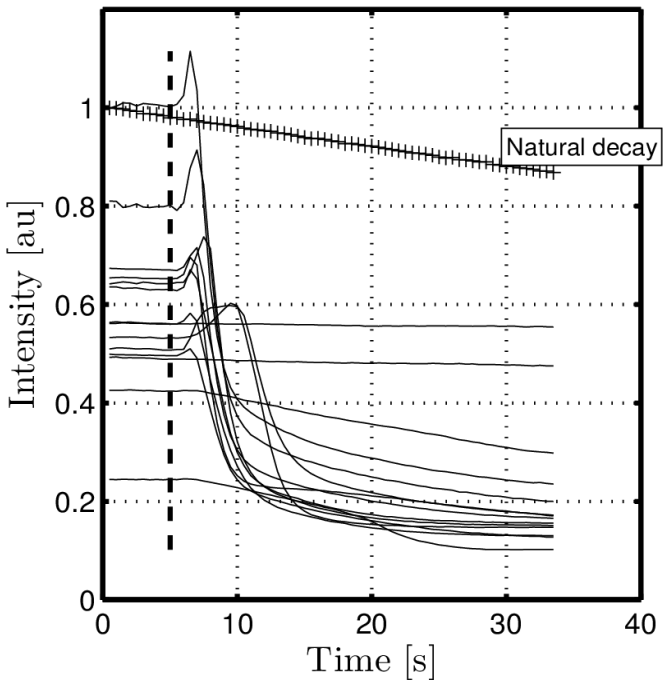

Figure 3-6 Total intensity of the square zones surrounding individual cells, exposed to an electric field turned on at t=5 s with operational voltage of V=3 V.

The last experiment was performed at the operational voltage of V=1 V. As shown in Figure 3-7, none of the target cells experienced full electroporation. It is understood that the strength of electric field is not high enough to affect membrane permeabilization of CHO cells.

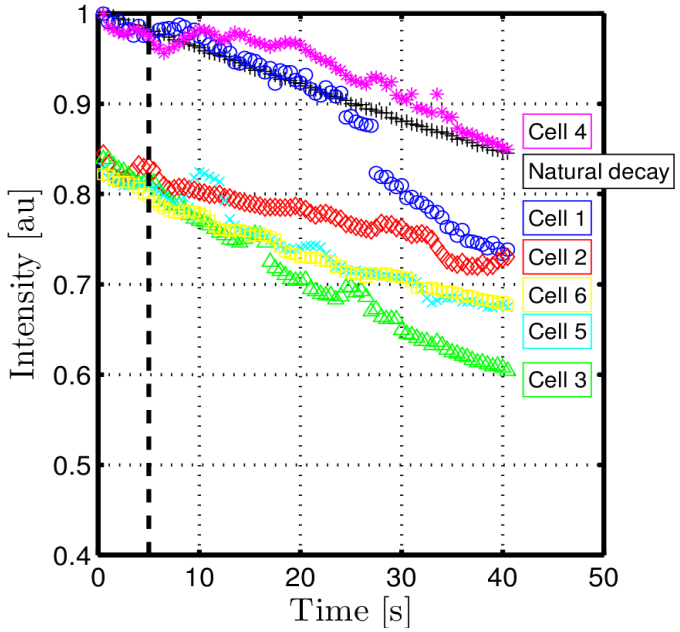

Figure 3-7 Total intensity of the square zones surrounding individual cells, exposed to an electric field turned on at t=5 s with operational voltage of V=1 V.

3.7 Discussion

The results presented here are samples to show the application of the electro-microchannel in electrical cell manipulation mechanisms. It is a promising approach to analyze behavior of single cells under electrical configurations. It should be noted that the capability of the proposed methodology is not limited to mammalian cells with relatively larger sizes. For electrical manipulation of smaller bio-samples, for example bacteria, ITO-coated cover slip, as one sample is seen in Figure 3-1, enables high magnification microscopic analysis. Moreover, the geometry customization of electrodes in deposition of ITO makes non-uniform electric fields in the microchannel. If such step is taken toward

development of the chip, a broad range of cell treatments based on dielectrophoresis will be also achievable. Customized patterning of polyimide with no extra cost is another possibility toward integration and customization of the electro-fluidic channel in other on-chip cell manipulation systems.

The proposed methodology presented in this chapter is ideal for LOC since it can be easy to produce and relatively cheap, but the fabrication methodology needs ITO coatings that increase the cost. It has been reported that ITO might be degraded during thermal lamination [115]. These are the two drawbacks of the methodology that should be taken into consideration.

The complexity in the proposed system is the requirement of an AC power supplier. In electroporation systems, usually AC fields have been preferred to DC because DC current causing more bubbling through electrolysis. In addition, an alternating electric field enhances the efficiency of electroporation because of what has been reported as "mechanical disturbance" that an alternating field exerts to the cell membranes [116]. However, AC brings with it a lot of complexity because of the number of variable it has and is harder to generate than DC.

By varying the shape of a microfluidic channel and running current through the cell solution, a channel with different electric fields can be made, such as the one developed by Wang et al. [117]. They have made a microchannel with varying cross-section area. The electrodes are two platinum probes that are inserted at the inlet and outlet of the channel. The geometrically-varying design of the channel creates varying electric field in the channel. It means the narrower cross-section area of the channel, the stronger electric field it has. However, the PDMS-based fabrication of their chip still involves soft lithography that is not as cheap and straight-forward as the methodology we introduced in this chapter.

The fabrication methodology presented in this chapter can be used to make such microchannels with varying design which are powered by a DC input and no ITO coatings are needed. It can be simply

achieved if ITO-coated glass slides are replaced by glass slides and two metal needles are placed at the inlet and outlet of the microchannel. The varying design of microchannel can also be simply made by customizing the laser-ablated pattern of polyimide which is simple. The fabrication of the electro-microfluidic device with varying design will be discussed in detail as a suggestion for future works in section 6.3. The proposed methodology of making electro-microfluidic channels is considered as an alternative for creating many other microchips not only for cell electroporation, but also for other stages of sample preparation procedure, for example DEP-based separation of micro-particles/biological cells. It is also presented in section 6.3 as a suggestion for future works.

3.8 Conclusion

In the present chapter, a cheap and fast fabrication methodology of making electric microchannel with Teflon-coated Kapton polyimide is presented. It is shown that a thin laser-ablated polyimide sheet thermally bonded to two ITO-coated glasses provides a cheap microchannel with electrical functionalities. The optical transparency and high throughput of the devices made by the methodology are the main features. Straight microchannels with 50 µm height were fabricated and their electrical performance was tested on electroporation of CHO cells. Different operational voltages (1-5 volt) were applied to the chip and the fluorescent imaging of electroporation in real-time for individual cells was carried out. The results show a promising practicability of the proposed methodology in analysis of single cell electroporation. Further developments of the proposed electrical microchip by customizing ITO-coatings and polyimide cutting patterns are practical. Such developments will extend the application of the electrical microchip so that it can be utilized and integrated to many other MEMS devices.

Chapter 4

Carbon Nanotube for Enhancement of Electrical Lysis of Bacteria

The content of this chapter has been published in Nanotechnology, DOI:10.1088/0957-4484/22/32/325705

4.1 Introduction

In this chapter, we report on the enhancement of electrical cell lysis using Carbon Nanotube (CNT). Electrical cell lysis systems utilize an external electric field to induce opposing charges across the membrane that leads to cell lysis [76,77,118–120]. No chemical is required and such electromechanical systems are easily integrated into LOC devices. Electrical cell lysis systems are widely utilized in microchips as they are well-suited to be integrated into LOC devices. However, cell lysis based on electrical mechanisms has high voltage requirements.

The developments to reduce required operational voltage are mainly based on reducing distance between electrodes. By employing micro-fabrication technologies, the micro-distant electrodes can be structured where electric intensity is locally enhanced between the electrodes [59,108]. Lee and Cho [59] have demonstrated a flow-through microchannel device featured by a narrow orifice gate for cell lysis. The cross section of the microchannel is narrowed 20 times at the orifice gate so that the electric field is strengthened up to 1.2 kV/cm with the operational DC voltage of 50 V. The three-dimensional electrodes in the shape of saw-tooth built in a microfluidic channel have been developed by Lu et al. [60] where cells are lysed while passing by electrode tips. They have reported that, with the

tip-to-tip distance of 30 μm between electrodes, an operational AC voltage of less than 10 V is enough to lyse mammalian cells with the average size of 10 μm. Although reducing the electrode distance down to the scale of sample cells leads to a locally strengthened electric field, the high cost of fabrication acts as a barrier to widely employ these systems for LOC cell lysis. Moreover, such microfluidic channels are likely to be blocked at the micro-gaps.

Here, we demonstrate that by incorporating CNT into microfluidic electrical lysis systems, the required voltage for lysis is reduced by half and the lysis throughput at low voltages is improved by ten times, compared to a no-CNT microchip. In our experiment, E. coli cells are lysed while passing through a forest of aligned CNT in a microchannel. Based on the lightning rod effect, the electric field is locally-strengthened at the tip of CNTs [121]. It enhances the efficiency of cell lysis so that cell lysis occurs at lower voltages or with higher throughput. This approach enables easy integration of cell lysis with other on-chip high-throughput sample preparation processes.

4.2 Theory

When a cell exposed to an electric field, the intrinsic membrane potential (typically 70 mV under normal condition [122]) resulting from gradient of ionic concentrations is imbalanced by the external electric field. If the transmembrane potential exceeds a threshold value, the induced opposing charges inside the cell squeeze the membrane until nano-pores are formed across the membrane. The nano-pores allow open paths between the cellular matrix and the external media suspending the cell. Depending on the magnitude, frequency and duration of the applied pulsed voltage, the created nano-pores can either be resealed (reversible electroporation) or remain open permanently (irreversible electroporation). Irreversible electroporation results in a failure of the cell membrane to maintain essential ionic balance across the membrane and the cell ruptures. The threshold transmembrane

potential over which the electroporation is irreversible can be estimated for spherical cells from Ref. [123]:

$$E = \frac{\Delta\varphi}{1.5a\cos\theta} \qquad (4.1)$$

where $\Delta\varphi$ is the transmembrane potential, a is the radius of the cell and θ is the angle between the direction of electric field and radial line at the point of interest on the membrane, as shown in Figure 4-1.

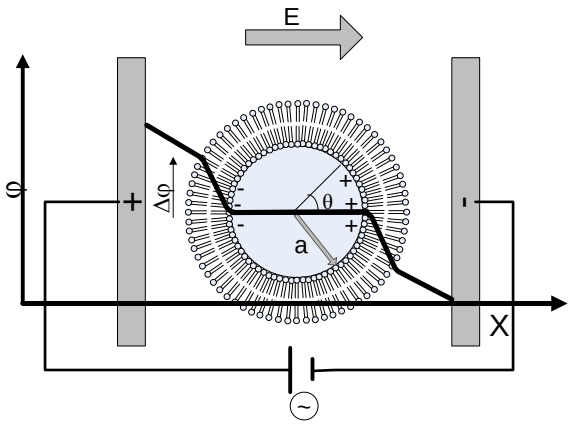

Figure 4-1 Illustration of a cell exposed to an electric with the graph of transmembrane potential induced across the cell membrane causing the build-up of the opposing charges on the membrane

The threshold transmembrane potential is also dependent on the pulse duration of the applied voltage as the structural change in cell membrane can go back to its original state if the duration of charging time is not long enough. The pulse duration (or charging time constant) required that transmembrane potential of a spherical cell reaches the threshold value is expressed by:

$$\tau = \left(\rho_1 + \frac{\rho_2}{2} \right) C\, a \qquad (4.2)$$

where ρ_1 and ρ_2 are, respectively, the resistivities of the external cell medium and internal cell medium (cytoplasm) and, C is the capacitance of the membrane. The threshold transmembrane potential for irreversible electroporation is typically 1 V for spherical cells with pulse duration of a few microseconds [123]. Considering $\Delta\varphi$=1 V, the critical electric field strength of tens to hundreds of kV/cm is obtained from the equation (4.1).

The high voltage requirements for electrical cell lysis limit the integration of the systems on LOC devices. Our approach has taken advantage of the uniquely high aspect ratio of CNT that provides locally concentrated electric field at the tip of CNTs, physically based on the lightning rod effect[121]. The simulation data for the distribution of electric field at the tip of CNT has been reported in literature [124] [125] [121]. It has been shown that the strength of electric field is greatly enhanced near the tip of CNTs. Rojas-chapana et al. [121] have studied the localized electric field at the tip of CNT for reversible electroporation. They have presented an expression of the degree to which the electric field is enhanced at the tips of CNTs:

$$\frac{E}{E_0} = \alpha \left(\frac{L}{D} \right) \qquad (4.3)$$

where α=3 is a constant, E is the electric field at the tip of CNT and L/D is the aspect ratio of CNT which is greatly high.

The results from Rojas-chapana et al [121] also indicated that there was a tendency of the CNTs to collect and adhere to lipid membrane structures. Later on, the application of CNT in voltage reduction in irreversible electroporation was presented in our group [126]. Here, we have employed the lightning rod effect of CNT for irreversible electroporation not only to reduce the voltage requirements but also to improve the throughput of electrical cell lysis.

4.3 Fabrication of Microfluidic channel

We fabricated a microfluidic channel containing aligned CNTs. The assembly diagram of the fabricated microfluidic chip is depicted in Figure 4-2.

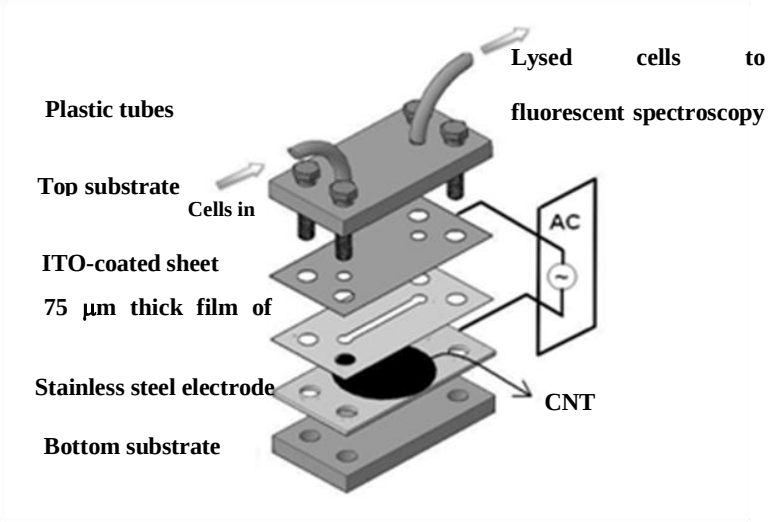

Figure 4-2 Assembly diagram of the components of the cell lysis microchip

The channel has been cut off from a 75-μm-thick kapton polyimide film (DuPont). The film is sandwiched between an Indium Titanium Oxide (ITO)-coated sheet and stainless steel electrodes. The stainless steel electrode is covered by a patch of randomly aligned Multi walled CNT (MWNT)

(Xintek Inc, North Carolina, USA). In Xintek products, pre-synthesized CNTs are coated on the stainless steel through electrophoretic deposition (EPD). EPD is achieved via migration of charged particles dispersed in a solution toward an electrode under the influence of electric field[127,128]. Chemical Vapor Deposition (CVD) is widely used for the direct growth of CNT on a substrate but through high-temperature chemical reactions. EPD is, in contrast, cheaper and simpler. In this technique, as-synthesized CNTs are purified and then dispersed in a suitable liquid by sonication in room temperature for about 2 hours. The stainless steel substrate and a counter electrode are immersed into the CNT-containing medium. When a constant DC voltage is applied to the electrodes, CNTs start migrating toward positive electron. The more detailed procedure for fabrication of Xntek Inc's products is found in literature [129,130].

In our designs, the channel is 1 cm long and 1 mm wide. SEM images of the Multi-walled CNT (MWNT) deposited on the electrode are illustrated in Figure 4-3. The length of the MWNTs is 6-8 μm and the diameter is 2-6 nm. The density of the aligned CNTs is estimated to be around $10^4/cm^2$.

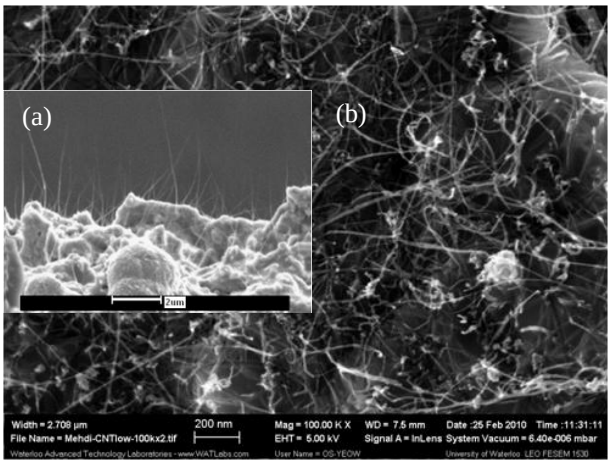

Figure 4-3 SEM Image of MWCNT deposited on stainless steel electrode in front (a) and top (b) views. The scale bars are 2 μm and 200 nm in (a) and (b), respectively

4.4 Preparation of Bacteria

We chose Escherichia coli (E. coli) cells for lysis because bacterial cells are typically smaller than mammalian cells and the voltage required for lysis of bacterial cells is higher than bigger cells, as governed by equation (4.1). However, the presented approach can be applied for other types of cells as well.

The E. coli cells were prepared as follows: Dh5α E. coli cells grown in Lysogeny Broth (LB) nutrient broth were incubated in a shaker at 37 °C for 16 hours. Three milliliters of the solution was centrifuged for 15 minutes at 1750 rpm speed for two times. The resulting concentrated bacterial culture was rinsed and diluted with deionized (DI) water to around 0.03 OD_{670}. The cells were kept in DI water no longer than half an hour before each experiment.

4.5 Fluorescent Microscopy

The cells were stained using the live/dead backlight bacterial viability kit (Invitrogen) consisting of two separate components of SYTO 9 and propidium iodide (PI). SYTO 9 and PI both stain nucleic acids. SYTO 9 penetrates through the bacteria membrane of all cells and stains them green so that it is used for counting the total number of cells while PI enters only bacteria with damaged membranes and the combination of the two stains produces red-fluorescing cells [131,132].

One milliliter of the prepared cell suspension was mixed with 1.5 μl of SYTO 9 and 1.5 μl propidium iodide. The cells with intact membrane stain green while the cells with compromised membrane stain red. Images were taken by a digital camera (Nikon Digital Sight DS-U1) on a fluorescent microscope (Nikon Eclipse E600FN). The ratio of lysed cells over the whole cells which was averaged over several snapshots of sample cells determines cell lysis rate. Figure 4-4 shows the control references for no electroporation and fully electroporation.

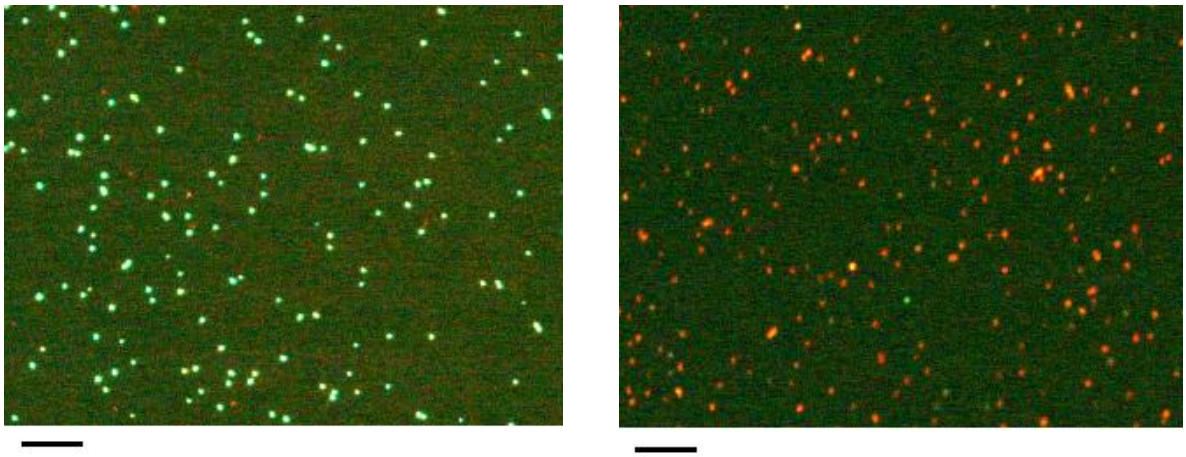

(a) (b)

Figure 4-4 The images of stained cells with dye as control references for no electroporation (a) and fully electroporation (b). The scale bars are 50 μm.

No electroporation refers to the sample cells prior to lysis experiment and fully electroporation refers to the sample cells with the maximum rate of electroporation. The lysis rate of each experiment was calculated by analyzing the number of red and green spots in cell images. Cell lysis rate was obtained from the ratio of the number of red to total cells compared to the ratio in control references. As an example, Figure 4-5 is a snapshot of E. coli cells stained with the fluorescent dye, signifying the lysis rate of 53%. This ratio has been obtained by counting the number of green and red spots in the fluorescent images and analyzing the ratio of red to total spots in comparison with references. The lysis rates reported in the present work are the values averaged over several such snapshots.

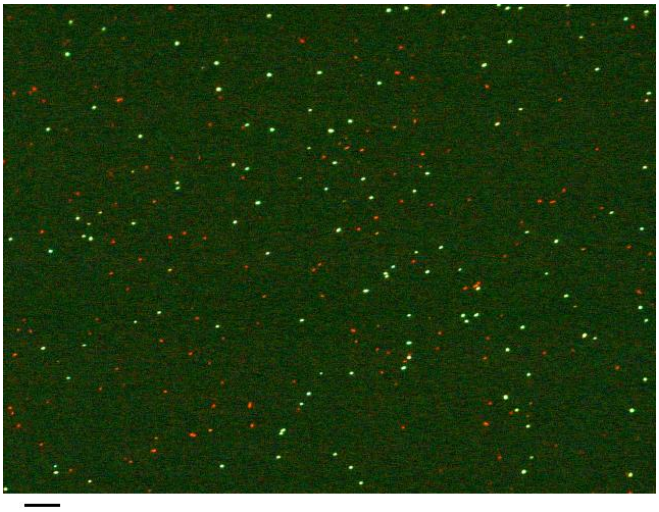

Figure 4-5 Sample picture of the cells stained with fluorescent dye. The green spots represent the cells with intact membrane and red ones are the cells with broken membranes. The scale bar is 50 μm

We verified the lysis rate by using Fluorospectrometer (NanoDrop, Wilmington, USA). The amount of live and lysed cells was quantified by the fluorescent emission intensities of the green (510-540 nm) and red (620-650 nm), respectively. It was carried out by following the protocol provided by Invitrogen Company [133]. The more detailed procedure is presented in Appendix A.

4.6 Experiment

The cell lysis experiment was performed as follows: cell media was prepared as described in section 4.4. The conductivity of the media containing DI water and fluorescent dye was as low as 1.4 μS/cm. Some control experiments were conducted prior to cell lysis experiments in both channels with and without CNT. At first we had to make sure that the microfluidic channels do not induce cell lysis. 50 μl of the prepared cell suspension was pumped to pass through the no-CNT channel, using a micro-

peristaltic pump with adjustable flow rates (Instech Model P720). The images taken from the sample cells before and after passing through the channel were identical. It proves that microfluidic channel does not induce lysis. This experiment was repeated with the channel with CNT to prove that the presence of CNT does not cause cell lysis when no electric field is applied. It is proved by the pictures of the cells before and after they pass through channel with CNT. As depicted in Figure 4-6, the ratio of the red to total spots, representing the rate of lysis, does not change after the cells pass by MWNTs in the channel. It provides evidence that cell lysis does not occur when no voltage is applied.

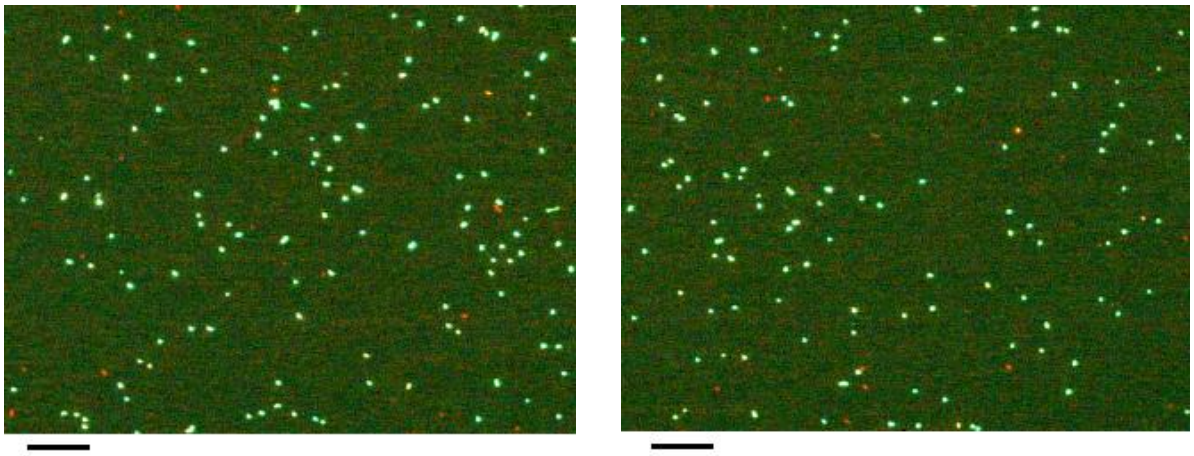

(a) (b)

Figure 4-6 The images taken from sample cells stained with dye before (a) and after (b) they passed through CNTs without electric field. The scale bars are 50 μm

A series of experiments were carried out with the operational voltage applied to the electrodes through chip carrier. AC voltages were supplied to the electrodes by a signal generator with the constant frequency of 100 kHz. It should be noted that even a normal DC voltage could be employed for cell lysis but would cause electrolysis and ohmotic heating. Therefore an AC field with high frequency is usually preferred to avoid electrolysis and consequent bubble generation. Nevertheless, the efficiency of AC field on cell lysis is diminished at very high frequencies [60]. We experimentally found that at the frequency of 100 kHz the bubble generation is minimized and the resulting electric field is effective to achieve lysis.

For each set of experiment, 50 μl of cell suspension was pumped into the channel and two microlitter of the suspension was picked up after the experiment for fluorescent analysis. The lysis rate of cells was monitored before and after they experienced the electric field. The sample cells before experiment was considered as reference sample. After each experiment, the number of lysed and live cells was counted and compared with the reference sample.

4.7 Results

To evaluate the enhancement of using CNT to reduce voltage requirement during cell lysis, the prepared cell medium was pumped into the channel with the constant flow speed of 10 ml/hour. Figure 4-7 shows the comparison of cell lysis yield rate at different voltages with and without CNT. The V=0 was applied to the device as a control experiment. The identical lysis rates of zero were resulted for the both channels, proving that there is no influence of CNT on cell survival without electric field. It is observed that cell lysis increased as the operational voltage was increased. As seen in Figure 4-7, complete lysis without the presence of CNTs is achieved when the voltage is greater than 85 V. Complete lysis with the CNT is accomplished when the voltage is only 40 V. The

corresponding cell lysis rate vs. operational voltage shows the enhancement of lysis in voltage reduction by using CNT.

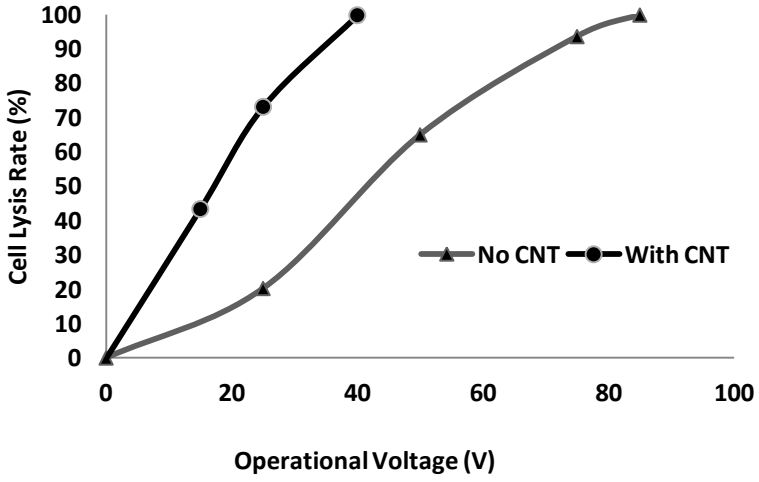

Figure 4-7 Comparison of cell lysis yield rate at different voltages with and without CNT. E. coli cells were continuously pumped into the microfluidic channel enclosed by electrodes

Since the point-of-care testing devices are miniaturized, the amount of lysate required for downstream processes is subsequently reduced. To provide enough amount of intracellular biomolecules such as DNA and proteins for biochemical analysis processes, improvement in throughput of sample-preparation processes, including cell lysis, has become more demanding. In our experiments, we characterized our device at two different flow rates, namely 20 ml/hour and 10 ml/hour, to investigate the effect of incorporating CNT on the throughput of cell lysis. We repeated the experiments of each set three times and four snapshots from each sample (similar to those depicted in Figure 4-6) were considered for cell counting. The results are presented in Figure 4-8.

With the higher flow rate, cells are exposed to the electric field for a shorter period of time and hence it is expected that the lysis yield rate is reduced, as seen in Figure 4-8. However, the device featuring CNT still maintains a higher lysis yield rate even at high flow rate. The enhancement of using CNT on the throughput of lysis is more considerable at lower operational voltages and higher flow rates. For example, at the voltage of 25 V, the lysis rate of the device with CNT is 10 times higher than the system without CNT at high flow speed. It demonstrates that the presence of CNT not only enhances the voltage requirements of electrical cell lysis but also it improves the throughput of the device.

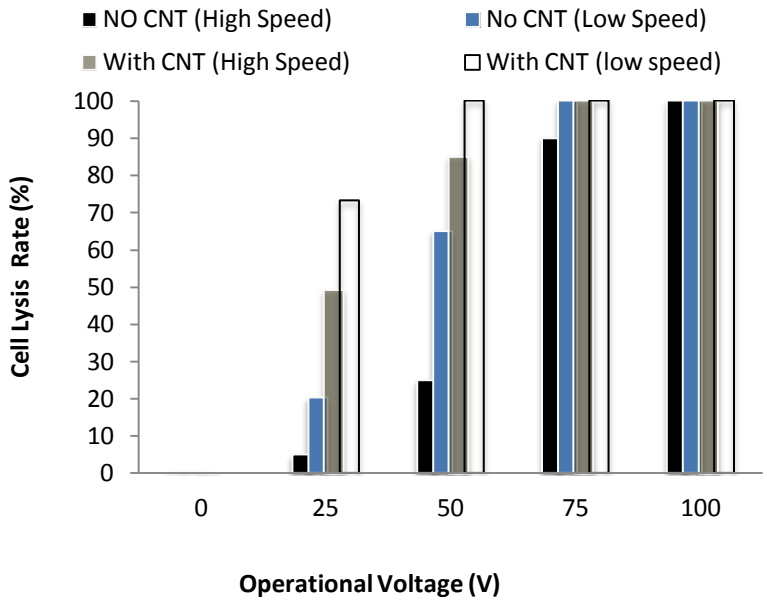

Figure 4-8 Comparison of cell lysis rate in two different speeds of stream flow with and without the presence of CNT on one electrode

4.8 Discussion

The CNT-mediated electrical cell lysis system presented in this chapter is considered as a great progress toward integration of cell lysis with other on-chip functions under the platform of LOC. However, there are a few points concerning the system that should be discussed.

The first point is that the fabrication methodology used for making the microchannels does not provide room for real-time microscopy. This drawback has been overcome by using fabrication methodology for making polyimide-based microchannel that will be presented in Chapter 5.

The second challenge in relation with cell lysis is the fluorescent microscopic technique that we have used for evaluation of lysis rate. By using the commercial viability kit with two nucleic acid-based stains (PI and SYTO 9), we have considered damage membrane as the sign for cell lysis in order to evaluate the efficiency of cell lysis with CNT compared with no CNT. The comparison results are reliable due to the fact that the compromised membrane of cells represents the increase in permeabilization of the cell membranes as a consequence of exposure to electric field. However, by considering that the release of nucleic acids from the cell membranes is the purpose of cell lysis, it would be more suitable if the amount of targeted lysis product (DNA, RNA or any cytoplasmic components of interest) were measured to confirm cell lysis has occurred.

As the last point, it should be noted that the enhancement of cell lysis achieved by the presence of CNT is analyzed in this chapter, but no investigation has been conducted for the influence of the configuration and orientation of CNT on the enhancement. The effect of morphology and density of CNT on field emission has been studied by Nilsson et al. [134]. They have predicted that CNTs in the distance of about two times of their height will reach the maximum field enhancement factor (α in equation 4.3). The prediction means further distance between CNTs does not increase the enhancement factor. The effects of inter-distance and morphology of CNT on the enhancement of cell

lysis should be theoretically and experimentally studied. We have suggested the study of these effective parameters for future works in section 6.3.

4.9 Conclusion

In this chapter, we have proposed a new electrical lysis system by incorporating aligned CNT on electrode. We proved that the incorporation of CNT reduces the required operational voltage to half due to the strengthened electric field at the tip of CNTs. Furthermore, CNT-featured lysis device maintains a higher lysis yield rate at high flow rate.

The presented approach enables integration of cell lysis with other LOC functions where the bulky instruments are going to be scaled down into a high-throughput point-of-care testing device and the requirement for a separate power supply needs to be diminished.

In addition to reduction in voltage requirements and improvement in throughput of cell lysis, strengthening electric field by CNT represents a useful approach for disrupting smaller cellular organelles and subunits that exist particularly in eukaryotic cells.

Chapter 5

Single Cell Electroporation by CNT-featured Microfluidic Chip

The content of this chapter has been published in Lab Chip, DOI: 10.1039/C3LC00014A

5.1 Introduction

Single cell lysis refers to the membrane disruption of individual cells in order to release and collect the intracellular components. Cell lysis is a part of sample-preparation procedures through which the lysis products, namely DNA, RNA and proteins, are provided for bio-genetics and point-of-care testing devices. Microelectromechanical systems (MEMS) have opened up tremendous possibilities for scaling down bulky laboratory instruments into micro-size chips with higher accuracy and sensitivity so that distinctions between individual cells can be analyzed. It has been understood that when bulky groups of cells are analyzed, the information obtained is averaged over a vast number of cells. As a result, individual characteristics are diminished. Therefore, single cell lysis has been of huge interest recently [65].

Here, we report on application of CNTs for electroporation of mammalian cells. CNT has been widely utilized in MEMS application due to its unique specifications. The greatly high aspect ratio of CNT enhances electric field at its sharpest point, which is the tip of CNT. This well-known phenomenon has been broadly used in field emission where CNT acts as an electron-gun emitter. CNT has been widely utilized as an electron source in field emission (FE) [135]. In applications of CNT in FE, the enhancement field at the tip of CNT, (which is applied in electroporation here), has been widely studied. The enhanced field by CNT is discussed under the physics of "lightning rod effect"

which justifies accumulation of charges over the sharpest feature of an object, thus leading to strongest electric field.

We have presented the enhancement of lysis of bacteria cells in terms of throughout and voltage reduction in Chapter 4. In this chapter, we examine the effect of field enhancement by CNT on electroporation of single mammalian cells.

5.2 Fabrication of CNT-embedded microfluidic chip

Microfluidic channels were made of polyimide sheets (DuPont Kapton FN 300FN929), ITO-coated slides (Sigma Aldrich, 8-12 Ω/sq, Cat. No. 703192) and customized CNT-coated substrates (Xintek Inc, North Carolina, USA). The pattern of microchannel was cut out the polyimide sheet by using 10.6 μm CO_2 laser engraving system (Universal Laser Systems, VLS2.30). As demonstrated at the left side of Figure 5-1, the polyimide sheet with the thickness of 75 μm was sandwiched between an ITO-coated microscope slide and a stainless steel sheet on which three patches of aligned CNT are pre-coated. The CNT coating by Xintek Inc. is explained in section 4.3. Inlet and outlet holes are featured through the stainless steel substrate at the sides of each CNT coatings.

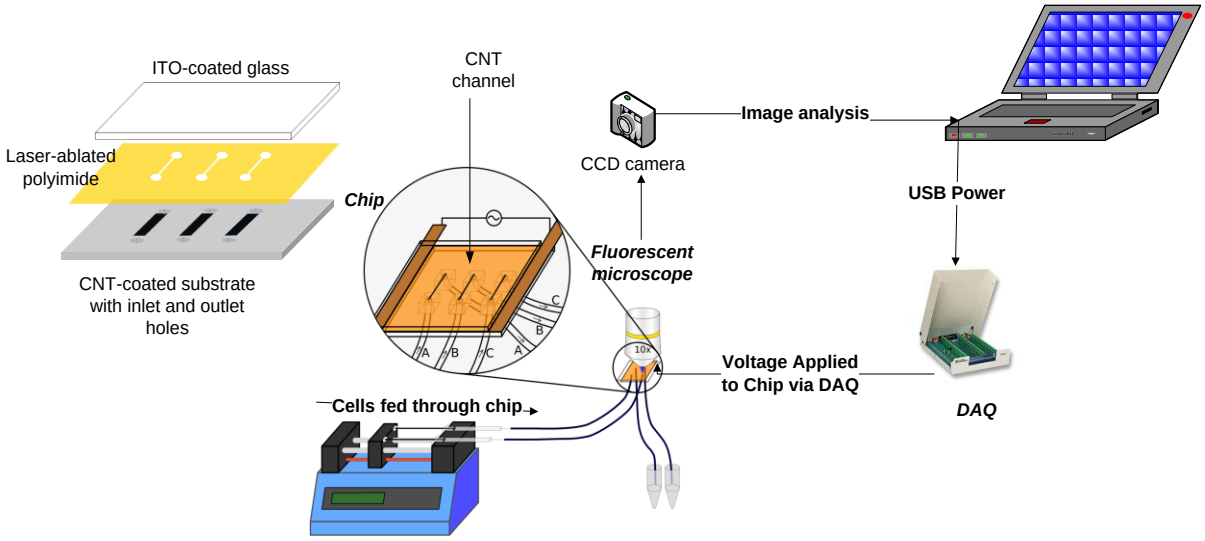

Figure 5-1 Simplified illustration of the set-up for cell electroporation experiment. The chip components (shown in left) are thermally bonded under pressure. Polyimide sheet has been sandwiched between the substrates to structure microchannels

The polyimide sheet has thin layers of Teflon FEP fluoropolymer on both sides as adhesion layers. Heated up to 280 ºC in vacuum, the Teflon layer rendered bonding to the top and bottom substrates under high pressure which was applied by a vise press. After bonding, six small blocks of prefabricated Polydimethylsiloxane (PDMS) were placed on the top of holes to secure attachment of tubing to the chip. Silicone tubing (VWR, Cat. No. CA62999-850) penetrated into the PDMS was connected to the channels' ports. The connection was then sealed by epoxy glue thickened with fumed silica. The tubes are attached to the tip of syringes in a pump.

Electrical connection to the ITO layer was attached, via extension in glass slide, to a conductive tape. Operational voltage was supplied by using a data acquisition system (DAQ) powered by USB port of a laptop. Fluorescent microscope (Nikon Eclipse E600FN) equipped with a CCD camera (CoolSNAP,

Turbo 1394 Series EZ) was used to take images of cells in microchannels in real-time. The overview of the set-up is schematically illustrated in Figure 5-1 and SEM images of a CNT array are depicted in Figure 5-2. Multi-walled CNTs with 2-6 nm diameter and 6 µm height are randomly distributed on a stainless steel with average concentration of 10^4/cm.

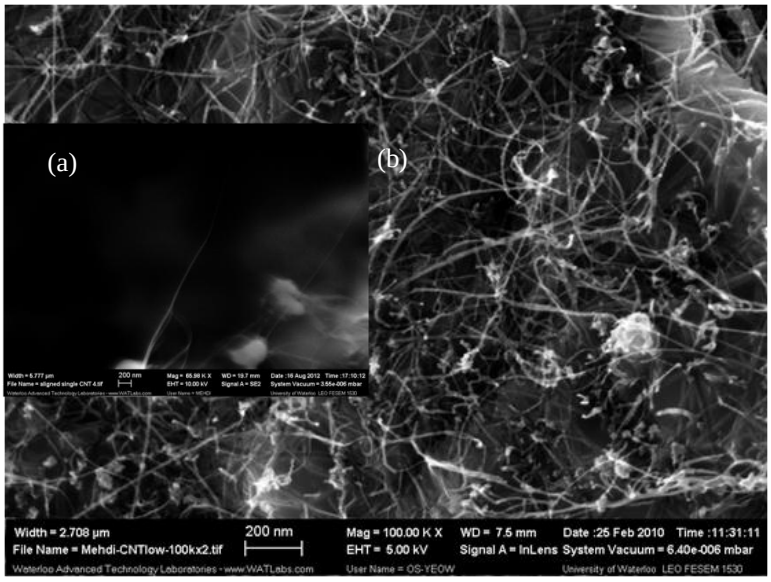

Figure 5-2 SEM image of randomly oriented CNT on stainless steel substrate a) side view of a single aligned CNT b) top view of a CNT array

5.3 Preparation of CHO cells

As a sample for mammalian cells, the Chinese Hamster Ovary cell line CHO-K1 (ATCC, Cat. No. CCL-61) was used in our experiments. Cell samples were prepared as follows: frozen cells were thawed in growth medium that was containing F-12 Kaighns (Fisher Scientific, Cat. No. SH3052601) and supplemented by 10% Fetal Bovine Serum (Fisher Scientific, Cat. No. SH3039602) and 1% Penicillin / Streptomycin (Bio Basic Canada, BS732). The cells were then transferred to a cell culture

flask followed by incubation at 37 °C with 5% CO_2. Cells were subcultured through the following procedure: the cell medium was aspirated from cell culture flask. After washing cells by PBS for two times, one milliliter of Trypsin 0.25% (Fisher Scientific, Cat. No. SH3004202) was added to detach cells. After five minutes incubation in room temperature, 7 ml of cell growth was added to the medium to stop trypsinization. Detached cells were then transferred into a tube and centrifuged at 300 g for 1 minute. The supernatant was discarded and electroporation buffer (10 mM phosphate buffer and 250 mM sucrose, pH 7.4) was replaced.

5.4 Experiments and results

Electroporation experiments were performed with two different types of chips: (i) with CNT; and (ii) without CNT. The prepared cells were loaded with Calcein AM dye, after being mixed with the dye solution in an incubator for 30 minutes at 37 ºC. The non-fluorescent Calcein AM which is cell-permeable hydrolyses to the green fluorescent Calcein inside the cell. The Calcein-AM loaded cells were then washed by the electroporation buffer in order to minimize the green background in the buffer. The concentration of cells was adjusted to 1×10^6/ml for the whole experiments. The cells were then pumped to the chips through the tubes. The pump was turned off once the cells reached the microchannel. When the target sample of cells became stationary, the pulse voltage with the frequency of 100 kHz was applied from the DAQ to the chip electrodes. The leakage of Calcein AM dye indicated electroporation. Electroporation of the target cells were imaged at frame rate of 2 Hz with exposure time of 30 ms.

The voltage of zero was applied to no-CNT and with-CNT chips to make sure cells are not automatically electroporated as a result of being in the channels or being in contact with CNTs. However, the intensity of green spots is reduced due to natural fluorescence decay under prolonged

excitation lighting. The fluorescent decay has been illustrated in Figure 5-3 for sample cells in with-CNT and no-CNT chips.

The normalized measured intensities are fitted with the exponential equation of $I=I_0 \exp^{(-t/\tau)}$, in which the decay time constant, τ, represents the time scale for dye deterioration. The time constants of 513 and 338 seconds are found for the sample cells in with and without CNT devices, respectively. Therefore the fluorescent decay is not significant during cell electroporation which normally occurred within a time scale of 10-20 seconds. And, no electroporation was indicated within this time scale when zero voltage was applied.

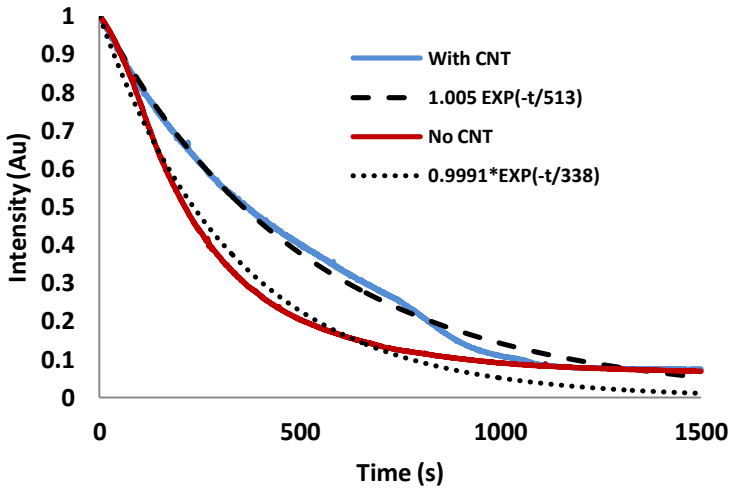

Figure 5-3 Fluorescent decay of Calcein AM-loaded cells stayed in the chips under zero voltage, along with the fitting exponential curves

For cell electroporation, the voltage of 3.75 V was applied to a no-CNT chip at the frequency of 100 kHz at t=5 s. As snapshots of cells in Figure 5-4 show, the cells experiencing electric field inside the channel were all electroporated.

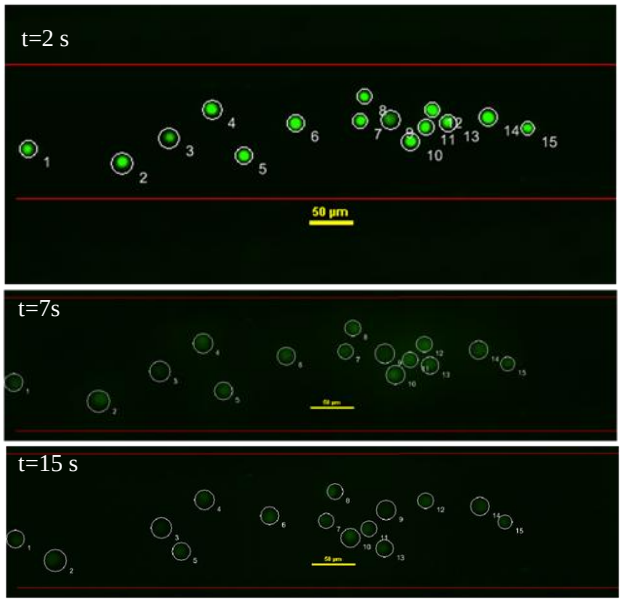

Figure 5-4 Electroporation of fifteen targeted cells loaded with green dye in a no-CNT microchannel. The walls of the channels are shown with red lines. The field (V=3.75 V) was applied at t=5 s; the dye leaked through the electroporated cell membranes. The yellow scale bar represents 50 µm

It shows the electric field provided inside the channel is strong enough to increase the permeability of CHO cell membrane so that the intercellular materials are released.

The same experiment was carried out with a CNT chip. It was interesting that the majority of targeted cells were electroporated as expected, except for a few cells that remained completely intact.

Snapshots of two examples of such survival have been depicted in Figure 5-5. It is an evidence that electroporation in CNT-featured device is position-dependent.

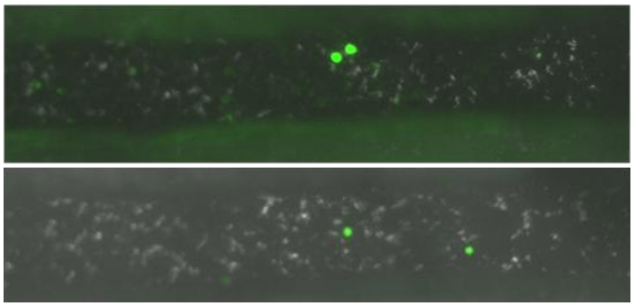

Figure 5-5 Examples of the few cells in a CNT-featured microchannel which survived high electric field

The survival against high electric field in a CNT-featured device should be due to the non-uniformity of electric field generated by the presence of CNTs. Electric field near the tips of aligned CNT is greatly enhanced due to the lightning rod effect. The enhancement field is found to be dependent on the aspect ratio of CNTs and the distance between them [136], even though there is no consensus in literature on enhancement factor (α in equation 4.3) for field enhancement at the apex of CNT arrays. The non-uniformity of electric field results in stronger field near the tips and weaker field at the base of CNTs. To show the concept, two aligned CNTs with the aspect ratio of 1000 and the inter-distance of 100 μm have been simulated. The details of simulation process are provided in Appendix B. The simulation results are shown in Figure 5-6. In the contour of electric field, demonstrated in Figure 5-6a, the high intensity of lines near the tips represents strong field while the low density of them represents weak field. The strength of electric field along the red line crossing the middle height of CNTs is shown in Figure 5-6b. Without CNT, the uniform electric field with the strength of 500

V/cm is provided (continuous line), by ignoring the fringe effect near the edges. With CNTs, the non-uniform field is achieved while its maximum strength is about half of that without CNTs (dotted line). This results prove that electroporation of cells at the CNT-coated electrode is position-dependent so that cells staying near the base of CNTs can survive high electric field. However the inter-distance of CNTs can be adjusted to minimize the chance of such survival.

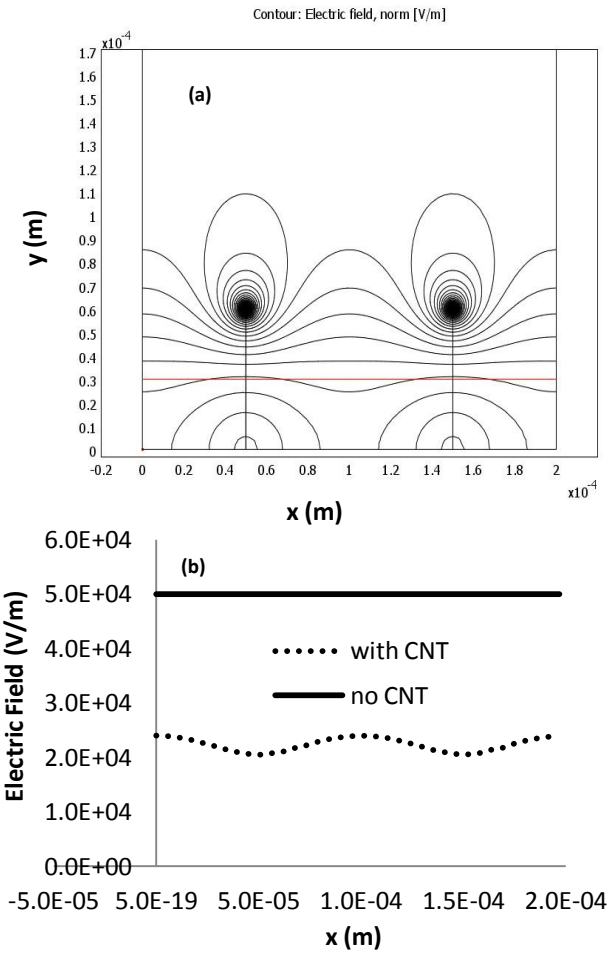

Figure 5-6 Simulation results for two aligned CNTs with the aspect ratio of 1000 and the inter-distance of 100 µm. The variation of strength of electric field along the red line in graph (a) is shown in graph (b).

The second experiment was performed under the operation voltage of 3 V. The electroporation was imaged from time t=0 until t=30 s. The electric field turned on at the time t=5 s. To quantify electroporation rate, the mean intensity of green spots were measured and normalized for targeted cells of each device in order to set the maximum to one. The image analysis results have been depicted in Figure 5-7. The number of target cells for no-CNT chip and with-CNT is 15 and 16, respectively. It is seen that at this voltage, the electric field is not strong enough to electroporate all the cells. It is also noticeable that single cells show individual rate of leakage through their membranes. Averagely, with the presence of CNT, electroporation was completed within a shorter time compared to when there was no CNT. It is also obvious that more cells have experienced electroporation when exposed to the field of CNT.

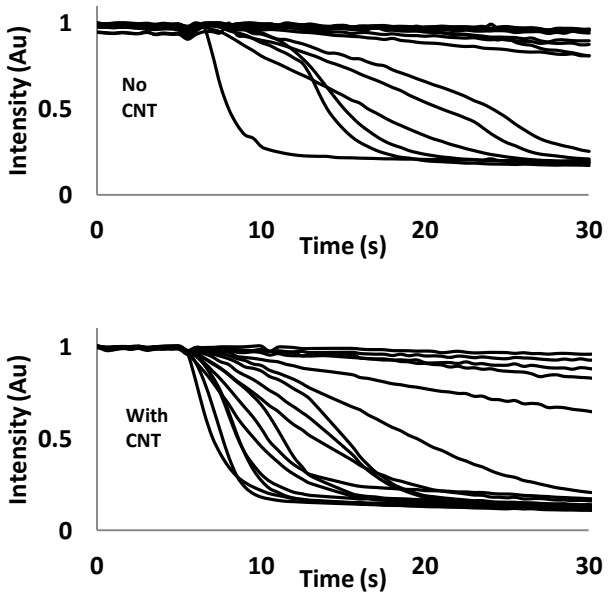

Figure 5-7 Degradation of the mean intensity of Calcein AM-loaded CHO cells when exposed to the field (V= 3 V) applied at t=5 s

To compare electroporation rate more accurately, more experiments were performed and the number of electroporated cells and survived ones was compared for a population of 95 cells and 54 cells in with-CNT and no-CNT devices, respectively. The result is illustrated in Figure 5-8. The electroporation rate is calculated based on the number of cells whose mean intensity has reduced (from 1 to 0.2), over the total targeted cells. It is found that the electroporation rate at the voltage of 3 V is 72% higher compared to a no-CNT chip

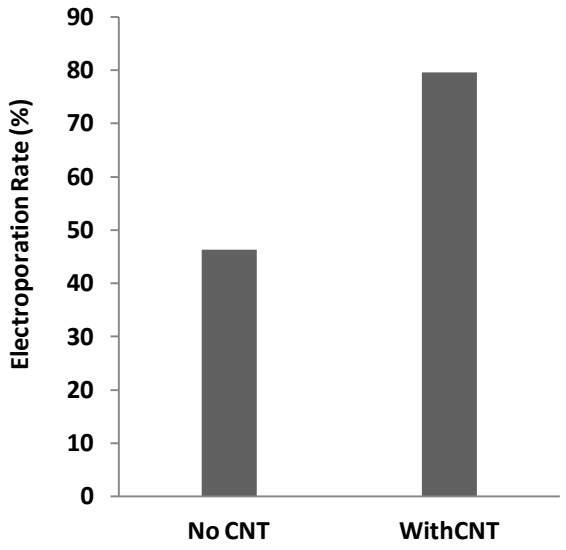

Figure 5-8 Comparison of electroporation rate of no-CNT and with-CNT devices for V=3 V

5.5 Discussion

This project has attained two goals: i) enhancement of single cell lysis by utilizing the field enhancement of CNT in cell lysis, ii) development of a great approach to integrate CNT with microfluidic channels. However, there are some challenges involved with CNT-mediated cell lysis that are discussed here.

Concerning the integration of CNT with electrical cell lysis, it is important to know how much of nucleic acids attach to CNTs after electroporation. It is known that DNA and proteins tend to attach CNT by their nature, but it occurs in a considerable quantity under certain conditions that are not met in our experiments. The adsorption of double-stranded DNA (dsDNA) on MWNT has been reported to occur after MWNTs are mixed with DNA solution for 24 hours [137]. In our experiments, the device electroporates cells in a few seconds and the lysate can be taken out of the chip immediately after. Therefore, we do not expect considerable adsorption of DNAs to CNTs within the short time. Modifications/functionalizations of CNTs, such as covalent functionalization of CNT, is often performed to promote attachment of DNA [138–140]. The fact that a broad range of functionalization techniques have been developed demonstrates that the adsorption is not significant without a functionalization process. Dwyer et al. [140] have presented the use of CNT for immobilization of DNA via covalent functionalization of CNT. They found from their control experiment that DNA does not interact with CNT non-specifically. They have reported near zero immobilization in experiments without involving functionalization. The adsorption of biomolecules to CNT can be minimized in different ways. It is reported that Single-walled CNTs (SWNTs) have fewer defects when compared to MWNTs so that they have fewer sites for immobilization of DNA [141]. Therefore SWNT is a preferred candidate if adsorption is to be minimized or even eliminated. Furthermore, CNTs could be functionalized in a way such that any absorption of DNA/protein can be minimized. .

Notwithstanding with the above-mentioned reasons, we were still interested to measure the content of DNA released out of the cell as a result of cell lysis. Cell lysis refers to the disruption of the cell membrane, with the goal of releasing the intracellular components out of the cell. Therefore, comparison between the content of DNA collected from the CNT chip with that collected from a no-CNT chip could explain the enhancement of cell lysis by CNT in terms of the obtained DNA. We followed a protocol of a commercial DNA extraction to measure the amount of DNA released from

the chips and compared them with a baseline as the reference for the maximum amount of DNA obtained after chemically lysing cells with a lysis buffer.

After cells experienced cell lysis in the chips, the lysate was collected and DNA extraction of the lysate was performed. This was done using a DNA extraction kit (illustra tissue and cells genomicPrep Mini Spin Kit, GE), designed for use with mammalian tissue and cells. The resulting DNA suspension was analysed using a spectrophotometer (Thermo Scientic Nanodrop-1000). Because the kit includes a chemical lysis step, it would lyse all the cells including those not lysed by the microfluidic chip. To avoid this, the lysate was first centrifuged at 2000 g to drive the live cells to the bottom of the tube while keeping the lysate in the suspension. The supernatant was used for the DNA extraction measurements. However, the results of these attempts at measuring lysis were inconclusive because the measured DNA content in lysate did not match the baseline. A very weak absorption across the entire spectrum was observed that could be indicative of sample contamination rather than the DNA content. It is most likely due to the fact that lysis of plasma membrane does not necessarily leads to disruption of nuclear membrane wherein DNA is enclosed.

The concept of selective lysis of nuclear membrane or plasma membrane has not been much addressed yet in the literature of LOC. Lu et al. [60] have presented a modeling scheme to predict an optimum frequency of electric field that causes the disruption of plasma membrane but not intracellular organelles. The basic of it is understood from the equation (4.2) that the charging time constant (representing the time required for transmembrane potential to be charged) is proportional to the size of the structure that is targeted for lysis. In AC fields, the charging time constant is determined by the frequency of electric field. Based on the modeling results of Lu et al. [60] it is found that 100 kHz frequency, which we have used throughout our experiments, is effective on lysis of

plasma membrane but should not be much effective on disruption of nuclear membrane. This assumption most likely explains why we could not detect much DNA in our experiments.

5.6 Conclusions

We reported on the field enhancement by CNT applied in cell electroporation. The point of the work is to show how enhanced electric field near the tips of CNT improves cell electroporation. To test the hypothesis, a straight-forward fabrication methodology was presented to embed randomly aligned CNT in a micro-electric channel. The cells exposed to electric filed inside the channel leaked their intercellular components. Calcein AM as a cell-permeant dye was used to show electroporation in real-time under fluorescent microscopy. The results show that at a lower voltage than the threshold (3V), the CNT chip provides 72% higher electroporation rate. The proposed device eases integration of cell electroporation with high-voltage requirements with other on-chip functionalities with low-voltage requirements.

Chapter 6

Contributions, Conclusions and Future Work

This thesis presents new developments in electrical cell lysis realized in lab-on-a-chip (LOC). LOC has raised unique possibilities to scale down cell manipulation systems into cellular level to achieve higher performance and accuracy. Among the systems employed for cell disruption, electroporation without chemical reagents provides many advantages but suffers from some limitations. Contributions of this work are the proposed schemes to overcome the limitations.

6.1 Contributions

The three major contributions are presented as follow:

1. To overcome the high-cost and difficult lithography processes involved in fabricating cell lysis microchips, a new methodology of making electro-microfluidic channels is proposed. Mostly derived from semiconductor industry, photolithography is currently the common method for fabricating microfluidic chips. Traditional lithography consists of several micromachining processes with high-tech instrument that is expensive, complicated and labour-intensive. We have developed a fast and easy-to-implement methodology of making electrical microfluidic devices using a 30 W CO_2 laser for patterning polyimide. Polyimide is used in microfluidic devices especially in those for biological treatments. It is because polyimide has excellent properties such as good thermal and chemical stability, low absorption of small molecules that makes it fairly biocompatible. Laser ablation of polyimide is fast, detailed, controllable and very flexible, and has been used in microfluidic fabrication. Nonetheless, laser systems are mostly excimer lasers that are massive with sophisticated

systems for handling the toxic gas used. Different from the recently-emerged idea of making biochips entirely out of polymers, we used ITO-coated glass slides in our chips as substrates. This removes the issue of thermal expansion mismatch when depositing metal on polymer. Unlike the common bonding techniques with involvement of solvents, we have bonded polyimide to ITO-coated glass by the use of thin layers of pre-coated FEP on polyimide, as adhesion layers. It is carried out via simple thermal lamination techniques. Optical transparency of ITO-coated glass slides enables convenient fluorescent microscopy, with high magnification, in real-time. By means of the fabricated lysing devices, the voltage produced by a USB port of a computer is found high enough for electroporating CHO cells. Although the proposed methodology is applied in electroporation, it has the potential to be utilized in any other electro-functional mechanisms such as cell/particle separation by DEP, described in section 6.3 as a future work.

2. To ease the high voltage requirement and to improve the low throughput of MEMS-based cell lysis devices, incorporation of CNT into electrical cell lysis has been presented. CNT has been broadly integrated with microdevices due to its unique physical, electrical and mechanical properties suitable for MEMS applications. We proposed taking advantage of the substantially-high aspect ratio of CNT in order to manipulate distribution of electric field so that it becomes more effective on cell lysis. To prove the proposed hypothesis, we have fabricated prototypes of microchannels in which one electrode is coated by vertically aligned CNT. Bacteria cells are passed through the forest of aligned CNT in the microchannel, experiencing non-uniform electric field that is much stronger near the tip of CNTs. Therefore, lower voltages supplied to the chip result in enhanced electric field or, alternatively, the locally-enhanced electric field performs cell lysis in a shorter time. The former outcome means a reduction in operational voltage and the latter represents

improvement in throughput of cell lysis.

3. The application of CNT in cell lysis has been further developed by utilizing CNT in single cell electroporation. We have advanced the microchannel fabrication methodology so that CNT-featured microfluidic chip with electrical functionality has been created. The fabricated electroporation device is capable of performing single cell electroporation of mammalian cells with higher efficiency. The fluorescent microcopy technique has been revised so that electroporation of individual cells through the forest of CNT is feasible in real time. The effect of the enhanced electric field by CNT on electroporation of CHO cells has been studied and the voltage requirement of it has been compared with a no-CNT device. In addition to voltage reduction for mammalian cell electroporation, the achievement toward integration of pre-synthesized CNT with microfluidic chips is considerable. The proposed integration scheme applied in cell electroporation can be employed for other applications in which CNT is desired to be placed inside microchannels.

6.2 Conclusions

The followings are the summarized conclusions of the thesis:

1. Among the variety of principles employed to perform cell lysis, electrical method is the best candidate for cell lysis to be integrated with other MEMS-based functions. However, high-cost and complexity in embedding electrodes in microchannels, along with the high voltage requirements for cell lysis as well as the low throughput of flow-through microfluidic devices are found the main limitations in electrical cell lysis.
2. We have presented a new methodology of fabricating electro-microfluidic chips for cell electroporation. The methodology combined several low-cost and straightforward techniques that lead to realization of micro-channels with electrical functionalities and suitability for

real-time microscopy. The performance of the fabricated chips has been tested on cell electroporation. The results confirm the feasibility of the use of the methodology in making electrical cell manipulation systems.

3. We have introduced the use of CNT in electrical cell lysis. Microfluidic chips with and without CNT have been fabricated and bacterial lysis has been performed. The enhancement by the use of CNT is evaluated in terms of voltage reduction and throughput improvement. The results show that by integrating CNT in electrical lysis, the required voltage for full lysis of bacteria is reduced by half and the lysis throughput at low voltages is improved by ten times.
4. We have exploited the electric field enhancement by CNTs to realize low-voltage single cell electroporation. A microchip with embedded aligned CNTs has been developed to test the effect of the enhanced electric field on electroporation of mammalian CHO cell. The results show that at a voltage as low as 3 volt, the electroporation yield rate is increased by 72% with the incorporation of CNT. This enhancement is a promising advancement towards integration of low-voltage electroporation with other low-voltage cell manipulation techniques.

6.3 Future Works

The following suggestions can be considered for the continuation of the work:

1. The influence of the form of electric field on cell electroporation has been widely studied but there is not yet a report on the optimum number of times that cells require to experience high field until electroporated. The results of the study will be valuable because of two reasons: first, the lysis products may be defected as a result of being exposed to electric field for more times

than required and second, the lysing process or the size of the lysis chip will be optimized if the optimum number of field exposure is known.

The study can be carried out by following the methodology of making cell lysis devices presented in Chapter 3, with some revisions. Instead of the ITO-coated substrates, glass slides can be used as the top and bottom substrates but the inlet and outlet fluidic ports are made with metal tubes. The straight channels have a number of orifice gates through which the cells experience high electric field while passing. A schematic view of such device is shown in Figure 6-1. A DC power supplier is enough to apply voltage to the metal inlet and outlet ports that are acting as electrodes as well.

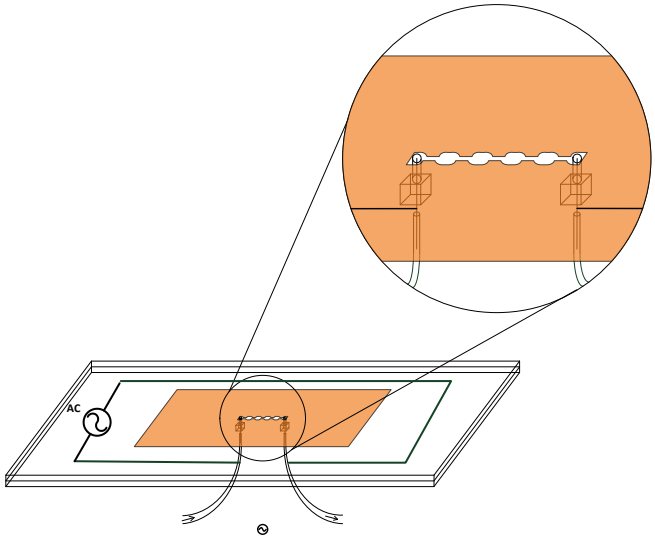

Figure 6-1 Illustrative scheme of the microchannels capable of lysing cells while experiencing high field at the orifice gates

Electric field along the channel will be non-uniform due to the variation of the cross-section of microchannels, as simulation result shows a sample in Figure 6-2.

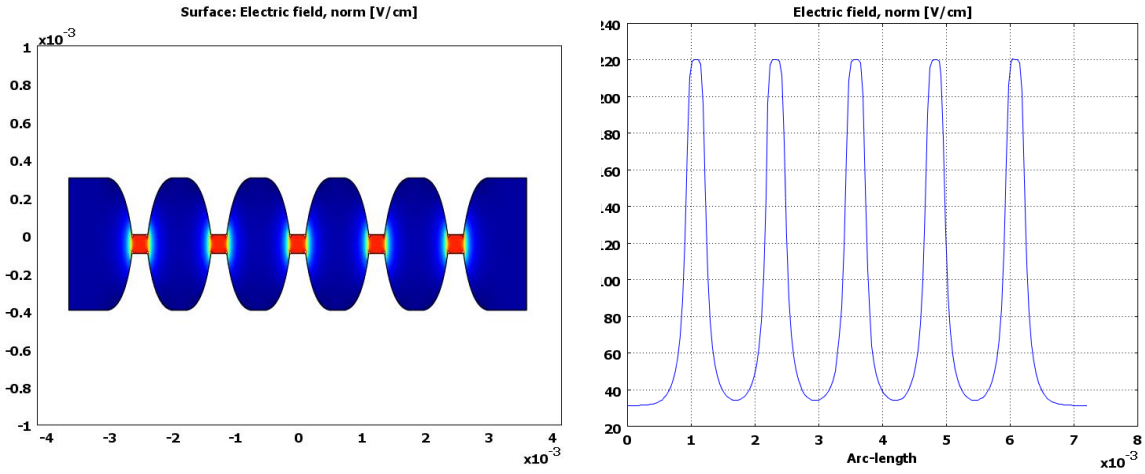

(a) (b)

Figure 6-2 a) A sample contour of electric field simulated by COMSOL in a microchannel with orifice gates, b) Variation of electric field along the middle of the channel

In this scheme, cells will experience alternating field not supplied with an AC signal generator but from a DC supplier inside a geometrically-varying channel. It makes fabrication and electrical operation straightforward. The number of spikes along the path of cells is considered as a representative of the number of times cells experience high electric field. The point of the research is to figure out the optimum number of field exposure to a certain type of biological cell until the cell is lysed. Individual cells can be tracked while passing through the gates and their health level can be monitored on-chip via fluorescent microscopic techniques, similar to the protocol that we followed for electroporation of CHO cells (described in Chapter 3). For the case of population cell lysis, microchannels with different number of gates can be

fabricated and off-chip fluorescent techniques can be utilized to analyze the lysis rate, similar to the one used for bacterial lysis (described in Chapter 4).

2. The fabrication methodology of electro-microfluidic channels (introduced in Chapter 3) can be implemented into other electrical cell manipulation techniques such as cell/particle separation through Dielectrophoresis, (DEP) concept. Separation under the physics of DEP refers to the phenomenon through which particles in a non-uniform electric field experience a force whose direction and strength is defined by the specifications of the particle and surrounding medium [142]. To achieve separation of two types of cells or particles, a micro-device with two diverging channels is suggested to be fabricated by following the fabrication procedure explained in Chapter 3. Two polyimide films, two ITO-coated glass slides and inlet/outlet tubes can be assembled in the order depicted in Figure 6-3. The pattern of each microchannel is cut off the polyimide sheet. The width of one channel must be wider than the other one.

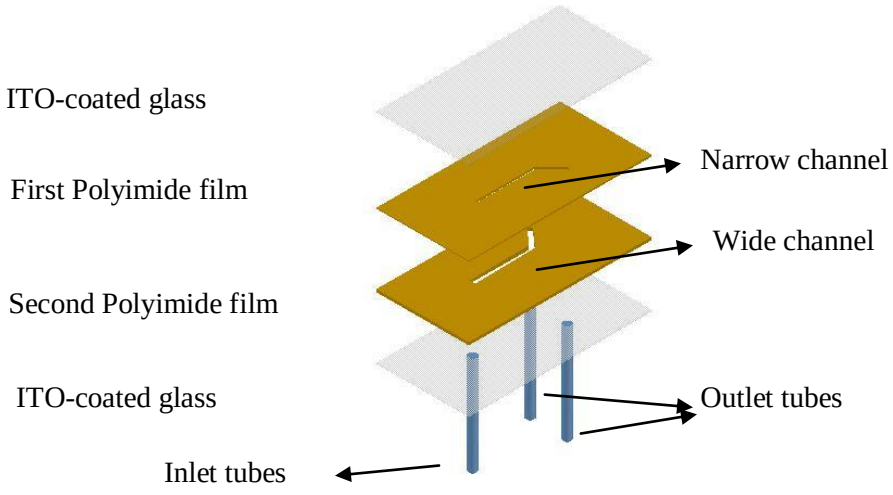

Figure 6-3 Schematic illustration of the assembly components of the microchip for cell/particle separation application

A simple simulation of the electric field at the step-shaped cross-section of the design reveals that elecric field will form non-uniformly in the channel so that cells or particles will approach toward either top or bottom of the channel, depending on DEP specifications. A sample of a non-uniform electric field across the separating channels is shown on the left side of Figure 6-4, and the variation of field along the vertical line (red line) at the middle of the cross section is shown on the right side of Figure 6-4. The top and bottom section of channel are in 100 µm and 200 µm width, respectively, and the height of each section is 50 µm. When particles are traveling toward the end of microchannels, the top and bottom sections of channel diverse. It leads to separation of the particles passing through the narrow section from those passing through the wide section.

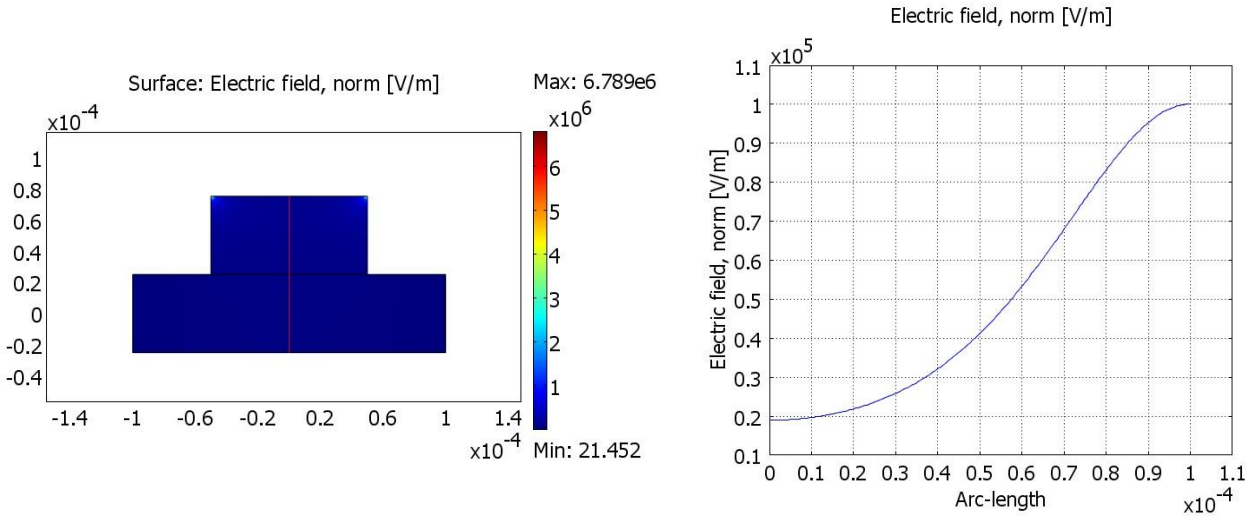

Figure 6-4 A sample simulation of electric field in a step-shaped channel (left); variation of the strength of electric field along the red line at the middle of channel (right). Dimensions are in cm.

3. As discussed in Chapter 4, the enhancement of cell lysis by means of CNT is studied in this thesis, but not on the influence of the configuration and orientation of CNT on the enhancement. A sample simulation of strengthened field around a group of three CNTs, shown in Figure 6-5, demonstrates that the adjacent CNTs have influence on the electric field of each other. The variation of electric field along the line across the tip of the three CNTs, depicted in Figure 6-5b, shows that the maximum strength of field at the tip of the middle CNT is lower than the other two.

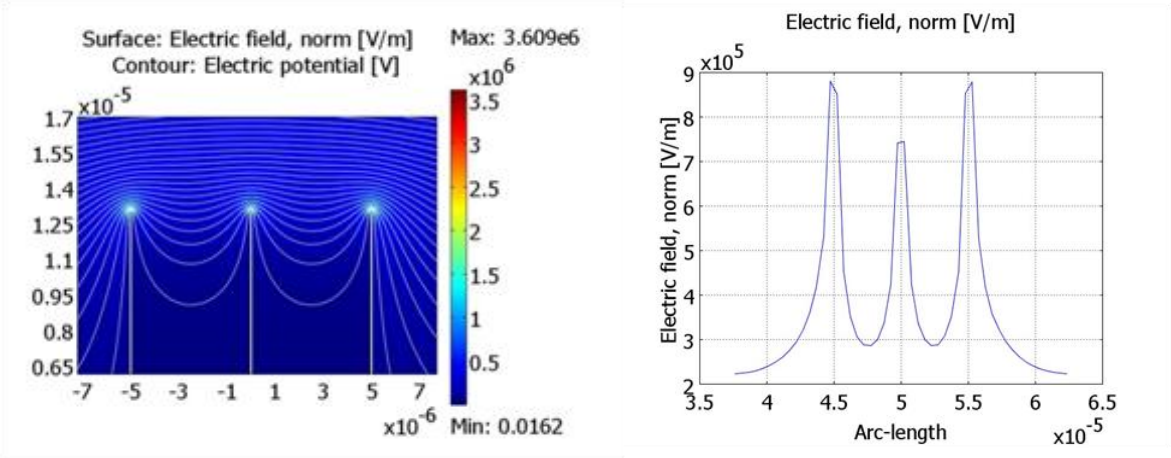

Figure 6-5 a) Sample of simulation results for the electric field and potential lines for three CNTs in 5μm distant away, b) Strength of electric field varying along the line across the tip of CNTs

To find the optimal inter-distance of CNTs for cell lysis, a parameter -we call it "*effective lysis area*"- can be defined. The effective lysis area is the area in which the electric field is high enough for cell lysis to the whole area of interest. The largest effective lysis area represents the

maximum enhancement of cell lysis. The variation of it against the inter-distance of CNTs will obtain the optimal state in which CNTs provide the maximum field enhancement. As a suggestion for the continuation of the application of CNT in electrical lysis, the optimum configuration of CNT can be studied analytically and experimentally.

Appendix A

Fluorescence Spectroscopy and Data Analysis

Fluorescent spectroscopy has been widely used in cell biology to quantify the viability of cells. We quantified the lysis rate based on the fluorescence emission spectrum of tagged cells. We used fluorescent dye to determine cell lysis rate, using the live/dead backlight bacterial viability kit (Invitrogen) consisting of two separate components of SYTO 9 and propidium iodide. One milliliter of the prepared cell suspension was mixed with the dye containing 1.5 μl of SYTO 9 and 1.5 μl propidium iodide.

By using Fluorospectrometer (NanoDrop, Wilmington, USA), emission spectrum of stained cells was obtained when the excitation wavelength was centered at 485 nm. The amount of live and dead cells was quantified by the fluorescent emission intensities of the green (510-540 nm) and red (620-650 nm), respectively.

We prepared different volumes of live and dead cell suspensions to achieve known relative proportion of live to dead cells. The reference live cells were cultured by following the protocol explained in section 4.4 and the reference dead cells were obtained when the live cells were stayed at room temperature until they all died. Two microlitter of each suspension was excited at the wavelength of 485 nm under the fluorospectrometer, and the emission spectra of these suspensions of dead and live cells were recorded, as illustrated in the following figure. This graph is used as a reference for quantifying cell lysis rates. The integral of the intensity curves of the green and red emission represent the amount of live and dead cells, respectively.

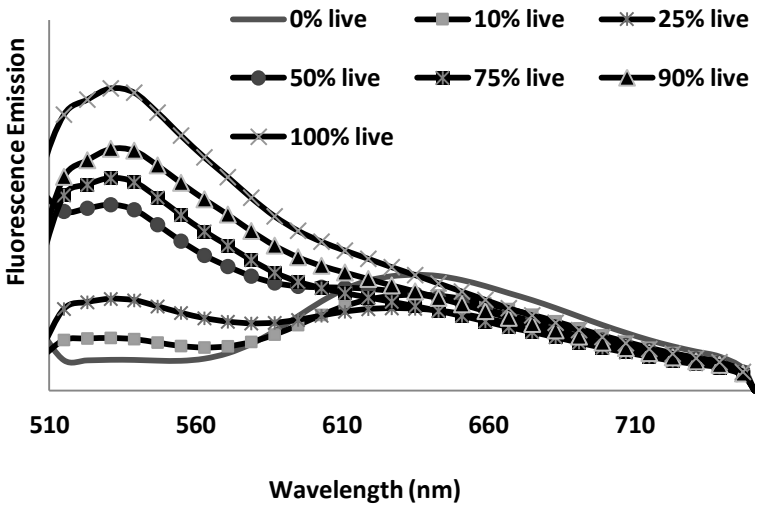

Reference emission spectra of various proportions of live and dead cells. The cells are stained with fluorescent dye and relative known proportions of live to dead cells are mixed. The integral of the intensity curves of the green and red emission represent the amount of live and dead cells, respectively

We calculated the ratio between these two integrals and fit a linear relationship between cell viability and the green/red fluorescence ratios, as shown in the graph below. We visually verified the cell viability by counting the green and red cell spots in the images of samples of cells taken through a fluorescent microscope before and after each experiment.

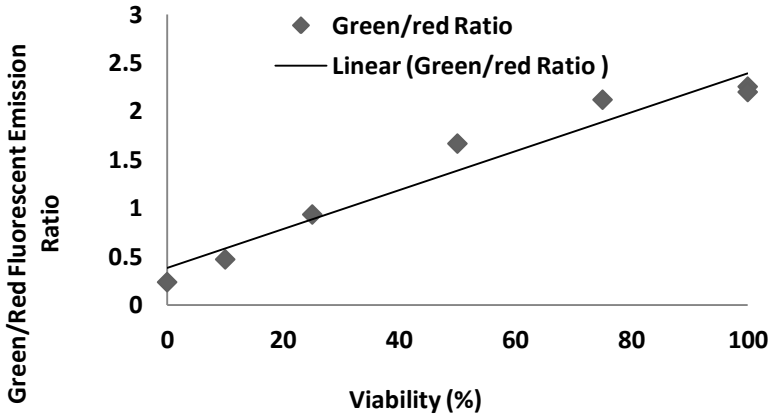

The fit of a linear relationship between the ratio of the green/red fluorescence intensity and viability rate of cells. The relation has been used as a reference to quantify cell lysis rate

Appendix B

Electrostatic Simulation

The 2-dimensional application of electrostatics of dielectric materials in COMSOL 3.5a has been used to simulate electric field between parallel electrodes with CNT arrays on one electrode[143]. The domain is a rectangle in 200 x 300 μm dimension. The CNT models are subtracted from the surrounding dielectric domain of air. Two CNTs in 60 nm diameter and 60 μm height are located at the bottom electrode with 100 μm distance between. As boundary conditions, the CNTs and the bottom electrode were grounded and the voltage of 15 V was applied to the top electrode. The condition of side walls were set as symmetric boundaries. Triangular mesh elements were applied in a non-uniform distribution, as created by the default settings of COMSOL. The maximum mesh density has been observed near the CNTs, illustrated in the following figure. To show the grid-size independency, the point x=100 and y= 30 μm has been considered as the reference point at which the strength of electric field with different number of mesh elements has been calculated. As seen, E at the reference point is not dependent on the mesh elements when more than 40,000 elements are created.

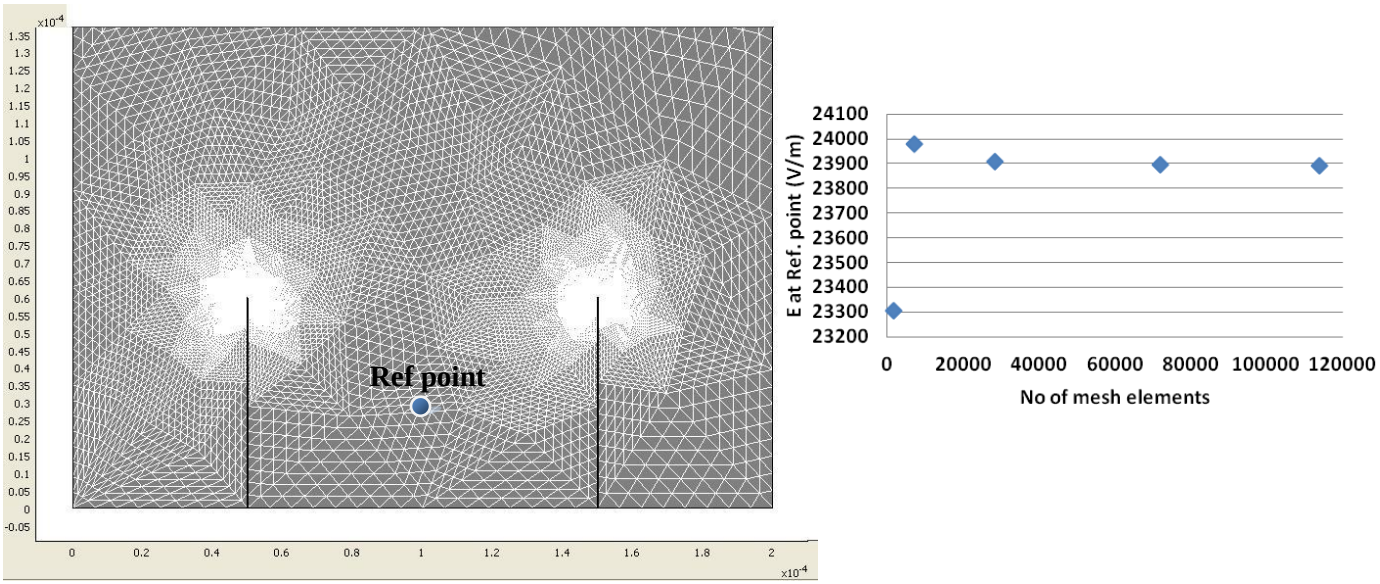

Scheme of mesh grids b) Strength of electric field (E) at the reference point (x=100 and y= 30 μm) vs. the number of mesh elements

Copyright Permissions

SPRINGER LICENSE
TERMS AND CONDITIONS

Jul 03, 2013

This is a License Agreement between University of Waterloo ("You") and Springer ("Springer") provided by Copyright Clearance Center ("CCC"). The license consists of your order details, the terms and conditions provided by Springer, and the payment terms and conditions.

All payments must be made in full to CCC. For payment instructions, please see information listed at the bottom of this form.

License Number	3181600429212
License date	Jul 03, 2013
Licensed content publisher	Springer
Licensed content publication	Biomedical Microdevices
Licensed content title	Fabrication of electro-microfluidic channel for single cell electroporation
Licensed content author	Mehdi Shahini
Licensed content date	Jan 1, 2013
Type of Use	Thesis/Dissertation
Portion	Full text
Number of copies	5
Author of this Springer article	Yes and you are the sole author of the new work
Order reference number	
Title of your thesis / dissertation	Developments on Cell Lysis Techniques In Lab on a chip Technologies
Expected completion date	Nov 2013
Estimated size(pages)	120
Total	0.00 CAD
Terms and Conditions	

Introduction

The publisher for this copyrighted material is Springer Science + Business Media. By clicking "accept" in connection with completing this licensing transaction, you agree that the following terms and conditions apply to this transaction (along with the Billing and Payment terms and conditions established by Copyright Clearance Center, Inc. ("CCC"), at the time that you opened your Rightslink account and that are available at any time at http://myaccount.copyright.com).

Limited License

With reference to your request to reprint in your thesis material on which Springer Science and

Business Media control the copyright, permission is granted, free of charge, for the use indicated in your enquiry.

Licenses are for one-time use only with a maximum distribution equal to the number that you identified in the licensing process.

This License includes use in an electronic form, provided its password protected or on the university's intranet or repository, including UMI (according to the definition at the Sherpa website: http://www.sherpa.ac.uk/romeo/). For any other electronic use, please contact Springer at (permissions.dordrecht@springer.com or permissions.heidelberg@springer.com).

The material can only be used for the purpose of defending your thesis, and with a maximum of 100 extra copies in paper.

Although Springer holds copyright to the material and is entitled to negotiate on rights, this license is only valid, subject to a courtesy information to the author (address is given with the article/chapter) and provided it concerns original material which does not carry references to other sources (if material in question appears with credit to another source, authorization from that source is required as well).

Permission free of charge on this occasion does not prejudice any rights we might have to charge for reproduction of our copyrighted material in the future.

Altering/Modifying Material: Not Permitted
You may not alter or modify the material in any manner. Abbreviations, additions, deletions and/or any other alterations shall be made only with prior written authorization of the author(s) and/or Springer Science + Business Media. (Please contact Springer at (permissions.dordrecht@springer.com or permissions.heidelberg@springer.com)

Reservation of Rights
Springer Science + Business Media reserves all rights not specifically granted in the combination of (i) the license details provided by you and accepted in the course of this licensing transaction, (ii) these terms and conditions and (iii) CCC's Billing and Payment terms and conditions.

Copyright Notice:Disclaimer
You must include the following copyright and permission notice in connection with any reproduction of the licensed material: "Springer and the original publisher /journal title, volume, year of publication, page, chapter/article title, name(s) of author(s), figure number(s), original copyright notice) is given to the publication in which the material was originally published, by adding; with kind permission from Springer Science and Business Media"

Warranties: None

Example 1: Springer Science + Business Media makes no representations or warranties with respect to the licensed material.

Example 2: Springer Science + Business Media makes no representations or warranties with respect to the licensed material and adopts on its own behalf the limitations and disclaimers

established by CCC on its behalf in its Billing and Payment terms and conditions for this licensing transaction.

Indemnity
You hereby indemnify and agree to hold harmless Springer Science + Business Media and CCC, and their respective officers, directors, employees and agents, from and against any and all claims arising out of your use of the licensed material other than as specifically authorized pursuant to this license.

No Transfer of License
This license is personal to you and may not be sublicensed, assigned, or transferred by you to any other person without Springer Science + Business Media's written permission.

No Amendment Except in Writing
This license may not be amended except in a writing signed by both parties (or, in the case of Springer Science + Business Media, by CCC on Springer Science + Business Media's behalf).

Objection to Contrary Terms
Springer Science + Business Media hereby objects to any terms contained in any purchase order, acknowledgment, check endorsement or other writing prepared by you, which terms are inconsistent with these terms and conditions or CCC's Billing and Payment terms and conditions. These terms and conditions, together with CCC's Billing and Payment terms and conditions (which are incorporated herein), comprise the entire agreement between you and Springer Science + Business Media (and CCC) concerning this licensing transaction. In the event of any conflict between your obligations established by these terms and conditions and those established by CCC's Billing and Payment terms and conditions, these terms and conditions shall control.

Jurisdiction
All disputes that may arise in connection with this present License, or the breach thereof, shall be settled exclusively by arbitration, to be held in The Netherlands, in accordance with Dutch law, and to be conducted under the Rules of the 'Netherlands Arbitrage Instituut' (Netherlands Institute of Arbitration).***OR:***

All disputes that may arise in connection with this present License, or the breach thereof, shall be settled exclusively by arbitration, to be held in the Federal Republic of Germany, in accordance with German law.

Other terms and conditions:

v1.3

If you would like to pay for this license now, please remit this license along with your payment made payable to "COPYRIGHT CLEARANCE CENTER" otherwise you will be invoiced within 48 hours of the license date. Payment should be in the form of a check or money order referencing your account number and this invoice number RLNK501058095. Once you receive your invoice for this order, you may pay your invoice by credit card. Please follow instructions provided at that time.

Make Payment To:

Copyright Clearance Center
Dept 001
P.O. Box 843006
Boston, MA 02284-3006

For suggestions or comments regarding this order, contact RightsLink Customer Support: customercare@copyright.com or +1-877-622-5543 (toll free in the US) or +1-978-646-2777.

Gratis licenses (referencing $0 in the Total field) are free. Please retain this printable license for your reference. No payment is required.

Bibliography

1. Andersson, H. & van den Berg, A. Microfluidic devices for cellomics: a review. *Sensors and Actuators B: Chemical* **92,** 315–325 (2003).

2. Huang, Y., Mather, E. L., Bell, J. L. & Madou, M. MEMS-based sample preparation for molecular diagnostics. *Analytical and bioanalytical chemistry* **372,** 49–65 (2002).

3. Yi, C., Li, C.-W., Ji, S. & Yang, M. Microfluidics technology for manipulation and analysis of biological cells. *Analytica Chimica Acta* **560,** 1–23 (2006).

4. Chen, X. & Cui, D.-F. Microfluidic devices for sample pretreatment and applications. *Microsystem Technologies* **15,** 667–676 (2009).

5. Kim, J., Johnson, M., Hill, P. & Gale, B. K. Microfluidic sample preparation: cell lysis and nucleic acid purification. *Integrative biology: quantitative biosciences from nano to macro* **1,** 574–86 (2009).

6. West, J., Becker, M., Tombrink, S. & Manz, A. Micro total analysis systems: latest achievements. *Analytical chemistry* **80,** 4403–19 (2008).

7. De Mello, A. J. & Beard, N. Focus. Dealing with "real" samples: sample pre-treatment in microfluidic systems. *Lab on a Chip* **3,** 11N (2003).

8. Wang, M., Kao, M., Liu, H., Kan, W. & Hsu, Y. A Microfluidic Device for Capture of Single Cells and Impedance Measurement. 711–714 (2007).

9. Morgan, H., Hughes, M. P. & Green, N. G. Separation of submicron bioparticles by dielectrophoresis. *Biophysical journal* **77,** 516–25 (1999).

10. Gascoyne, P. R. C. & Jody Vykoukal. Review Particle separation by dielectrophoresis. 1973–1983 (2002).

11. Chen, D. F., Du, H. & Li, W. H. Bioparticle separation and manipulation using dielectrophoresis. *Sensors and Actuators A: Physical* **133,** 329–334 (2007).

12. Zhang, C., Khoshmanesh, K., Mitchell, a & Kalantar-Zadeh, K. Dielectrophoresis for manipulation of micro/nano particles in microfluidic systems. *Analytical and bioanalytical chemistry* **396,** 401–20 (2010).

13. Enger, J., Goksör, M., Ramser, K., Hagberg, P. & Hanstorp, D. Optical tweezers applied to a microfluidic system. *Lab on a chip* **4,** 196–200 (2004).

14. Lichtenberg, J., de Rooij, N. F. & Verpoorte, E. Sample pretreatment on microfabricated devices. *Talanta* **56,** 233–66 (2002).

15. James S. G. Brookman. Mechanism of cell disintegration in a high pressure homogenizer. *Biotechnology and Bioengineering* **16,** 371–383 (1974).

16. Sauer, T., Robinson, C. W. & Glick, B. R. Disruption of native and recombinant Escherichia coli in a high-pressure homogenizer. *Biotechnology and bioengineering* **33,** 1330–42 (1989).

17. Rehacek, J., Products, N., Assistance, T. & Schaefer, J. Disintegration of Microorganisms in an Industrial Horizontal Mill of Novel Design. *Biotechnology and Bioengineering* **19,** 1523–1534 (1974).

18. Limon-Lason, J., Hoare, M., Orsborn, C. B., Doyle, D. J. & Dunnill, P. Reactor Properties of a High-speed Bead Mill for Microbial Cell Rupture. *Biotechnology and Bioengineering* **21,** 745–774 (1974).

19. Brookman, J. S. G. Further Studies on the Mechanism of Cell Disruption by Extreme Pressure Extrusion. *Biotechnology and Bioengineering* **17,** 465–479 (1975).

20. Englert, C. R. & Robinson, C. W. Disruption of Candida utiZis Cells in High Pressure Flow Devices *. *Biotechnology and Bioengineering* **XXIII,** 765–780 (1981).

21. Kido, H. *et al.* A novel, compact disk-like centrifugal microfluidics system for cell lysis and sample homogenization. *Colloids and surfaces. B, Biointerfaces* **58,** 44–51 (2007).

22. Kim, J. *et al.* Cell lysis on a microfluidic CD (compact disc). *Lab on a chip* **4,** 516–22 (2004).

23. Di Carlo, D., Jeong, K.-H. & Lee, L. P. Reagentless mechanical cell lysis by nanoscale barbs in microchannels for sample preparation. *Lab on a chip* **3,** 287–91 (2003).

24. Harju, S., Fedosyuk, H. & Peterson, K. R. Rapid isolation of yeast genomic DNA: Bust n' Grab. *BMC biotechnology* **4,** 8 (2004).

25. Tsuchido, T., Katsui, N., Takeuchi, a, Takano, M. & Shibasaki, I. Destruction of the outer membrane permeability barrier of Escherichia coli by heat treatment. *Applied and environmental microbiology* **50,** 298–303 (1985).

26. Holmes, D. S. & Quigley, M. A Rapid Boiling Method for the Preparation. **197,** 193–197 (1981).

27. Lee, A. L. & Sagar, S. A Method for Large-Scale Plasmid Purification. (2001).

28. Lander, R. J., Winters, M. a, Meacle, F. J., Buckland, B. C. & Lee, A. L. Fractional precipitation of plasmid DNA from lysate by CTAB. *Biotechnology and bioengineering* **79,** 776–84 (2002).

29. Zhu, K. *et al.* A continuous thermal lysis procedure for the large-scale preparation of plasmid DNA. *Journal of biotechnology* **118,** 257–64 (2005).

30. Zhu, K., Jin, H., He, Z., Zhu, Q. & Wang, B. A continuous method for the large-scale extraction of plasmid DNA by modified boiling lysis. *Nature protocols* **1,** 3088–93 (2006).

31. Belgrader, P. *et al.* PCR detection of bacteria in seven minutes. *Science (New York, N.Y.)* **284,** 449–50 (1999).

32. Waters, L. C. *et al.* Microchip device for cell lysis, multiplex PCR amplification, and electrophoretic sizing. *Analytical chemistry* **70,** 158–62 (1998).

33. Liu, R. H., Yang, J., Lenigk, R., Bonanno, J. & Grodzinski, P. Self-contained, fully integrated biochip for sample preparation, polymerase chain reaction amplification, and DNA microarray detection. *Analytical chemistry* **76,** 1824–31 (2004).

34. Tho, P., Manasseh, R. & Ooi, A. Cavitation microstreaming patterns in single and multiple bubble systems. *Journal of Fluid Mechanics* **576,** 191 (2007).

35. Hameed, B. A., Olsen, K. J., Lee, M., Lichtenheld, M. G. & Podack, E. R. Degradation and Cell Lysis Materials and Methods. **169,** (1989).

36. Podack, E. R., Young, J. D. & Cohn, Z. a. Isolation and biochemical and functional characterization of perforin 1 from cytolytic T-cell granules. *Proceedings of the National Academy of Sciences of the United States of America* **82,** 8629–33 (1985).

37. Takamatsu, H., Takeya, R., Naito, S. & Sumimoto, H. On the mechanism of cell lysis by deformation. *Journal of biomechanics* **38,** 117–24 (2005).

38. Feril, J. L. B., Kondo, T., Takaya, K. & Riesz, P. Enhanced ultrasound- induced apoptosis and cell lysis by a hypotonic medium. *International Journal of Radiation Biology* **80,** 165–175 (2004).

39. Prinz, C., Tegenfeldt, J. O., Austin, R. H., Cox, E. C. & Sturm, J. C. Bacterial chromosome extraction and isolation. *Lab on a chip* **2,** 207–12 (2002).

40. Lepeschkin, W. W. The Effect of Ultrasonic Waves on Serum Proteins. *Physical Chemistry* **53,** 335–343 (1949).

41. Martins, B. I., Raju, M. R., Hayes, T. L. & Tobias, C. a. Survival of cultured mammalian cells exposed to ultrasound. *Radiation and environmental biophysics* **14,** 243–50 (1977).

42. Neppiras, E. a. & Hughes, D. E. Some experiments on the disintegration of yeast by high intensity ultrasound. *Biotechnology and Bioengineering* **6,** 247–270 (1964).

43. Brayman, A. A., Doida, Y. & Miller, M. W. OOriginal Contribution. **18,** 701–714 (1992).

44. Belgrader, P. *et al.* A minisonicator to rapidly disrupt bacterial spores for DNA analysis. *Analytical chemistry* **71,** 4232–6 (1999).

45. Feril, L. B. *et al.* Enhancement of ultrasound-induced apoptosis and cell lysis by echo-contrast agents. *Ultrasound in Medicine & Biology* **29,** 331–337 (2003).

46. Ogino, C., Farshbaf Dadjour, M., Takaki, K. & Shimizu, N. Enhancement of sonocatalytic cell lysis of Escherichia coli in the presence of TiO2. *Biochemical Engineering Journal* **32,** 100–105 (2006).

47. Marentis, T. C. *et al.* Microfluidic sonicator for real-time disruption of eukaryotic cells and bacterial spores for DNA analysis. *Ultrasound in medicine & biology* **31,** 1265–77 (2005).

48. Warner, C. L. *et al.* A Flow-Through Ultrasonic Lysis Module for the Disruption of Bacterial Spores. *Journal of the Association for Laboratory Automation* **14,** 277–284 (2009).

49. Khanna, P. *et al.* Nanocrystalline diamond microspikes increase the efficiency of ultrasonic cell lysis in a microfluidic lab-on-a-chip. *Diamond and Related Materials* **18,** 606–610 (2009).

50. Fredricks, D. N., Smith, C. & Meier, A. Comparison of Six DNA Extraction Methods for Recovery of Fungal DNA as Assessed by Quantitative PCR. **43,** 5122–5128 (2005).

51. Reed, G. & Peppler, H. J. *Yeast Technology*. 355–366 (AVI Publshing Company, 1973).

52. Darbyshire, J. in *Topics in enzyme and fermentation biotechnology* **5,** 147–186 (John Wiley & Sons, 1977).

53. Heo, J., Thomas, K. J., Seong, G. H. & Crooks, R. M. A microfluidic bioreactor based on hydrogel-entrapped E. coli: cell viability, lysis, and intracellular enzyme reactions. *Analytical chemistry* **75,** 22–6 (2003).

54. Chen, X., Cui, D., Liu, C. & Cai, H. Microfluidic Biochip for Blood Cell Lysis. *Chinese Journal of Analytical Chemistry* **34,** 1656–1660 (2006).

55. Di Carlo, D., Ionescu-Zanetti, C., Zhang, Y., Hung, P. & Lee, L. P. On-chip cell lysis by local hydroxide generation. *Lab on a chip* **5,** 171–8 (2005).

56. Schilling, E. A., Kamholz, A. E. & Yager, P. Cell lysis and protein extraction in a microfluidic device with detection by a fluorogenic enzyme assay. *Analytical chemistry* **74,** 1798–804 (2002).

57. Tsong, T. Y. Electroporation of cell membranes. *Biophysical journal* **60,** 297–306 (1991).

58. Calvin, N. M. & Hanawalt, P. C. High-Efficiency Transformation of Bacterial Cells by Electroporation division. *Journal of Bacteriology* **170,** 2796–2801 (1988).

59. Lee, D. W. & Cho, Y.-H. A continuous electrical cell lysis device using a low dc voltage for a cell transport and rupture. *Sensors and Actuators B: Chemical* **124,** 84–89 (2007).

60. Lu, H., Schmidt, M. a & Jensen, K. F. A microfluidic electroporation device for cell lysis. *Lab on a chip* **5,** 23–9 (2005).

61. Park, K., Akin, D. & Bashir, R. Electrical capture and lysis of vaccinia virus particles using silicon nano-scale probe array. *Biomedical microdevices* **9,** 877–83 (2007).

62. Schuster, K. C., Reese, I., Urlaub, E., Gapes, J. R. & Lendl, B. Multidimensional information on the chemical composition of single bacterial cells by confocal Raman microspectroscopy. *Analytical chemistry* **72,** 5529–34 (2000).

63. Chao, T.-C. & Ros, A. Microfluidic single-cell analysis of intracellular compounds. *Journal of the Royal Society, Interface / the Royal Society* **5 Suppl 2,** S139–50 (2008).

64. Svahn, H. A. & van den Berg, A. Single cells or large populations? *Lab on a chip* **7,** 544–6 (2007).

65. Brown, R. B. & Audet, J. Current techniques for single-cell lysis. *Journal of the Royal Society, Interface / the Royal Society* **5 Suppl 2,** S131–8 (2008).

66. Zeng, Y., Novak, R., Shuga, J., Smith, M. T. & Mathies, R. a. High-performance single cell genetic analysis using microfluidic emulsion generator arrays. *Analytical chemistry* **82,** 3183–90 (2010).

67. Huang, W.-H., Ai, F., Wang, Z.-L. & Cheng, J.-K. Recent advances in single-cell analysis using capillary electrophoresis and microfluidic devices. *Journal of chromatography. B* **866,** 104–22 (2008).

68. Liu, J., Hansen, C. & Quake, S. R. Solving the "world-to-chip" interface problem with a microfluidic matrix. *Analytical chemistry* **75,** 4718–23 (2003).

69. Marcus, J. S., Anderson, W. F. & Quake, S. R. Parallel picoliter rt-PCR assays using microfluidics. *Analytical chemistry* **78,** 956–8 (2006).

70. Bontoux, N. *et al.* Integrating whole transcriptome assays on a lab-on-a-chip for single cell gene profiling. *Lab on a chip* **8,** 443–50 (2008).

71. Ocvirk, G. *et al.* -Galactosidase Assays of Single-Cell Lysates on a Microchip : A Complementary Method for Enzymatic Analysis of Single Cells. **92,** (2004).

72. Shoemaker, G. K., Lorieau, J., Lau, L. H., Gillmor, C. S. & Palcic, M. M. Multiple sampling in single-cell enzyme assays using CE-laser-induced fluorescence to monitor reaction progress. *Analytical chemistry* **77,** 3132–7 (2005).

73. He, M. *et al.* Selective encapsulation of single cells and subcellular organelles into picoliter- and femtoliter-volume droplets. *Analytical chemistry* **77,** 1539–44 (2005).

74. Zhang, H. & Jin, W. Determination of different forms of human interferon-gamma in single natural killer cells by capillary electrophoresis with on-capillary immunoreaction and laser-induced fluorescence detection. *Electrophoresis* **25,** 1090–5 (2004).

75. Zhang, H. & Jin, W. Single-cell analysis by intracellular immuno-reaction and capillary electrophoresis with laser-induced fluorescence detection. *Journal of chromatography. A* **1104,** 346–51 (2006).

76. Han, F. *et al.* Fast electrical lysis of cells for capillary electrophoresis. *Analytical chemistry* **75,** 3688–96 (2003).

77. Mcclain, M. A. *et al.* Microfluidic Devices for the High-Throughput Chemical Analysis of Cells. **75,** 5646–5655 (2003).

78. Sambrook, J. & Russell, D. *Molecular Cloning: A Laboratory Manual , Third Edition (3 Volume Set)*. (Cold Spring Harbor Laboratory Press, 2000).

79. Chomczynski, P. & Sacchi, N. The single-step method of RNA isolation by acid guanidinium thiocyanate-phenol-chloroform extraction: twenty-something years on. *Nature protocols* **1,** 581–5 (2006).

80. Price, C. W., Leslie, D. C. & Landers, J. P. Nucleic acid extraction techniques and application to the microchip. *Lab on a chip* **9,** 2484–94 (2009).

81. Christel, L. a, Petersen, K., McMillan, W. & Northrup, M. a. Rapid, automated nucleic acid probe assays using silicon microstructures for nucleic acid concentration. *Journal of biomechanical engineering* **121,** 22–7 (1999).

82. Cady, N. C., Stelick, S. & Batt, C. a. Nucleic acid purification using microfabricated silicon structures. *Biosensors and Bioelectronics* **19,** 59–66 (2003).

83. Tian, H., Hühmer, a F. & Landers, J. P. Evaluation of silica resins for direct and efficient extraction of DNA from complex biological matrices in a miniaturized format. *Analytical biochemistry* **283,** 175–91 (2000).

84. Hagan, K. a, Bienvenue, J. M., Moskaluk, C. a & Landers, J. P. Microchip-based solid-phase purification of RNA from biological samples. *Analytical chemistry* **80,** 8453–60 (2008).

85. Wen, J., Legendre, L. a, Bienvenue, J. M. & Landers, J. P. Purification of nucleic acids in microfluidic devices. *Analytical chemistry* **80,** 6472–9 (2008).

86. Dittrich, P. S., Tachikawa, K. & Manz, A. Micro total analysis systems. Latest advancements and trends. *Analytical chemistry* **78,** 3887–908 (2006).

87. Jakeway, S. C., de Mello, a J. & Russell, E. L. Miniaturized total analysis systems for biological analysis. *Fresenius' journal of analytical chemistry* **366,** 525–39 (2000).

88. Hong, J. W., Studer, V., Hang, G., Anderson, W. F. & Quake, S. R. A nanoliter-scale nucleic acid processor with parallel architecture. *Nature biotechnology* **22,** 435–9 (2004).

89. Irimia, D., Tompkins, R. G. & Toner, M. Single-cell chemical lysis in picoliter-scale closed volumes using a microfabricated device. *Analytical chemistry* **76,** 6137–43 (2004).

90. Lee, C.-Y., Lee, G.-B., Lin, J.-L., Huang, F.-C. & Liao, C.-S. Integrated microfluidic systems for cell lysis, mixing/pumping and DNA amplification. *Journal of Micromechanics and Microengineering* **15,** 1215–1223 (2005).

91. Becker, H. & Gärtner, C. Polymer microfabrication technologies for microfluidic systems. *Analytical and bioanalytical chemistry* **390,** 89–111 (2008).

92. Yoo, J.-C., La, G.-S., Kang, C. J. & Kim, Y.-S. Microfabricated polydimethylsiloxane microfluidic system including micropump and microvalve for integrated biosensor. *Current Applied Physics* **8,** 692–695 (2008).

93. Brown, L., Koerner, T., Horton, J. H. & Oleschuk, R. D. Fabrication and characterization of poly(methylmethacrylate) microfluidic devices bonded using surface modifications and solvents. *Lab on a chip* **6,** 66–73 (2006).

94. Abgrall, P. *et al.* A novel fabrication method of flexible and monolithic 3D microfluidic structures using lamination of SU-8 films. *Journal of Micromechanics and Microengineering* **16,** 113–121 (2006).

95. Metz, S., Holzer, R. & Renaud, P. Polyimide-based microfluidic devices. *Lab on a chip* **1,** 29–34 (2001).

96. Richardson, R. R., Miller, J. a & Reichert, W. M. Polyimides as biomaterials: preliminary biocompatibility testing. *Biomaterials* **14,** 627–35 (1993).

97. Toepke, M. W. & Beebe, D. J. PDMS absorption of small molecules and consequences in microfluidic applications. *Lab on a chip* **6,** 1484–6 (2006).

98. Haraldsson, K. T. *et al.* 3D polymeric microfluidic device fabrication via contact liquid photolithographic polymerization (CLiPP). *Sensors and Actuators B: Chemical* **113,** 454–460 (2006).

99. Oh, S. R. Thick single-layer positive photoresist mold and poly(dimethylsiloxane) (PDMS) dry etching for the fabrication of a glass–PDMS–glass microfluidic device. *Journal of Micromechanics and Microengineering* **18,** 115025 (2008).

100. Yin, H. *et al.* Microfluidic Chip for Peptide Analysis with an Integrated HPLC Column, Sample Enrichment Column, and Nanoelectrospray Tip. *Analytical Chemistry* **77,** 527–533 (2005).

101. Kim, J. & Xu, X. Excimer laser fabrication of polymer microfluidic devices. **15,** 255–260 (2003).

102. Lee, D. W. & Cho, Y.-H. A continuous electrical cell lysis device using a low dc voltage for a cell transport and rupture. *Sensors and Actuators B: Chemical* **124,** 84–89 (2007).

103. Liu, C. C. & Cui, D. F. Design and fabrication of poly(dimethylsiloxane) electrophoresis microchip with integrated electrodes. *Microsystem Technologies* **11,** 1262–1266 (2005).

104. Rajaraman, S., Noh, H. (Moses), Hesketh, P. J. & Gottfried, D. S. Rapid, low cost microfabrication technologies toward realization of devices for dielectrophoretic manipulation of particles and nanowires. *Sensors and Actuators B: Chemical* **114,** 392–401 (2006).

105. Kasahara, T. *et al.* Microfluidic organic light emitting diode (OLED) using liquid organic semiconductors. in *2012 IEEE 25th International Conference on Micro Electro Mechanical Systems (MEMS)* 1069–1072 (IEEE, 2012). doi:10.1109/MEMSYS.2012.6170256

106. Shin, B. S., Oh, J. Y. & Sohn, H. Theoretical and experimental investigations into laser ablation of polyimide and copper films with 355-nm Nd:YVO4 laser. *Journal of Materials Processing Technology* **187-188,** 260–263 (2007).

107. Klank, H., Kutter, J. P. & Geschke, O. CO(2)-laser micromachining and back-end processing for rapid production of PMMA-based microfluidic systems. *Lab on a chip* **2,** 242–6 (2002).

108. Wang, H. & Lu, C. Electroporation of Mammalian Cells in a Microfluidic Channel with Geometric Variation exogenous molecules into cells . Rapid electrical lysis. *Analytical chemistry* **78,** 5158–5164 (2006).

109. Valic, B. *et al.* Effect of electric field induced transmembrane potential on spheroidal cells: theory and experiment. *European biophysics journal: EBJ* **32,** 519–28 (2003).

110. Wang, H. & Lu, C. Electroporation of mammalian cells in a microfluidic channel with geometric variation. *Analytical chemistry* **78,** 5158–64 (2006).

111. Stroh, T., Erben, U., Kühl, A. a, Zeitz, M. & Siegmund, B. Combined pulse electroporation--a novel strategy for highly efficient transfection of human and mouse cells. *PloS one* **5,** e9488 (2010).

112. Knox, R. S. THEORY OF POLARIZATION QUENCHING BY EXCITATION TRANSFER. *Physica* **39,** 361–386 (1968).

113. Bao, N., Le, T. T., Cheng, J.-X. & Lu, C. Microfluidic electroporation of tumor and blood cells: observation of nucleus expansion and implications on selective analysis and purging of circulating tumor cells. *Integrative biology* **2,** 113–120 (2010).

114. Wang, H. & Lu, C. High-Throughput and Real-Time Study of Single Cell Electroporation Using Microfluidics: Effects of Medium Osmolarity. *Biotechnology and bioengineering* **95,** 1116–1125 (2006).

115. Hamasha, M. M. *et al.* Stability of ITO Thin Film on Flexible Substrate Under Thermal Aging and Thermal Cycling Conditions. *Journal of Display Technology* **8,** 385–390 (2012).

116. Chang, D. C. in *Electroporation and Electrofusion in Cell biology* (Neumann, E., Sowers, A. E. & Jordan, C. A.) 215–227 (Plenum Press, 1989).

117. Wang, H. & Lu, C. Electroporation of Mammalian Cells in a Microfluidic Channel with Geometric Variation. **78,** 5158–5164 (2006).

118. Gao, J., Yin, X.-F. & Fang, Z.-L. Integration of single cell injection, cell lysis, separation and detection of intracellular constituents on a microfluidic chip. *Lab on a chip* **4,** 47–52 (2004).

119. Khine, M., Lau, A., Ionescu-Zanetti, C., Seo, J. & Lee, L. P. A single cell electroporation chip. *Lab on a Chip* **5,** 38–43 (2005).

120. Zhan, Y., Wang, J., Bao, N. & Lu, C. Electroporation of cells in microfluidic droplets. *Analytical chemistry* **81,** 2027–31 (2009).

121. Rojas-Chapana, J. A., Correa-Duarte, M. A., Ren, Z., Kempa, K. & Giersig, M. Enhanced Introduction of Gold Nanoparticles into Vital Acidothiobacillus ferrooxidans by Carbon Nanotube-based Microwave. *Nano Letters* **4,** (2004).

122. Neumann E. *Electroporation and Electrofusion in Cell Biology*. 61–82 (Springer, 1989).

123. Tsong T Y. *Electroporation and Electrofusion in Cell Biology*. 149–163 (Springer, 1989).

124. Ba, L. *et al.* Probing local electric field distribution of nanotube arrays using electrostatic force microscopy. *Journal of Applied Physics* **93,** 9977 (2003).

125. Vieira, S. M. C. *et al.* Investigation of field emission properties of carbon nanotube arrays defined using nanoimprint lithography. *Applied Physics Letters* **89,** 022111 (2006).

126. Yantzi, J. D. & Yeow, J. T. W. Carbon Nanotube Enhanced Pulsed Electric Field Electroporation for Biomedical Applications. in *IEEE ICMA* 1872–1877 (2005).

127. Vandeperre, L. J. ELECTROPHORETIC DEPOSITION OF MATERIALS. *Annual Review of Materials Science* 327–52 (1999).

128. Boccaccini, A. R. *et al.* Electrophoretic deposition of carbon nanotubes. *Carbon* **44,** 3149–3160 (2006).

129. Du, C. *et al.* Method of synthesizing small-diameter carbon nanotubes with electron field emission properties. (2005).

130. Gao, B. *et al.* Fabrication and Electron Field Emission Properties of Carbon Nanotube Films by Electrophoretic Deposition. *Advanced Materials* **13,** 1770–1773 (2001).

131. Berney, M., Hammes, F., Bosshard, F., Weilenmann, H.-U. & Egli, T. Assessment and interpretation of bacterial viability by using the LIVE/DEAD BacLight Kit in combination with flow cytometry. *Applied and environmental microbiology* **73,** 3283–90 (2007).

132. Desjardins, R., Boulos, L. & Barbeau, B. Methods LIVE / DEAD ® Bac Light E□: application of a new rapid staining method for direct enumeration of viable and total bacteria in drinking water. *Microbiological Methods* **37,** 77–86 (1999).

133. Molecular Probes Inc. LIVE/DEAD BacLight Bacterial Viability Kits. (2004). at <http://probes.invitrogen.com/media/pis/mp07007.pdf>

134. Nilsson, L. *et al.* Scanning field emission from patterned carbon nanotube films. *Applied Physics Letters* **76,** 2071 (2000).

135. Yaghoobi, P. & Nojeh, A. Electron emission from carbon nanotubes. *Modern Physics Letters B* **21,** 1807–1830 (2007).

136. Wang, M., Li, Z. H., Shang, X. F., Wang, X. Q. & Xu, Y. B. Field-enhancement factor for carbon nanotube array. *Journal of Applied Physics* **98,** 014315 (2005).

137. Wang, G., Xu, J.-J. & Chen, H.-Y. Interfacing cytochrome c to electrodes with a DNA – carbon nanotube composite film. *Electrochemistry Communications* **4,** 506–509 (2002).

138. Williams, K. A., Veenhuizen, P. T. M., De la Torre, B. G., Eritja, R. & Dekker, C. Carbon nanotubes with DNA recognition. *Nature* **420,** 761 (2002).

139. Wang, S. G., Wang, R., Sellin, P. J. & Zhang, Q. DNA biosensors based on self-assembled carbon nanotubes. *Biochemical and biophysical research communications* **325,** 1433–7 (2004).

140. Dwyer, C. *et al.* DNA-functionalized single-walled carbon nanotubes. *Nanotechnology* **13,** 601–604 (2002).

141. Guo, M., Chen, J., Nie, L. & Yao, S. Electrostatic assembly of calf thymus DNA on multi-walled carbon nanotube modified gold electrode and its interaction with chlorpromazine hydrochloride. *Electrochimica Acta* **49,** 2637–2643 (2004).

142. Gascoyne, P. R. C. Particle separation by dielectrophoresis. *Electrophoresis* **23,** 1973–1983 (2002).

143. Crossley, B. L., Kossler, M., Starman, L. A., Coutu, R. A. & Peter, J. Optimization of Carbon Nanotube Field Emission Arrays. in *Proceedings of the COMSOL Conference 2009 Boston* (2009).